1983

An encoder system for the 18-inch telescope and uvbyHB photometry of bright UV stars

Brian R. Wade

University of Wollongong

AN ENCODER SYSTEM FOR THE 18-INCH TELESCOPE AND uvbyHβ PHOTOMETRY OF BRIGHT UV STARS

A thesis submitted in fulfilment of the requirements for the award of the degree of

MASTER OF SCIENCE

from

THE UNIVERSITY OF WOLLONGONG

by

Brian R. Wade, B.Sc.(A.N.U.), Dip.Ed.(Sydney).

DEPARTMENT OF PHYSICS

1983

764978

The original work reported in this thesis is that of the candidate alone, except for photometry of twenty one of the program stars obtained by Dr. L. F. Smith.

All subsequent reductions and interpretations based on these observations were, however, carried out by the candidate.

The telescope encoding system was constructed by Mr. P. Ihnat to the design of the candidate.

ACKNOWLEDGEMENTS

It is a great pleasure to express my thanks to Dr. L. F. Smith for advice and guidance which has been cheerfully and generously provided throughout this study.

I wish to thank Dr. D.J. Carnochan and Professor R. Wilson for making available preprints of their ultraviolet catalogues and their 1983 paper.

To the director of MSSSO, my thanks for the granting of observing time for this program.

Dr. R. R. Shobbrook kindly provided calculator programs which greatly eased the task of reducing the data.

To Dr. J. E. Norris and Dr. E. B. Newell for their helpful suggestions in interpreting the photometric results, I am most grateful.

To Dr. G. Hovey and Mr. G. Bothwell I am indebted for advice during the preliminary planning stage of the encoding system.

I am deeply grateful for the assistance of Mr. P. Ihnat who so ably constructed the encoding system and provided helpful discussions on digital circuits.

Special thanks to Dr. K. Ausburn for his encouragement, and to Professor P. Fisher for making available the facilities of the University of Wollongong Physics Department.

SUMMARY

An observation program of uvbyHβ photometry was performed on 90 stars taken from Carnochan and Wilson's (1976) catalogue of objects that appear to be very ultraviolet as detected by the S2/68 experiment in the ESRO TD-1A satellite.

The classification of most of the stars by visible photometry, published spectrographic class, and ultraviolet photometry from the TD-1A data is consistent to within two subclasses. The initial appearance of excessive UV for these objects would appear to be due to incorrect HD classification.

Two objects (HD36629 and HD81307) appear to have genuinely excessive ultraviolet flux, and it is suggested that this could be due to the presence of faint, hot companions with size and luminosity comparable to planetary nebulae.

A few stars show peculiarities for which there is no obvious explanation.

An examination is made of the suggestion of Carnochan and Wilson (1983) that a large number of the objects in Wilson's (1978) catalogue with very ultraviolet colours are subdwarfs, with luminosities two magnitudes below the main sequence. It is shown that the results of this program do not support the suggestion, and the alternative proposal is made that the unexpectedly large number of faint objects could result from a

selection effect in favour of objects with unusually low interstellar extinction.

The design of a position encoding system installed on the University of Wollongong's 18-inch telescope is described; the system employs incremental optical shaft encoders and an economical digital display. It was originally intended that the uvbyHβ photometry program be conducted with that telescope and encoding system; however, time factors dictated the use of MSSSO telescopes instead.

CONTENTS

Page

CHAPT. 1: THE TD-1A ULTRAVIOLET OBSERVATIONS 1

CHAPT. 2: uvbyHβ PHOTOMETRY 4

CHAPT. 3: OBSERVATIONAL DATA.................... 7

CHAPT. 4: CLASSIFICATION OF PROGRAM STARS

4.1 Photometric Classification......... 27

4.2 Ultraviolet Classification......... 40

4.3 Comparison of Classifications...... 47

CHAPT. 5: SPECTRAL ENERGY DISTRIBUTIONS.......... 55

CHAPT. 6: DISCUSSION OF RESULTS

6.1 The Search for Anomalies........... 77

6.2 HD36629, HD81307 and HD81694 78

6.3 Anomalous early B stars 85

6.4 Anomalous late B stars 88

6.5 Subdwarfs 90

CHAPT. 7: AN ENCODING SYSTEM FOR THE 18-INCH TELESCOPE 106

BIBLIOGRAPHY............................131

1. THE TD-1A ULTRAVIOLET OBSERVATIONS

The European Satellite TD-1A was launched from California in March 1972. One of the experiments on board, coded S2/68, comprised an ultra-violet telescope feeding a spectrophotometer and photometer which gave low dispersion spectra over the range 1350-2550 Å and a broadband measurement centred on 2750 Å (Boksenberg et al, 1973).

Each observation of a star yielded 21 data points in each of the three spectrophotometric channels, one measurement every 19.4 Å.

The Ultraviolet Bright Star Catalogue (Jamar et al, 1976) lists fluxes for 60 wavelengths from 1360-2540 Å and the flux at 2740 Å for 1356 bright stars (the limiting magnitude for B-type stars being 6.0 to 7.0).

The Catalogue of Stellar Ultraviolet Fluxes (Thompson et al, 1978) contains 31215 stars and gives for each three broadband (about 330 Å) fluxes centred on 2365, 1965 and 1565 Å. The 2740 Å broadband measure is listed as a fourth flux.

The broadband absolute fluxes obtained can be put onto the visual magnitude scale using the calibration of Hayes and Latham (1975):

$$m(\lambda) = -2.5 \log_{10} F(\lambda) - 21.175$$

where $F(\lambda)$ is the flux at wavelength λ Å in units of erg cm^{-2} s^{-1} $Å^{-1}$.

Carnochan and Wilson (1976) list a selection of stars for which $(A_2-A_1) = (m_{1565}-m_{2740}) < -1.4$ and for which $A_1 = m_{2740} > 6.4$.

The University College London Ultraviolet Star Catalogue (Wilson, 1978) lists broadband fluxes and corresponding magnitudes and colours for almost 3,000 stars.

Carnochan and Wilson (1983) (henceforth referred to as CW) list 464 objects with (A_2-A_1) less than -1.50, corresponding to an unreddened B4V star.

Numbers of objects from Carnochan and Wilson's 1976 and 1978 catalogues have been identified as subdwarfs, or binaries with a subdwarf component - see for example Giddings and Dworetsky (1978) and Dworetsky et al (1977). Berger and Fringant (1980) detected 13 new hot subluminous stars, most with m_v greater than 10 and (A_2-A_1) less than -1.8 .

CW state that a statistical analysis of their list of ultraviolet objects indicates that many of them are subdwarf stars lying at least two magnitudes below the main sequence in the spectral range O to B3. A preliminary study by Carnochan et al (1975) reached a similar conclusion.

(With regard to the accuracy of the TD-1A data, CW say that high background counts and noise spikes could seriously affect the 1965 Å and 2365 Å channels; 1965 Å suffered the worst and its data were not used by CW, and all 2365 Å data were examined to remove spikes.

The 1565 Å channel, with a high work-function cathode and the 2740 Å channel with a large bandwidth were relatively trouble-free.)

For this study, 90 stars were taken from Carnochan and Wilson's (1976) catalogue. It should be noted that the more recent fluxes given by Thompson et al (1978) indicate that for some of the stars, (A_2-A_1) is greater than -1.4 .

2. uvbyHβ PHOTOMETRY

The uvbyHβ photometry system is described by Stromgren (1966). Filters of intermediate bandwidth (180-300 Å), with mean wavelengths of 3500, 4110, 4670 and 5470 Å define four bands. The magnitudes u, v, b and y corresponding to intensities measured in these four bands define three indices:

(b-y), the colour index;

c_1 = (u-v)-(v-b), the Balmer discontinuity index;

m_1 = (v-b)-(b-y), the metal-line index.

Stromgren (1966) also defines indices unaffected by interstellar reddening:

$$[c_1] = c_1 - 0.20(b-y)$$

$$[m_1] = m_1 + 0.18(b-y)$$

$$[u-b] = [c_1] + 2[m_1]$$

Crawford's derivation of interstellar reddening (Crawford, 1975) gives

$$[m_1] = m_1 + 0.32(b-y)$$

which is the definition adopted in this study.

The β index is obtained as the magnitude difference corresponding to the ratio of the intensities measured through interference filters centred on Hβ (4861 Å) with half-widths of about 30 Å and 150 Å respectively (Stromgren, 1966).

Crawford and Mander (1966) list 80 stars used as standards for photoelectric Hβ photometry and describe the observational technique used.

Crawford and Barnes (1970) establish a standard uvby system based on 304 stars, and present procedures for reducing observations.

Crawford (1975) presents uvbyHβ data on 123 O-type stars and uses them to obtain the interstellar reddening slopes for the uvby system which are used in this study.

Crawford (1978) provides empirical calibrations of the uvbyHβ system for B-type stars.

Figure 2 shows the passbands of the uvbyHβ photometry and TD-1A ultraviolet observations related to a model atmosphere flux distribution for a star with $T_e = 14{,}000^{\circ}$ (Klinglesmith, 1971), corresponding to a B5 star (Nandy and Schmidt, 1975).

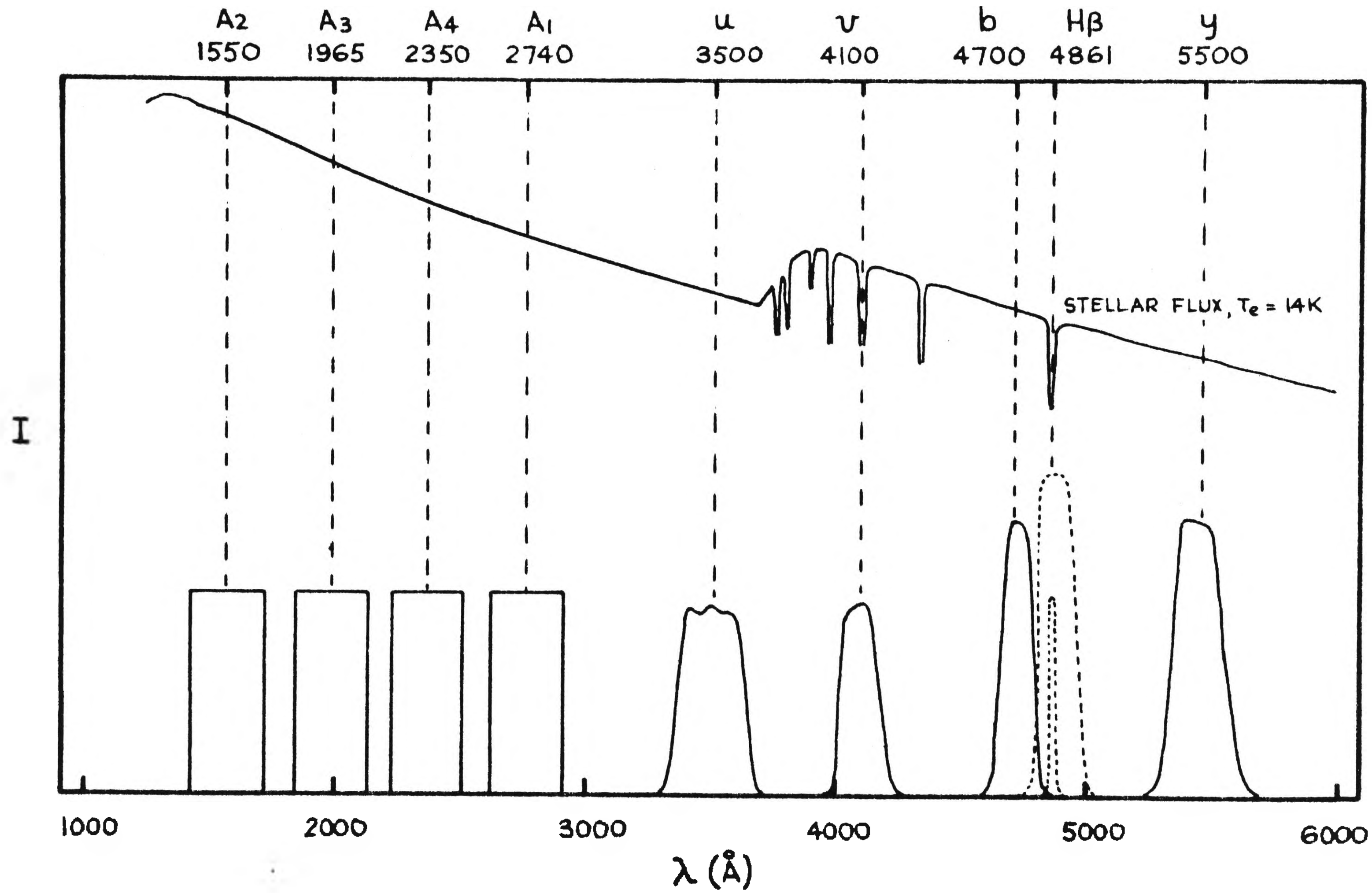

Fig 2. Passbands of uvbyHβ and TDI UV observations.

3. OBSERVATIONAL DATA

3.1 Selection of Stars

3.11 Standard Stars.

Standards chosen were listed both as uvby standards by Crawford and Barnes (1970) and as Hβ standards by Crawford and Mander (1966). All were south of declination +20° and accessible on one of our runs. The standards observed on each night were chosen to obtain the greatest possible range of photometric indices.

TABLE 3.11 STANDARD STARS

HR	HD
812	17093
1412	28319
1552	30836
3849	83754
4119	90994
4133	91316
4405	99211
4540	102870
5270	122563
5511	130109
5530	130819
5993	144470
5997	144608
6141	148605
6629	161868
6714	164353
7377	182640
7446	184915
7447	184930
8634	214923
8969	222368

3.12 Program Stars

A Catalogue of Ultraviolet Objects by Carnochan and Wilson (1976) lists objects that appear to be very ultraviolet as detected by the S2/68 experiment in the ESRO TD1 satellite and for which the difference in magnitudes between the fluxes at 1550 and 2740 Angstroms is less than -1.4.

Program stars were selected from the catalogue if they were south of declination $+20^{\circ}$, brighter than magnitude 8.4 and accessible on one of our runs. A few stars to magnitude 9.5 were also included.

Most of the program stars are listed in the Ultraviolet Star Catalogue by Wilson (1978).

3.2 The Photoelectric System and Filters

In January and May 1979, the 16-inch telescope at Siding Spring Observatory was used with a single-channel MSSSO photometer, 1P21 photomultiplier refrigerated with dry ice, direct low-current integrator, digital voltmeter and printer. In September 1980 the SSO 24-inch telescope, Princeton pre-amplifier and pulse counter were used.

Transmission curves for the uvby interference filters were provided by the makers, Spectrofilm Inc.; the curves for the Hβ filters were provided by MSSSO (see figures 3.2(a) and 3.2(b)).

Central wavelengths and half-widths of the filters are listed in Table 3.2.

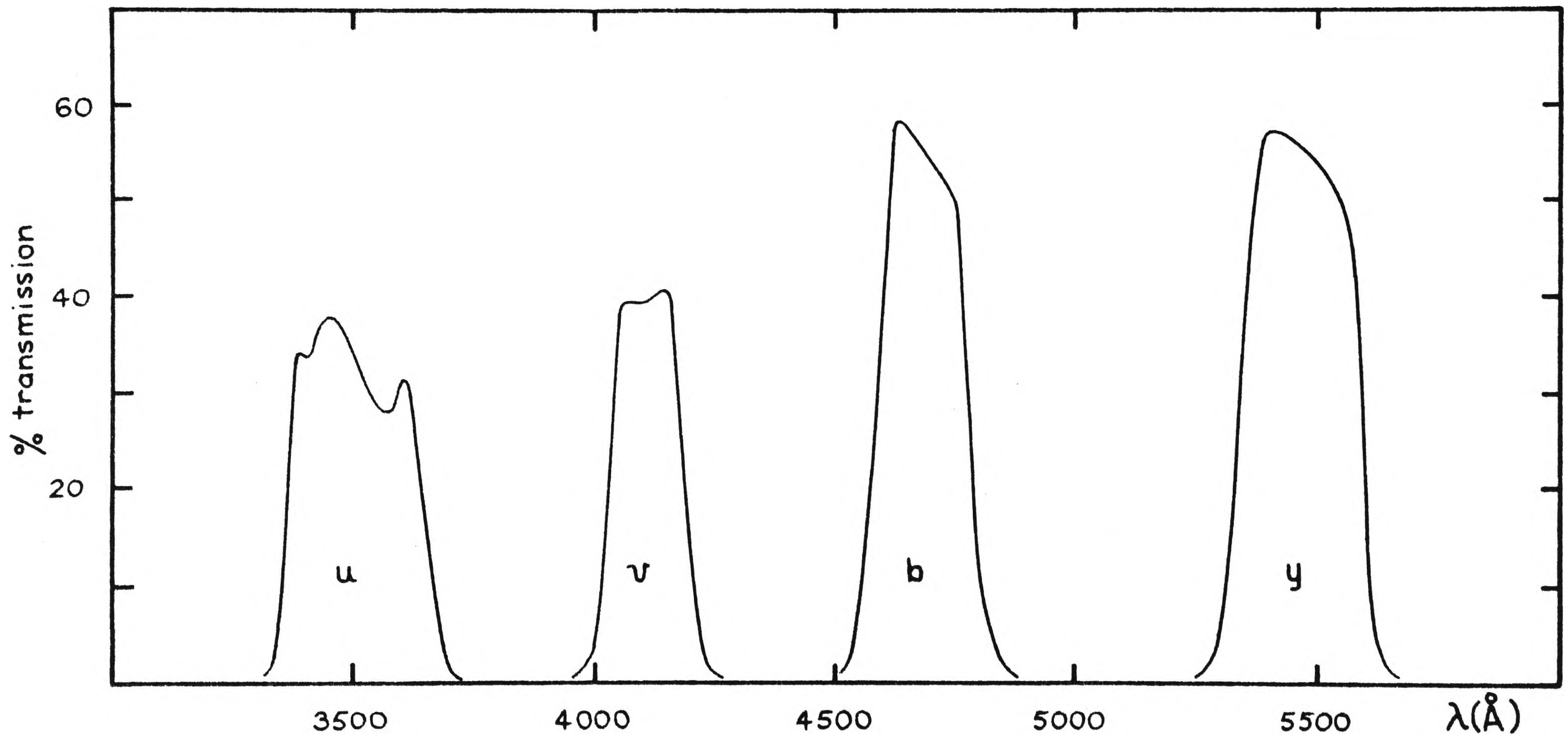

Fig. 3.2 (a). Transmission curves for u, v, b, y filters.

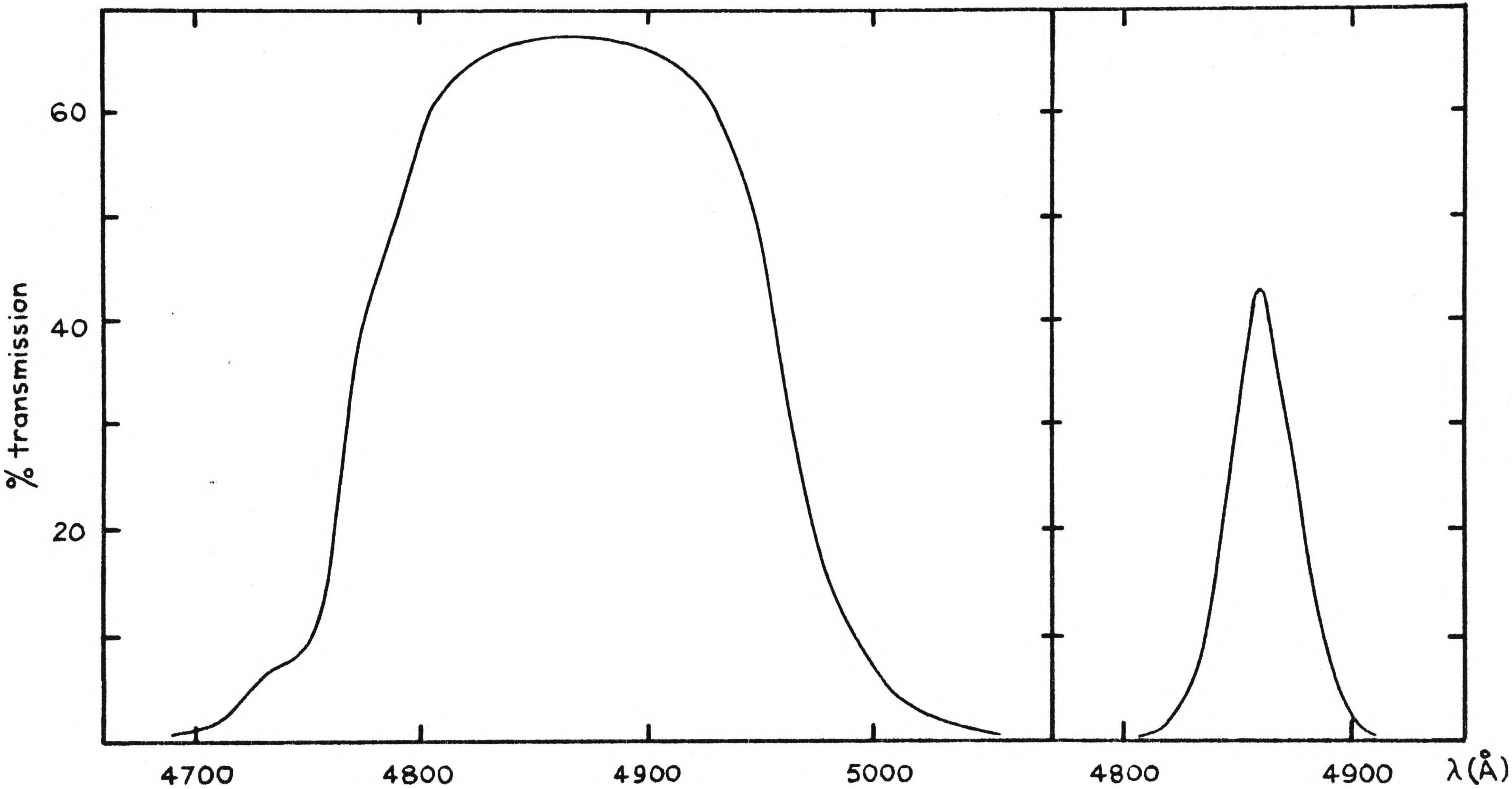

Fig. 3.2 (b). Transmission curves for the Hβ filters.

TABLE 3.2 FILTER CHARACTERISTICS

FILTER	CENTRAL WAVELENGTH (ANGSTROMS)	HALF WIDTH (ANGSTROMS)
u	3490	268
v	4110	180
b	4680	180
y	5460	230
Hβ wide	4861	180
Hβ narrow	4861	30

3.3 Observation at the Telescope

Published star coordinates were corrected for precession. Finding charts were prepared by tracing from the Smithsonian Atlas.

The observational sequence adopted was u,v,b,y, Hβ wide, Hβ narrow for star plus sky; the sequence was repeated for sky only, and again for star plus sky. Integration time for each filter was usually 10 seconds.

Standard stars were observed at intervals of about once per hour.

3.4 Reductions

3.41 Instrumental magnitude for each filter

As light flux ϕ passed through a filter to the photomultiplier, the amplified current I from the photomultiplier (which was proportional to ϕ) charged a capacitance C to a potential difference V in time t, where

$$I = \frac{CV}{t}$$

Hence $$\phi \propto \frac{CV}{t}$$

Three voltage readings were taken for each filter:

V1: star + sky

V2: sky only

V3: star + sky

The voltage which would have resulted from the star only was thus

$$V = \frac{V1 + V3}{2} - V2$$

The observed magnitude was then

$$m'' = -2.5 \log_{10} \frac{CV}{t} \quad .$$

Magnitudes for u, v, b and y defined in this way are then combined into colours b-y, c_1 and m_1 .

3.42 Air Mass for each observation

The relative air mass, X, in units of the atmospheric thickness at the zenith, is given to good accuracy by the secant of the zenith distance, z, for z less than 60° (Hardie, 1962).

The value for sec z is given by

$$\sec z = \{\sin\phi\sin\delta + \cos\phi\cos\delta\cos(\tau-\alpha)\}^{-1}$$

where ϕ is the observer's latitude, δ the declination of the star, τ the sidereal time and α the right ascension of the star.

Hardie (1962) also gives an expression for air mass which is "accurate to better than 1/10 per cent up to X = 6.8" :

$$X = \sec z - A(\sec z - 1) - B(\sec z - 1)^2 - C(\sec z - 1)^3$$

where A = 0.0018167, B= 0.002875, C = 0.0008083.

The more complex expression was adopted for calculation, since little extra effort was needed to use it with a programmable calculator.

3.43 Extinction Coefficients

Correction for atmospheric extinction is according to the relationship

$$m' = m'' - kX$$

where m' = the extinction-corrected magnitude

m'' = the observed magnitude

X = the airmass

k = the extinction coefficient.

To find the extinction coefficient k, the magnitude of any non-variable star (usually a standard star) was measured at differing airmasses. On a plot of magnitude versus airmass, a line of best fit was obtained by eye; the gradient of the line was the extinction coefficient k.

Extinction coefficients k_y, k_{b-y}, k_m and k_c were found, where -

$$y' = y'' - k_y X$$
$$(b-y)' = (b-y)'' - k_{b-y} X$$
$$m_1' = m_1'' - k_m X$$
$$c_1' = c_1'' - k_c X$$

Table 3.43 lists the average observed extinction coefficients which were adopted, and the mean extinction coefficients, "adequate for most nights" found by Crawford and Barnes (1970) for Kitt Peak Observatory.

TABLE 3.43 EXTINCTION COEFFICIENTS

COEFFICIENT	MEAN OBSERVED (ADOPTED)	CRAWFORD & BARNES (1970)
k_y	0.144	0.150
k_{b-y}	0.068	0.068
k_m	0.065	0.053
k_c	0.181	0.187

3.44 Transformation to the Standard System

Transformation coefficients were applied to the instrumental system indices to obtain indices on the standard system. Crawford and Barnes (1970) give the relationships as:

$$V - y' = A + B(b-y)$$

$$(b - y) = C + D(b-y)'$$

$$m_1 = E + Fm_1' + J(b-y)$$

$$c_1 = G + Hc_1' + I(b-y)$$

In the case of m_1 and c_1 , linear transformations were initially obtained with J and I set to zero; since the central wavelengths and bandwidths of the filters were very close to those of the standard system, no colour term was expected. The remaining discrepancies from the mean line showed no correlation with (b-y), confirming J = 0 and I = 0 as adequate.

Transformation coefficients were determined by eye and by least-squares solutions with close agreement, the eye-determined values being those adopted. Crawford and Barnes (1970) caution against giving too much weight to a least-squares derived value for the coefficient F, and that a "carefully checked mean value" is generally preferable for B, D and H as well.

Figures 3.44 (a), (b), (c) and (d) show the eye-fitted linear transformations from each night of the May 1979 run. Table 3.44 lists the adopted transformation coefficients.

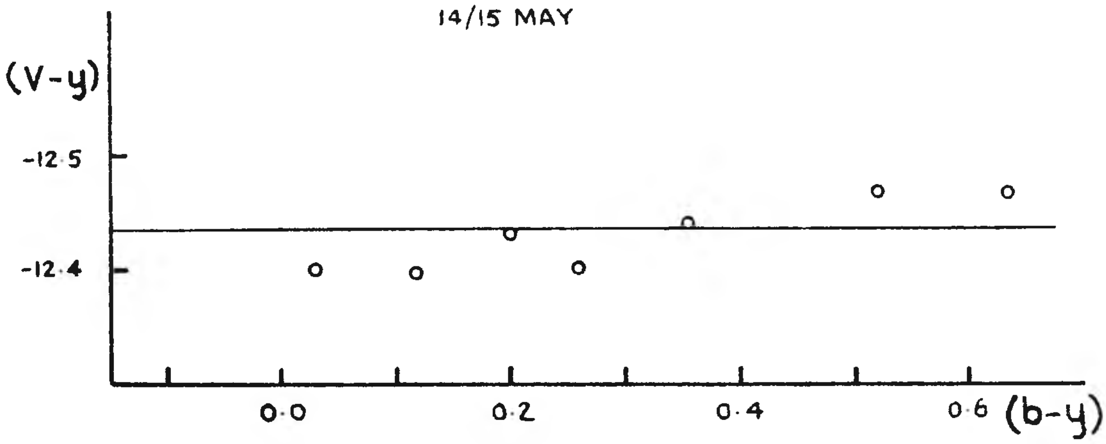

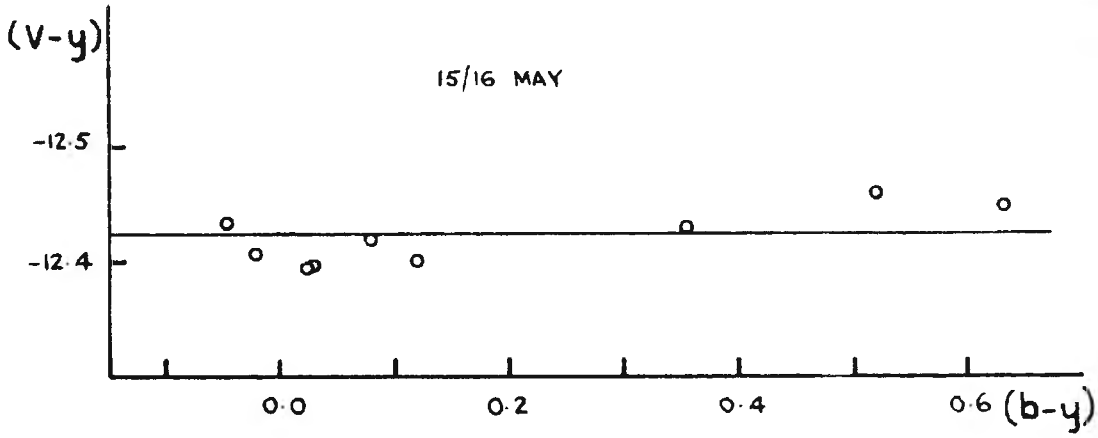

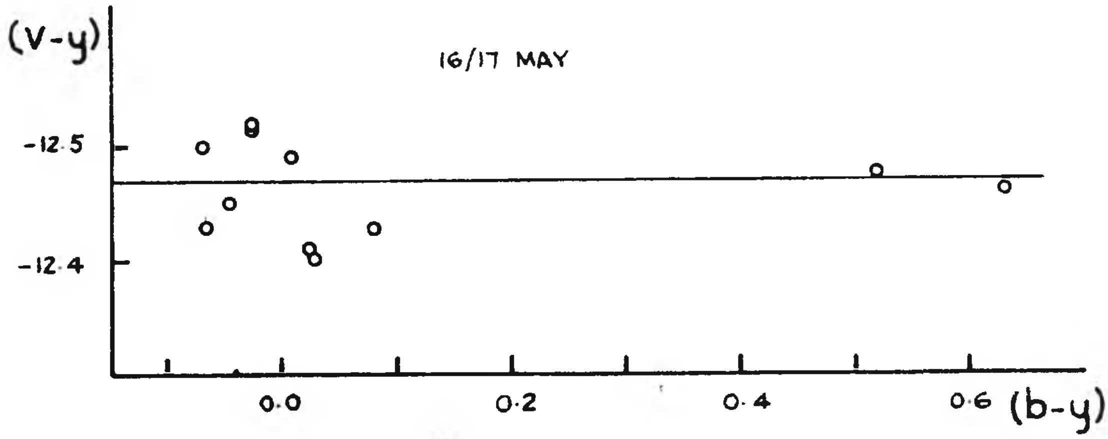

Fig. 3.44 (a) Transformations to standard system.

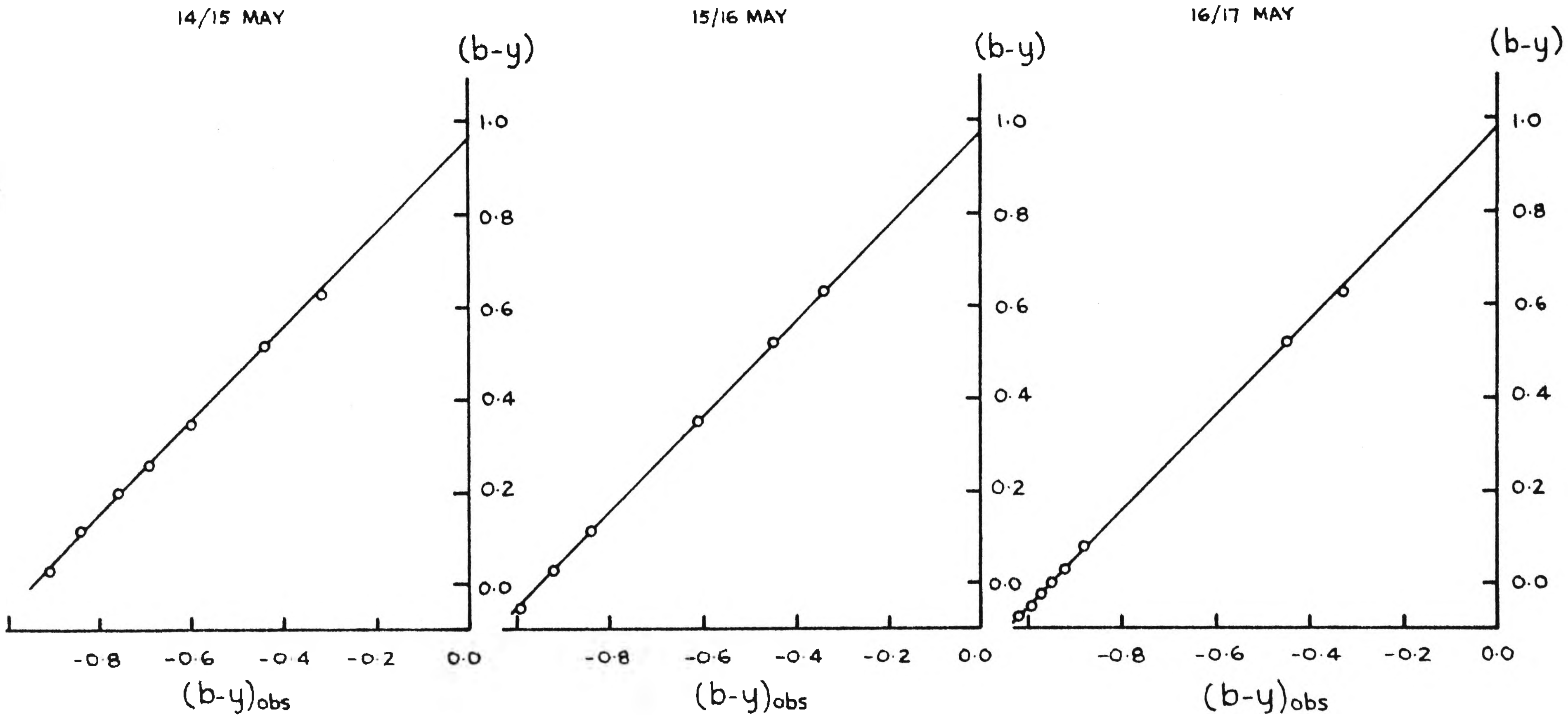

Fig. 3.44(b). Transformations to standard system.

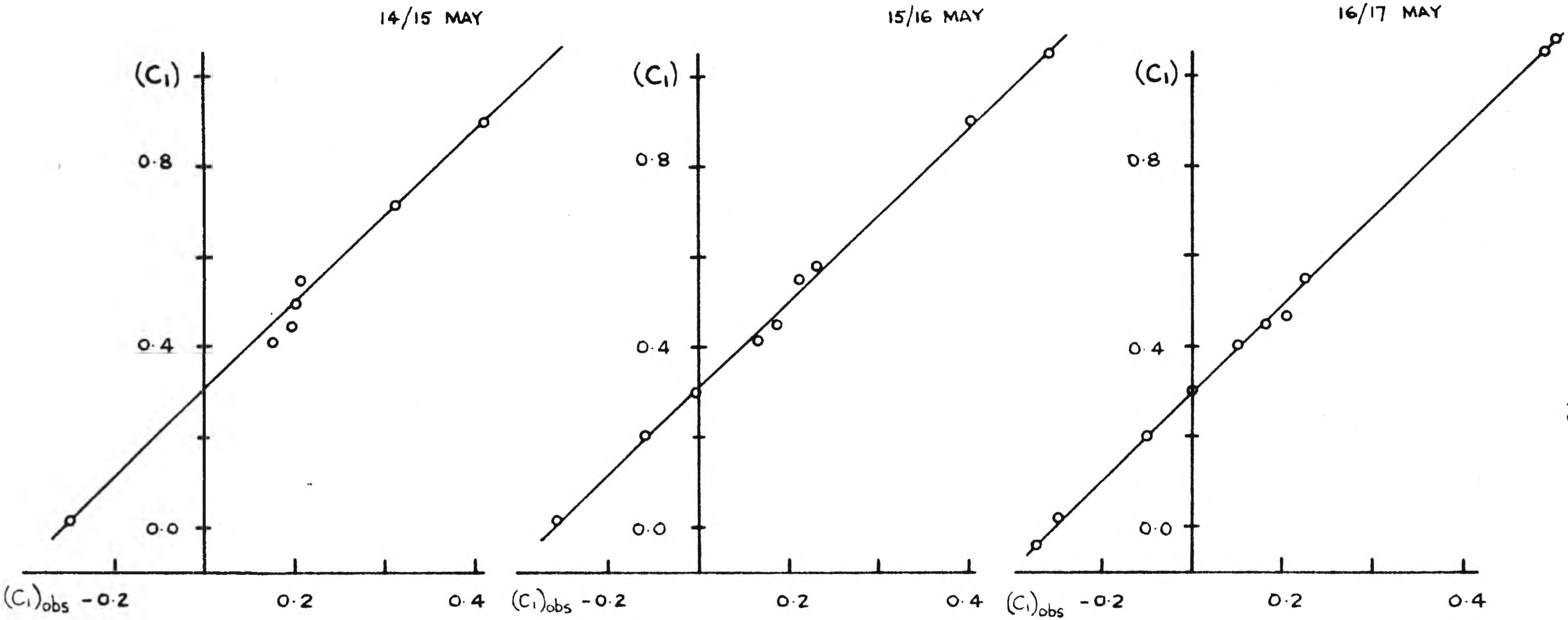

Fig 3.44 (c) Transformations to standard system.

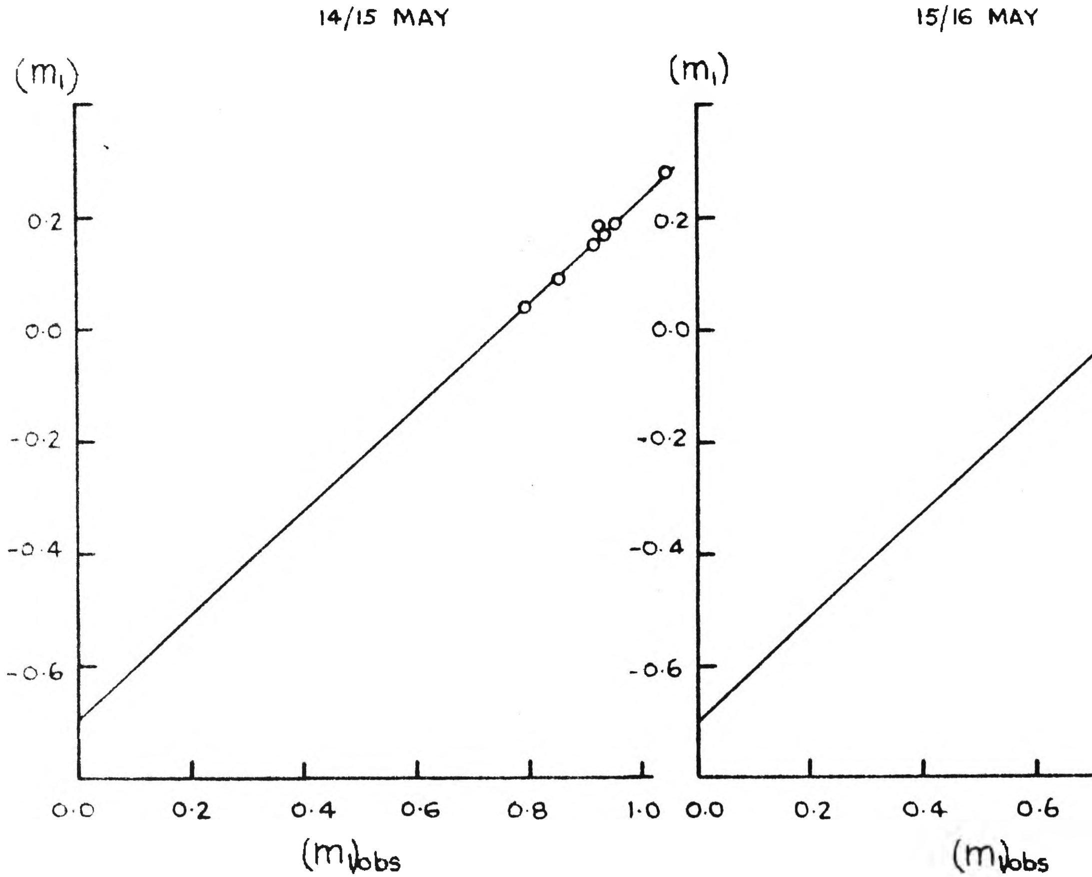

Fig. 3.44(d). Transformations

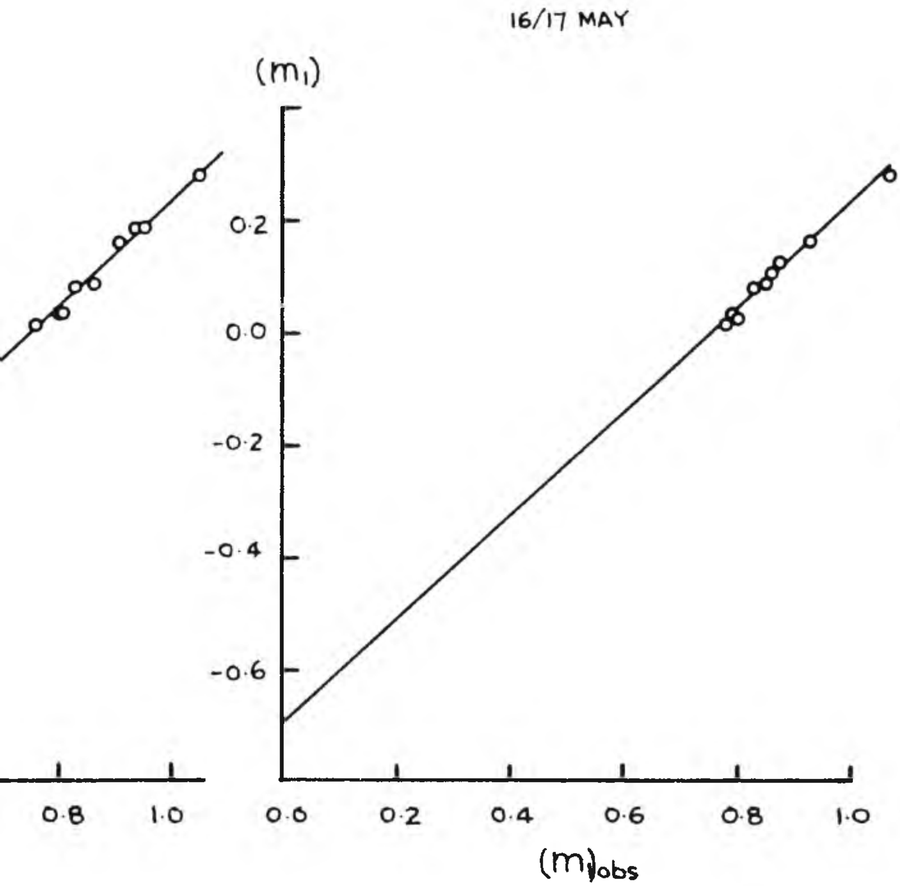

to standard system.

TABLE 3.44 TRANSFORMATION COEFFICIENTS

COEFFICIENT	14/15 May	15/16 May	16/17 May
A	-12.44	-12.44	-12.47
B	0.00	0.00	0.00
C	0.97	0.98	0.98
D	1.02	1.03	1.03
E	-0.70	-0.70	-0.70
F	0.93	0.93	0.93
G	0.31	0.31	0.29
H	0.96	0.96	0.96

3.45 Hβ reductions

The procedure followed is described by Crawford and Mander (1966).

The observed values of beta (β") are obtained from the relationship:

$$\beta'' = -2.5 \log \left(\frac{\frac{1}{2}(H_{n1} + H_{n2}) - S_n}{\frac{1}{2}(H_{w1} + H_{w2}) - S_w} \right)$$

where H_{n1} and H_{n2} are the two magnitudes of (star plus sky) obtained through the narrow filter in each observational sequence; H_{w1} and H_{w2} are the corresponding magnitudes obtained through the wide filter; and S_n and S_w are the sky only magnitudes obtained through the narrow and wide filters respectively.

For each standard star, the average of all values of β'' over all nights was taken to give the instrumental system value (β') for each standard star.

For each standard star, the difference was found between the average of β'' for each night and β'. The differences across all the standard stars were averaged to find the night correction.

We found the night corrections sufficiently small to be able to neglect them.

The instrumental system values (β') of the standard stars were compared with the standard values (β) of Crawford and Mander (1966) to obtain the transformation coefficients needed to convert from the instrumental system to the standard system. The transformation is linear:

$$\beta = A + B\beta'$$

and we found the transformation coefficients to be

$$A = 0.268$$

$$B = 1.059$$

3.46 Accuracy of Photometric Results

So that the maximum number of stars could be surveyed in the time available, most of the program stars were observed only once. For the standard stars and program stars which were observed several times, indices usually agreed within ±0.01 magnitudes.

3.47 Photometric Results

Table 3.47 gives y, (b-y), m_1 and c_1 for all the program stars.

β was not measured for stars observed in January 1979.

The ultraviolet colours

$$A_2 - A_1 = (m_{1550} - m_{2740})$$

$$A_2 - A_4 = (m_{1550} - m_{2350})$$

given by Wilson (1978) are included for convenience.

TABLE 3.47

uvbyHβ INDICES AND ULTRAVIOLET COLOURS OF PROGRAM STARS

HD	y	b-y	m_1	c_1	β	A_2-A_1	A_2-A_4
36629	7.757	0.124	0.124	0.308	2.686	-1.52	-1.40
37526	7.582	-0.062	0.100	0.442	2.719	-1.37	-0.91
42204	8.457	-0.060	0.104	0.312	2.678	-1.39	-0.98
42551	7.574	-0.087	0.129	0.418	2.659	-1.36	-0.89
48165	8.093	-0.031	0.103	0.379	-	-1.36	-0.89
49188	7.659	-0.055	0.113	0.359	-	-1.36	-0.96
51255	8.203	-0.078	0.104	0.243	2.658	-1.47	-1.02
51285	8.162	-0.094	0.089	0.175	2.585	-1.54	-0.92
52942	8.143	0.169	0.037	0.148	2.647	-1.41	-1.24
53824	8.107	-0.046	0.095	0.515	2.733	-1.16	-0.85
54197	7.968	0.018	0.049	0.051	2.618	-1.51	-1.17
58441	8.062	-0.052	0.096	0.247	-	-1.49	-0.91
60757	7.855	-0.060	0.095	0.336	2.606	-1.47	-1.02
61193	8.194	0.019	0.046	0.091	2.649	-1.52	-1.11
63274	8.045	-0.035	0.090	0.434	-	-1.44	-0.88
64301	7.824	-0.068	0.154	0.553	-	-1.11	-0.82
64455	7.730	-0.065	0.095	0.374	2.678	-1.38	-0.83
66134	8.023	-0.006	0.117	0.633	-	-1.21	-0.53
68030	8.241	0.054	0.086	0.311	-	-1.37	-1.03
68046	8.106	-0.068	0.105	0.282	2.675	-1.41	-0.97
68982	7.564	0.139	0.048	0.257	-	-1.44	-1.35
69120	8.622	-0.015	0.091	0.579	-	-1.41	-0.85
70550	8.509	-0.018	0.073	0.800	2.753	-1.15	-0.77

Table 3.47 continued.

uvbyHβ and UV colours

HD	y	b-y	m_1	c_1	β	A_2-A_1	A_2-A_4
71336	8.001	-0.028	0.094	0.372	-	-1.43	-0.89
71945	7.808	-0.062	0.076	0.389	2.670	-1.39	-0.86
72771	7.886	-0.005	0.074	0.195	-	-1.34	-0.93
72973	8.276	-0.029	0.114	0.674	-	-1.27	-0.74
73215	8.126	-0.034	0.075	0.113	-	-1.48	-1.02
77904	8.158	-0.015	0.106	0.541	-	-1.26	-0.46
79368	8.388	-0.038	0.099	0.319	2.692	-1.38	-0.87
81307	6.544	0.012	0.162	0.803	2.886	-1.45	-0.95
81694	6.887	-0.015	0.144	0.789	2.851	-1.65	-1.22
81769	8.049	0.066	0.070	0.402	2.695	-1.21	-1.09
81921	6.789	0.007	0.077	1.005	2.716	-0.61	-0.46
82111	7.771	-0.030	0.077	0.436	2.686	-1.27	-0.95
82811	8.315	-0.037	0.117	0.483	2.740	-1.22	-0.95
83335	7.959	-0.035	0.101	0.473	2.716	-1.33	-0.88
83866	7.635	-0.023	0.067	0.355	2.691	-1.23	-0.81
84361	8.351	0.085	0.012	0.062	2.507	-1.47	-0.97
86385	7.897	-0.034	0.073	0.424	2.688	-1.36	-0.93
86441	7.501	-0.047	0.064	0.394	2.626	-1.32	-1.00
87295	7.668	0.006	0.062	0.343	2.660	-1.29	-1.09
88556	7.839	-0.025	0.063	0.426	2.687	-1.49	-1.00
88844	8.522	-0.025	0.020	-0.004	2.623	-1.33	-0.74
89403	7.671	0.016	0.035	0.287	2.650	-1.35	-1.04
89876	7.926	0.052	0.051	0.402	2.737	-1.34	-1.21

Table 3.47 continued

uvbyHβ and UV colours

HD	y	b-y	m_1	c_1	β	A_2-A_1	A_2-A_4
90288	8.119	-0.050	0.051	0.032	2.595	-1.66	-1.10
90786	8.795	0.018	0.032	0.132	2.654	-1.56	-0.86
91041	8.092	-0.015	0.090	0.526	2.707	-1.46	-0.96
94108	7.760	-0.059	0.095	0.381	2.703	-1.29	-0.94
95275	8.553	0.044	0.005	-0.115	2.596	-1.30	-0.88
118256	8.014	-0.013	0.080	0.471	2.684	-1.23	-0.73
118553	8.528	0.037	0.088	0.363	2.690	-1.32	-1.05
118571	8.762	0.075	-0.003	-0.028	2.607	-1.40	-1.40
119926	7.597	0.061	0.022	0.319	2.641	-1.33	-1.03
127449	7.725	0.038	0.065	0.253	2.656	-1.31	-1.09
130903	7.955	-0.008	0.063	0.882	2.639	-1.07	-1.30
135241	8.036	0.024	0.064	0.108	2.658	-1.50	-1.03
135786	7.946	-0.001	0.073	0.299	2.669	-1.37	-0.97
139300	7.501	-0.011	0.082	0.384	2.677	-1.45	-1.03
139579	8.361	0.010	0.083	0.726	2.748	-1.01	-1.06
143156	8.146	-0.042	0.096	0.418	2.686	-1.26	-0.86
146224	7.533	0.032	0.041	0.420	2.694	-1.03	-1.17
147889	7.906	0.655	-0.091	0.106	2.597	-1.56	-1.32
149065	8.438	0.055	0.037	0.156	2.669	-1.31	-1.28
149770	8.049	-0.039	0.078	0.328	2.626	-1.38	-0.91
149922	7.930	0.022	0.059	0.177	2.597	-1.48	-1.21
153084	8.335	0.031	0.055	0.113	2.657	-1.29	-1.03
153140	7.496	0.339	-0.040	0.039	2.573	-1.13	-1.11

Table 3.47 continued

uvbyHβ and UV colours

HD	y	b-y	m_1	c_1	β	A_2-A_1	A_2-A_4
154535	8.323	0.127	-0.020	0.068	2.611	-1.35	-1.20
155600	7.955	0.143	0.038	0.685	2.695	-0.85	-1.07
155754	7.955	0.057	0.014	0.071	2.639	-1.47	-1.23
156070	7.539	0.039	0.058	0.290	2.624	-1.25	-1.13
160109	7.484	0.067	0.060	0.412	2.695	-1.28	-1.16
161972	8.355	-0.034	0.077	0.398	2.660	-1.31	-0.95
162973	8.401	0.000	0.091	0.440	2.676	-1.45	-1.04
163430	8.172	0.009	0.080	0.190	2.622	-1.29	-1.01
163442	7.369	0.046	0.044	0.350	2.673	-1.32	-1.20
163927	8.351	-0.009	0.064	0.490	2.763	-1.25	-0.73
164320	7.565	0.032	0.063	0.566	2.679	-1.08	-0.79
165132	8.101	0.133	-0.014	-0.061	2.582	-1.61	-1.48
165246	7.716	0.134	-0.003	-0.066	2.586	-1.54	-1.36
165477	8.552	0.011	0.075	0.468	2.725	-1.16	-0.96
167003	8.449	-0.015	0.029	-0.050	2.555	-1.26	-0.67
170385	7.896	-0.062	0.086	0.331	2.673	-1.44	-0.98
172535	7.791	-0.024	0.082	0.338	2.695	-1.43	-1.02
172850	7.784	0.016	0.089	0.760	2.764	-0.99	-0.71
174395	8.167	0.063	0.056	0.635	2.733	-1.11	-1.02
175934	8.194	-0.024	0.098	0.566	2.724	-1.25	-1.06
180124	7.184	0.071	0.018	0.391	2.697	-1.25	-1.18

4. CLASSIFICATION OF PROGRAM STARS

4.1 Photometric Classification

4.11 Reddening-independent indices

Stromgren (1966) defined indices $[c_1]$, $[m_1]$ and $[u-b]$ which are "unaffected by interstellar reddening that obeys the standard law", and based on reddening ratios:

$$E(c_1) = 0.20\ E(b-y)$$
$$E(m_1) = -0.18\ E(b-y)\ .$$

Crawford (1975) gives, from four-colour photometry of O-type stars, the reddening ratios to be:

$$E(c_1) = 0.20\ E(b-y)$$
$$E(m_1) = -0.32\ E(b-y)\ .$$

Using Crawford's ratios in Stromgren's indices give the adopted values:

$$[c_1] = c_1 - 0.20(b-y)$$
$$[m_1] = m_1 + 0.32(b-y)$$
$$[u-b] = [c_1] + 2[m_1] = (u-b) - 1.56(b-y)\ .$$

4.12 The $[m_1]$ vs $[c_1]$ diagram

The $[m_1]$ versus $[c_1]$ diagram "yields coarse two-dimensional classification for the great majority of B stars", and segregates luminosity classes Ia, Ib and II from main sequence stars. It does not generally separate luminosity class III from luminosity classes IV and V (Stromgren, 1966).

Figure 4.12 shows the diagram for the program stars, which are represented by HD numbers with the two least significant figures deleted.

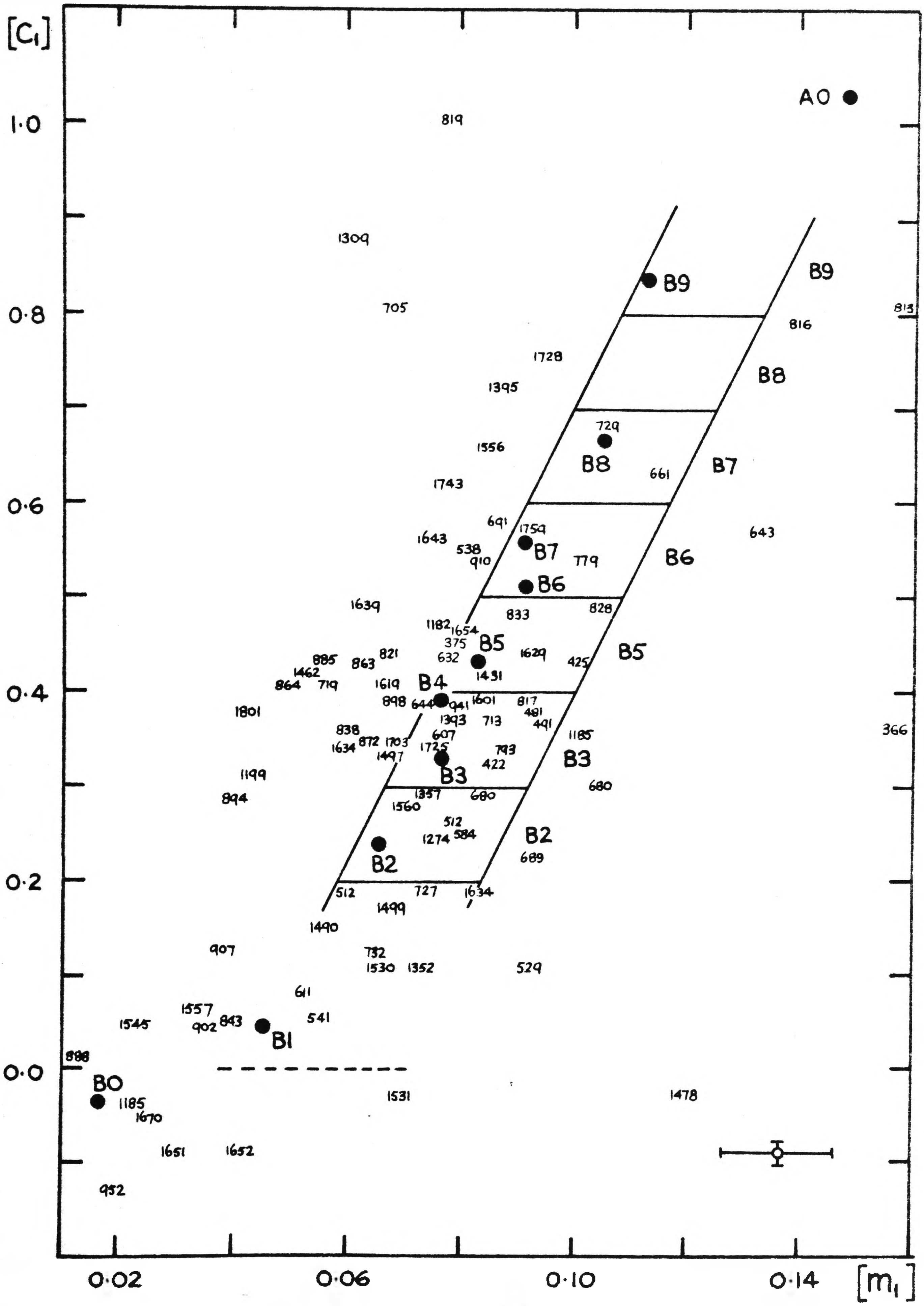

Fig. 4.12 [m1] vs [c1] for program stars.

The boxes labelled B2 to B9 enclose main sequence stars of the respective MK types (Stromgren, 1966). The dots represent the average location of MK types, calculated from average intrinsic values m_o, c_o, and $(b-y)_o$ for luminosity class V stars (Crawford, 1978).

The different reddening correction used in $[m_1]$ would shift Stromgren's main sequence to slightly more positive values. However the position of Crawford's stars indicates that the position of the main sequence stars is more negative than assigned by Stromgren.

The boundary between B0 and B1 was chosen as $[c_1] = 0.0$ on the basis of the Crawford values. The Stromgren $[c_1]$ boundaries were adopted for classes B1 to B9; disagreement with the more recent Crawford values is at most 0.1 of a class.

4.13 The [u-b] vs β diagram

This diagram can accomplish "high accuracy classification" for B stars, "with very few exceptions". (Stromgren, 1966).

Figure 4.13 shows the diagram for the program stars, represented by HD numbers with the two least significant figures deleted.

The boxes B2 to B9 enclose main sequence stars, with the zero-age line being the lower boundary (Stromgren, 1966). The dots are for average MK types with luminosity class V (Crawford, 1978).

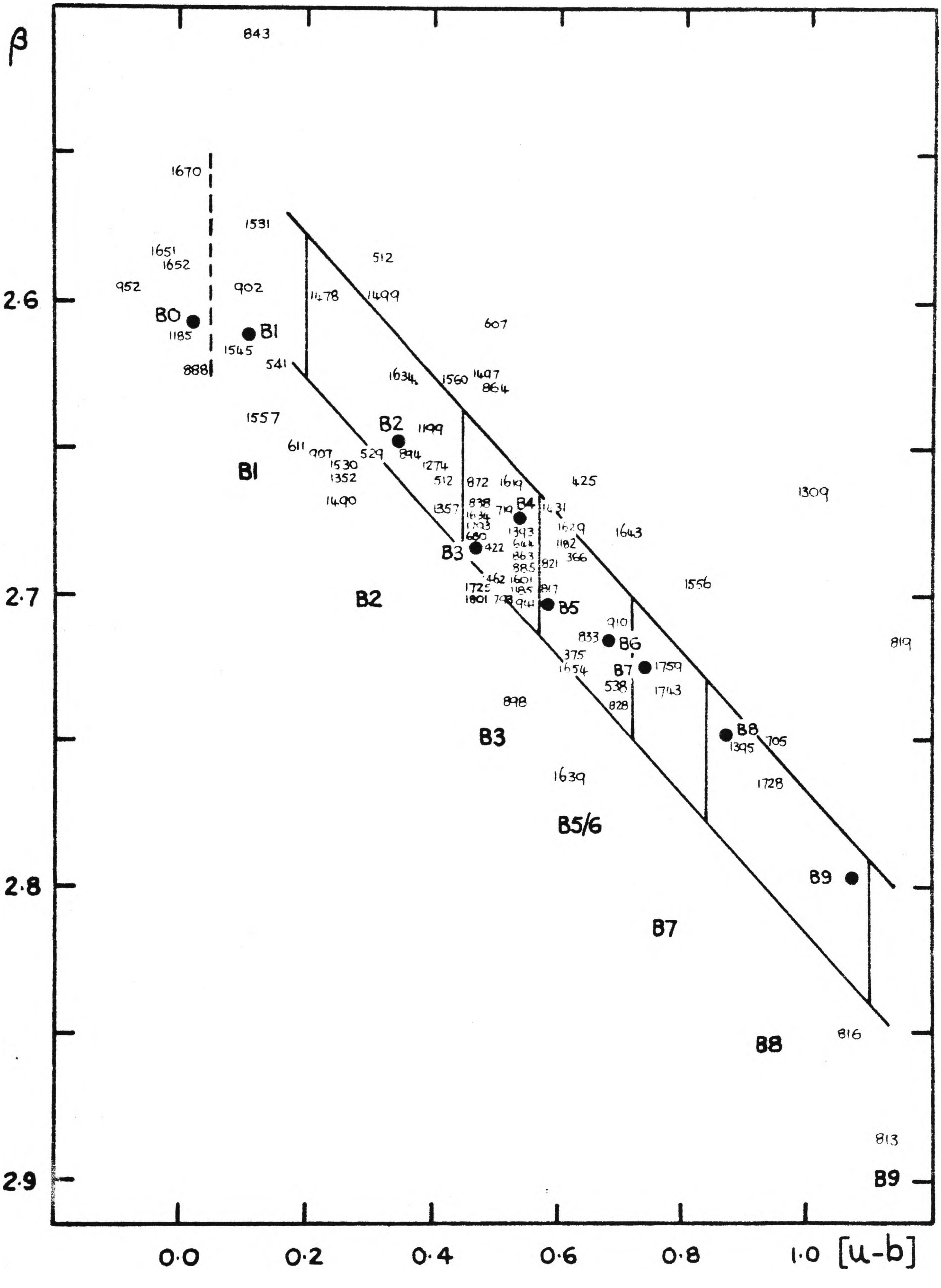

Fig. 4.13 [u-b] vs β for program stars.

The different reddening correction used in $[m_1]$ will cause the [u-b] values of the Stromgren main sequence to become slightly more positive (typically about 0.02 magnitudes). However, the original Stromgren values agree more closely with those of Crawford (1978) and have been adopted.

The boundary between B0 and B1 was chosen as [u-b]= 0.06 on the basis of the Crawford values, and the boundaries for classes B1 to B9 are after Stromgren (1966). No division is provided for B4 stars, since none appears in Stromgren's diagram. Classes 5 and 6 have been combined because of the lack of obvious separation on Stromgren's diagram.

Stars falling above or below the main sequence were classified by their [u-b] colours.

Table 4.1 lists the classification obtained for each star from the $[m_1]$ vs $[c_1]$ diagram, and from the [u-b] vs β diagram where β was measured.

4.14 Luminosity class

In the $[m_1]$ vs $[c_1]$ diagram, stars of luminosity classes Ia, Ib and II - and later than B5 - are expected to be well separated from the main sequence, while luminosity class III stars other than B9 to A5 show no clear separation (Stromgren 1966). Oblak et al (1976) show that, for classes B0 to B9, $[m_1]$ for luminosity class III stars is at most 0.01 magnitudes less than for luminosity class V stars; for luminosity class I and II stars, [m_1] ranges from 0.02 magnitudes (for B0) to 0.1 magnitudes (for B9) less than for main sequence stars.

In the [u-b] vs β diagram, Stromgren (1966) says that luminosity class III stars lie generally above the main sequence band, and that separation of luminosity classes is less satisfactory for B0 than for later B stars. Crawford (1978) says that "for the B-type stars, the Hβ line strength of a star is primarily a function of luminosity". However, for B0 to A0 stars, β for luminosity class III stars is typically only 0.02 magnitudes less than for luminosity class V (Oblak et al, 1976 and Crawford, 1978). For luminosity class I and II stars, β ranges from 0.05 magnitudes less than luminosity class V for B0 stars, to 0.25 magnitudes less for A0 stars.

Therefore, in the diagrams 4.12 and 4.13 for the program stars, we expect:

(a) No clear separation between luminosity class III and luminosity class V stars;

(b) Clear separation of luminosity class I and II stars from the main sequence only for stars later than about B5.

To test these expectations, luminosity classes of those program stars listed by Houk and Cowley (1975) and Jaschek et al (1964) are shown on an [m_1] vs [c_1] diagram (Figure 4.14a) and on a [u-b] vs β diagram (Figure 4.14b).

The only stars which are clearly separated from the main sequence in both diagrams, HD81921 and HD130903, are classified by Houk and Cowley (1975) as B9.5 II/III and B2(p) respectively.

The diagrams show no separation between luminosity classes III and V.

The giants HD156070 and HD153140, classified by Houk and Cowley as B2 II/III and B1 II are earlier than B5 and are not separated from the main sequence.

HD83866 is classified as B8 II by Houk and Cowley, as a B3 by the photometry which does not separate it from the main sequence.

Stars to the left of the Stromgren main sequence other than HD81921 and HD130903 are probably main sequence stars.

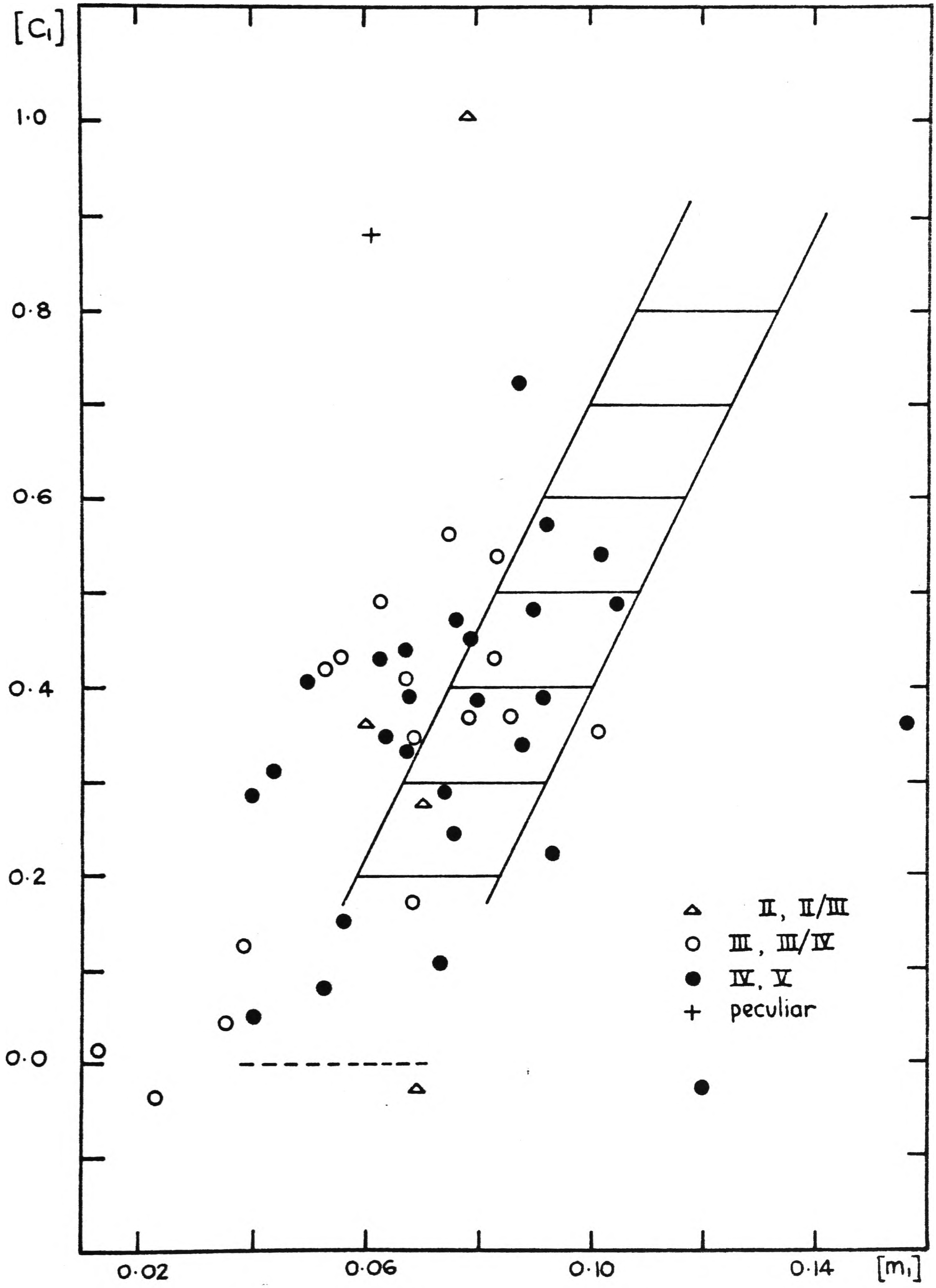

Fig. 4.14(a) [m_1] vs [c_1] for program stars with known luminosity class.

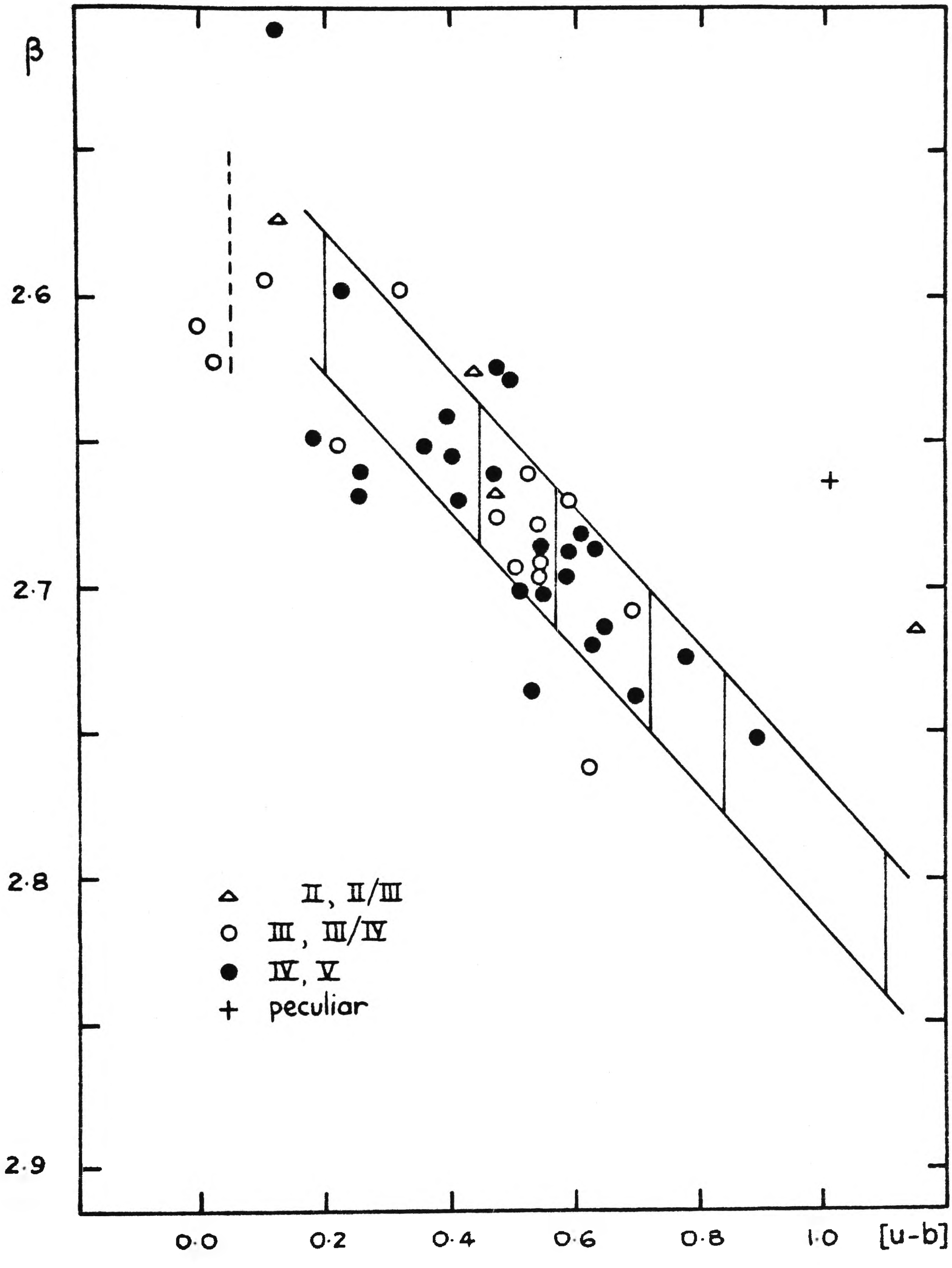

Fig. 4.14 (b) [u-b] vs β for program stars with known luminosity class.

TABLE 4.1

PHOTOMETRIC CLASSIFICATION OF PROGRAM STARS

HD	$[m_1]$	$[c_1]$	CLASS	$[u-b]$	β	CLASS
36629	0.164	0.283	B3	0.611	2.686	B5/6
37526	0.080	0.454	B5	0.615	2.719	B5/6
42204	0.085	0.324	B3	0.494	2.678	B3
42551	0.101	0.435	B5	0.638	2.659	B5/6
48165	0.093	0.385	B3	0.572	-	-
49188	0.095	0.370	B3	0.561	-	-
51255	0.079	0.259	B2	0.417	2.658	B2
51285	0.059	0.194	B1	0.312	2.585	B2
52942	0.091	0.114	B1	0.296	2.647	B2
53824	0.080	0.524	B6	0.685	2.733	B5/6
54197	0.055	0.047	B1	0.157	2.618	B1
58441	0.080	0.257	B2	0.417	-	-
60757	0.076	0.348	B3	0.500	2.606	B3
61193	0.052	0.087	B1	0.191	2.649	B1
63274	0.079	0.441	B5	0.599	-	-
64301	0.132	0.567	B6	0.831	-	-
64455	0.074	0.387	B3	0.535	2.678	B3
66134	0.115	0.634	B7	0.865	-	-
68030	0.104	0.300	B3	0.508	-	-
68046	0.083	0.296	B2	0.462	2.675	B3
68982	0.092	0.229	B2	0.413	-	-
69120	0.086	0.582	B6	0.754	-	-
70550	0.067	0.804	B9	0.938	2.753	B8

Table 4.1 continued

Photometric classifications

HD	$[m_1]$	$[c_1]$	CLASS	[u-b]	β	CLASS
71336	0.085	0.378	B3	0.547	-	-
71945	0.056	0.401	B5	0.514	2.670	B3
72771	0.073	0.196	B1	0.341	-	-
72973	0.105	0.680	B7	0.889	-	-
73215	0.064	0.120	B1	0.248	-	-
77904	0.101	0.544	B6	0.746	-	-
79368	0.087	0.327	B3	0.500	2.692	B3
81307	0.166	0.801	B9	1.132	2.886	B9
81694	0.139	0.792	B8	1.070	2.851	B8
81769	0.091	0.389	B3	0.571	2.695	B5/6
81921	0.079	1.004	B9	1.162	2.716	B9
82111	0.067	0.442	B5	0.577	2.686	B5/6
82811	0.105	0.490	B5	0.701	2.740	B5/6
83335	0.090	0.480	B5	0.660	2.716	B5/6
83866	0.060	0.360	B3	0.479	2.691	B3
84361	0.039	0.045	B1	0.123	2.507	B1
86385	0.062	0.431	B5	0.555	2.688	B3
86441	0.049	0.403	B5	0.501	2.626	B3
87295	0.064	0.342	B3	0.470	2.660	B3
88556	0.055	0.431	B5	0.541	2.687	B3
88844	0.012	0.001	B1	0.025	2.623	B0
89403	0.040	0.284	B2	0.364	2.650	B2
89876	0.068	0.392	B3	0.527	2.737	B3

Table 4.1 continued

Photometric Classifications

HD	$[m_1]$	$[c_1]$	CLASS	$[u-b]$	β	CLASS
90288	0.035	0.042	B1	0.112	2.595	B1
90786	0.038	0.128	B1	0.204	2.654	B2
91041	0.085	0.529	B6	0.699	2.707	B5/6
94108	0.076	0.393	B3	0.545	2.703	B3
95275	0.019	-0.124	B0	-0.086	2.596	B0
118256	0.076	0.474	B5	0.625	2.684	B5/6
118553	0.100	0.356	B3	0.555	2.690	B3
118571	0.021	-0.043	B0	-0.001	2.607	B0
119926	0.042	0.307	B3	0.390	2.641	B2
127449	0.077	0.245	B2	0.400	2.656	B2
130903	0.060	0.884	B9	1.004	2.639	B8
135241	0.072	0.103	B1	0.247	2.658	B2
135786	0.073	0.299	B2	0.445	2.669	B2
139300	0.078	0.386	B3	0.543	2.677	B3
139579	0.086	0.724	B8	0.896	2.748	B8
143156	0.083	0.426	B5	0.592	2.686	B5/6
146224	0.051	0.414	B5	0.516	2.694	B3
147889	0.119	-0.025	B0	0.212	2.597	B2
149065	0.055	0.145	B1	0.254	2.669	B2
149770	0.066	0.336	B3	0.467	2.626	B3
149922	0.066	0.173	B1	0.305	2.597	B2
153084	0.065	0.107	B1	0.237	2.657	B2
153140	0.068	-0.029	B0	0.108	2.573	B1

Table 4.1 continued

Photometric classifications

HD	$[m_1]$	$[c_1]$	CLASS	$[u-b]$	β	CLASS
154535	0.021	0.043	B1	0.084	2.611	B1
155600	0.084	0.656	B7	0.824	2.695	B7
155754	0.032	0.060	B1	0.124	2.639	B1
156070	0.070	0.282	B2	0.423	2.624	B2
160109	0.081	0.399	B3	0.561	2.695	B3
161972	0.066	0.405	B5	0.537	2.660	B3
162973	0.091	0.440	B5	0.622	2.676	B5/6
163430	0.083	0.188	B1	0.354	2.622	B2
163442	0.059	0.341	B3	0.458	2.673	B3
163927	0.061	0.492	B5	0.614	2.763	B5/6
164320	0.073	0.560	B6	0.706	2.679	B5/6
165132	0.029	-0.088	B0	-0.030	2.582	B0
165246	0.040	-0.093	B0	-0.013	2.586	B0
165477	0.079	0.466	B5	0.623	2.725	B5/6
167003	0.024	-0.047	B0	0.001	2.555	B0
170385	0.066	0.343	B3	0.476	2.673	B3
172535	0.074	0.343	B3	0.491	2.695	B3
172850	0.094	0.757	B8	0.945	2.764	B8
174395	0.076	0.622	B7	0.775	2.733	B7
175934	0.090	0.571	B6	0.751	2.724	B7
180124	0.041	0.377	B3	0.458	2.697	B3

4.2 Ultraviolet Classification

4.21 The Ultraviolet colours

Absolute fluxes for the program stars in the passbands centred at 2740 Å (A_1), 2365 Å (A_4), 1965 Å (A_3) and 1565 Å (A_2) given by Thompson et al (1978) were transformed to the visual magnitude scale using the absolute calibration of Hayes and Latham (1975):

$$m(\lambda) = -2.5 \log_{10} F(\lambda) - 21.175$$

Corrections were made for interstellar extinction using the absorption ratios $A(\lambda)/E_{B-V}$ of Thompson et al (1978) and taking $E(b-y) = 0.74E(B-V)$ (Crawford, 1975):

TABLE 4.21 ABSORPTION RATIOS

NAME	CENTRAL WAVELENGTH (ANGSTROMS)	$A(\lambda)/E_{B-V}$	$A(\lambda)/E_{b-y}$
A_2	1565	8.08	10.92
A_3	1965	8.23	11.12
A_4	2365	8.42	11.38
A_1	2740	6.10	8.24

Since $$m(\text{unreddened}) = m(\lambda) - \left[A(\lambda)/E_{b-y} \right] E_{b-y}$$

the unreddened ultraviolet colours will be -

$$(A_2 - A_4)_o = (A_2 - A_4) + 0.46E_{b-y}$$

$$(A_2 - A_1)_o = (A_2 - A_1) - 2.68E_{b-y}$$

Adopted E_{b-y} are given in Table 6.3(2) together with adopted spectral classifications. They are derived (see section 5.21) from the uvby photometry and intrinsic colours given by Crawford (1978). Since one purpose of the investigation was to discover UV anomalies, it was not assumed at this stage that the stars lay on the main sequence line defined by Carnochan and Wilson (1983).

4.22 The Ultraviolet colour-colour diagram

Figure 4.22 shows the (A_2-A_4) versus (A_2-A_1) diagram for the program stars, where the plotted colours are the unreddened ones. The dots give positions of main sequence stars from B0 to B8, and the diagonal line is the intrinsic line for main sequence stars (Carnochan and Wilson, 1983).

Class boundary lines were chosen perpendicular to the main sequence intrinsic line and agreeing with Carnochan and Wilson's colours.

As in the [u-b] versus β diagram, there is little separation between B3 and B4, and B5 and B6. In deriving classifications from this diagram, class B4 is again omitted and classes B5 and B6 combined.

Table 4.2 lists the unreddened colours for the program stars, and the classifications obtained from the colour-colour diagram.

The unreddened magnitudes for each of the passbands are listed in Table 5.23.

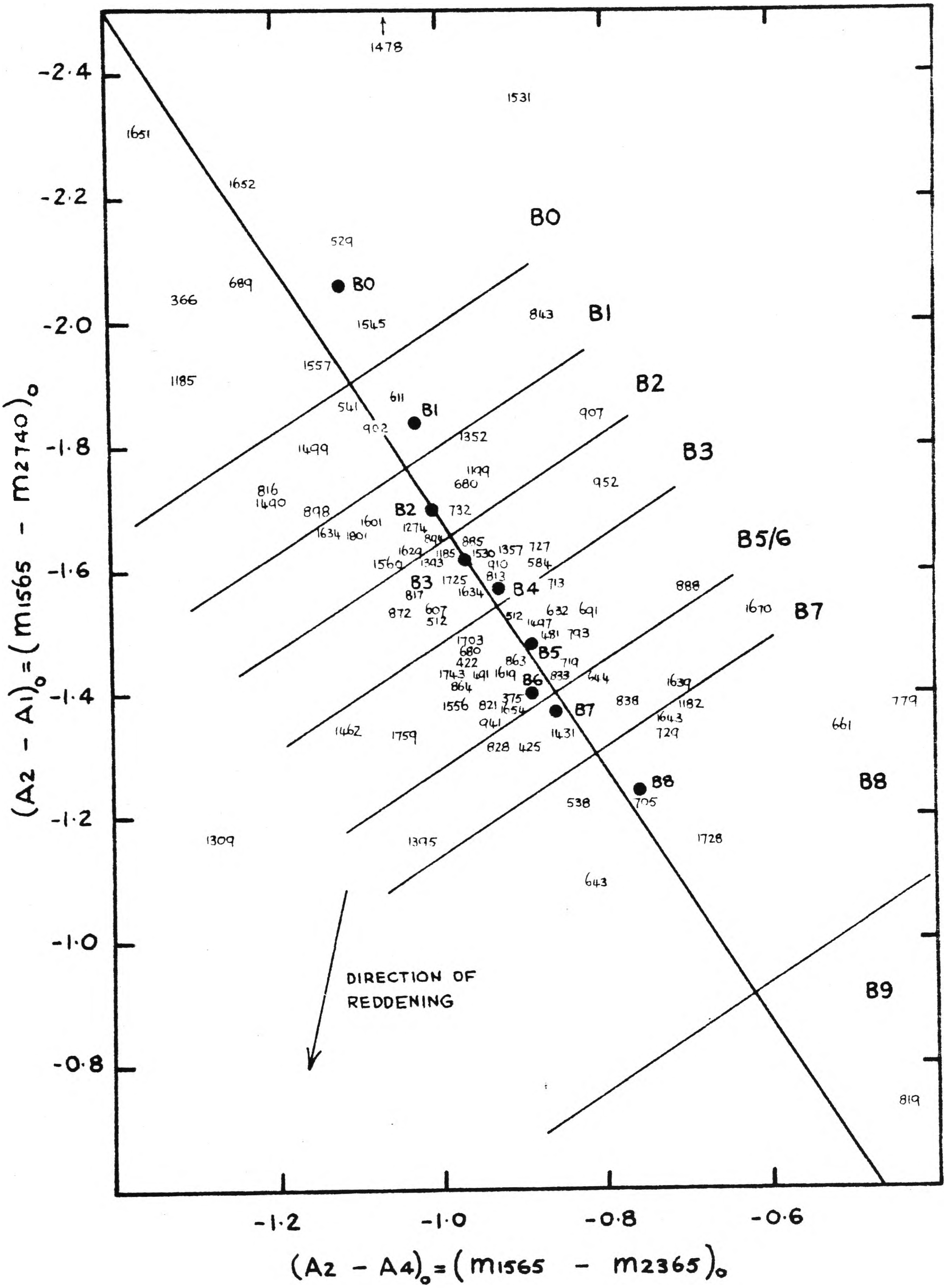

Fig. 4.22 $(A_2-A_4)_o$ vs $(A_2-A_1)_o$ for program stars.

TABLE 4.2

ULTRAVIOLET CLASSIFICATION OF PROGRAM STARS

HD	$(A_2-A_1)_o$	$(A_2-A_4)_o$	CLASS
36629	-2.04	-1.31	B0
37526	-1.39	-0.91	B5/6
42204	-1.45	-0.97	B5/6
42551	-1.31	-0.90	B7
48165	-1.50	-0.87	B5/6
49188	-1.43	-0.95	B5/6
51255	-1.52	-1.01	B3
51285	-1.54	-0.92	B5/6
52942	-2.13	-1.12	B0
53824	-1.22	-0.84	B8
54197	-1.87	-1.11	B1
58441	-1.61	-0.89	B3
60757	-1.53	-1.01	B3
61193	-1.88	-1.05	B1
63274	-1.53	-0.86	B5/6
64301	-1.09	-0.82	B8
64455	-1.43	-0.82	B7
66134	-1.34	-0.51	B8
68030	-1.74	-0.97	B2
68046	-1.45	-0.96	B5/6
68982	-2.07	-1.24	B0
69120	-1.53	-0.83	B5/6
70550	-1.22	-0.76	B8

Table 4.2 contd.

Ultraviolet classification

HD	$(A_2-A_1)_o$	$(A_2-A_4)_o$	CLASS
71336	-1.58	-0.86	B5/6
71945	-1.44	-0.85	B5/6
72771	-1.64	-0.88	B3
72973	-1.34	-0.73	B8
73215	-1.70	-0.98	B2
77904	-1.38	-0.44	B8
79368	-1.50	-0.85	B5/6
81307	-1.58	-0.93	B3
81694	-1.73	-1.21	B1
81769	-1.57	-1.03	B3
81921	-0.73	-0.44	B9
82111	-1.38	-0.93	B5/6
82811	-1.31	-0.93	B7
83335	-1.42	-0.86	B5/6
83866	-1.39	-0.78	B7
84361	-2.01	-0.88	B1
86385	-1.45	-0.91	B5/6
86441	-1.42	-0.98	B5/6
87295	-1.53	-1.05	B3
88556	-1.64	-0.97	B3
88844	-1.57	-0.70	B5/6
89403	-1.65	-0.99	B2
89876	-1.70	-1.15	B1

Table 4.2 contd.

Ultraviolet classification

HD	$(A_2-A_1)_o$	$(A_2-A_4)_o$	CLASS
90288	-1.83	-1.07	B1
90786	-1.87	-0.81	B2
91041	-1.61	-0.93	B3
94108	-1.35	-0.93	B5/6
95275	-1.74	-0.80	B3
118256	-1.38	-0.70	B8
118553	-1.64	-0.99	B3
118571	-1.91	-1.31	B0
119926	-1.75	-0.96	B2
127449	-1.67	-1.03	B2
130903	-1.17	-1.28	B5/6
135241	-1.82	-0.97	B2
135786	-1.63	-0.93	B3
139300	-1.64	-1.00	B3
139579	-1.16	-1.03	B7
143156	-1.33	-0.85	B7
146224	-1.34	-1.12	B5/6
147889	-3.59	-0.97	B0
149065	-1.72	-1.21	B1
149770	-1.50	-0.89	B5/6
149922	-1.80	-1.16	B1
153084	-1.63	-0.97	B3
153140	-2.36	-0.90	B0

Table 4.2 contd.

Ultraviolet classification

HD	$(A_2-A_1)_o$	$(A_2-A_4)_o$	CLASS
154535	-2.00	-1.09	B0
155600	-1.38	-0.98	B5/6
155754	-1.93	-1.15	B0
156070	-1.61	-1.07	B2
160109	-1.68	-1.09	B2
161972	-1.44	-0.93	B5/6
162973	-1.64	-1.01	B2
163430	-1.57	-0.96	B3
163442	-1.67	-1.14	B2
163927	-1.41	-0.70	B7
164320	-1.35	-0.74	B8
165132	-2.30	-1.36	B0
165246	-2.23	-1.24	B0
165477	-1.38	-0.92	B5/6
167003	-1.53	-0.62	B7
170385	-1.49	-0.97	B5/6
172535	-1.59	-0.99	B3
172850	-1.16	-0.68	B8
174395	-1.43	-0.97	B5/6
175934	-1.33	-1.05	B5/6
180124	-1.66	-1.11	B2

4.3 Comparison of Classifications

In Table 4.3(1), stars are grouped according to their [u-b] vs β classifications when known (column 2); otherwise by their Stromgren [m_1] versus [c_1] classification (column 3). Column 4 gives the classification from the ultraviolet (A_2-A_1) versus (A_2-A_4) diagram.

Columns 5 and 7 give spectrographic classifications from the Michigan Catalogue and Jaschek et al (1964).

Column 6 was obtained from a compilation by Mrs. Pam Kennedy of Mount Stromlo and Siding Spring Observatories of published spectrographic classifications of southern O and B type stars. For all of the stars common to this program the original source was Garrison et al (1977).

The HD spectral types (column 8) are as listed by Wilson (1978) except for HD's 155600, 174395, 139579, 172850 and 81921, for which Carnochan and Wilson (1976) reference the SAO Catalogue.

In discussing the consistency of the classifications, the HD types will be disregarded because of their evident inaccuracy; however it should be noted that the apparently excessive ultraviolet flux of most of the program stars disappears when they are correctly assigned to earlier classes than indicated by the HD classification.

Sixty two stars have classifications by various criteria which differ from each other by no more than one subclass, where the subclasses are taken as those in the classification diagrams, namely B0, B1, B2, B3, B5/6, B7, B8 and B9.

Three stars (165246, 135241 and 90288) differ by no more than one subclass in the photometric and ultraviolet classifications, but differ by up to two subclasses in the spectrographic classifications.
Twenty five stars have classifications which differ by two or more subclasses in the photometric and ultraviolet classifications. They are listed in Table 4.3(2).

Figure 4.3 illustrates the general consistency between classifications obtained from the visible and ultraviolet data.

Ultraviolet Class \ Photometric Class	B0	B1	B2	B3	B5/6	B7	B8	B9
B0	1185 1651 1652	1531 1545 1557	529 689 1478		366			
B1		541 611 843 902	1490 1499	898			816	
B2		732	894 907 1199 1274 1352 1560	680 1601 1634 1801	1629			
B3	952	727	512 584 1357 1530 1634	607 872 885 1185 1393 1725	375 910 817			813
B5/6	888		512	422 481 491 680 713 719 793 863 864 941 1462 1497 1619 1703	632 691 821 833 1654	1556 1743 1759	1309	
B7	1670			644 838	425 828 1431 1639 1639		1395	
B8					538 643 779 1182 1643	661 729	705 1728	
B9								819

Fig. 4.3 Comparison of visible and UV classifications.

TABLE 4.3(1)

COMPARISON OF CLASSIFICATIONS

HD	β	St	UV	Michigan	Stromlo	Jaschek	HD
95275	B0	B0	B3	08/9		09 V/B0 I	09.5II/III
165132	B0	B0	B0		09.5 V		B3
165246	B0	B0	B0		08 V N		B9
88844	B0	B1	B5/6	B0.5 III	B0.5 III		B8
118571	B0	B0	B0	B1 III			B0.5IV/V N
167003	B0	B0	B7		B1 II		B2
54197	B1	B1	B1				B8
72771	-	B1	B3				B4 V
61193	B1	B1	B1	B2 V n			B3
73215	-	B1	B2				B5
84361	B1	B1	B1	B2/3 V			B8
90288	B1	B1	B1	B2 IV		B3 V	B3 V
153140	B1	B0	B0	B1 II	B1 II		B3
154535	B1	B1	B0		B1 IV N		B5
155754	B1	B1	B0		B1 IV		B3 V
51255	B2	B2	B3				B3
51285	B2	B1	B5/6				B3
52942	B2	B1	B0				B5
58441	-	B2	B3				A0
68982	-	B2	B0			B3 V	B3 V
89403	B2	B2	B2	B2/3 IV			B2 V
90786	B2	B1	B2	B2 III			B8
119926	B2	B3	B2	B2/3 V			B5
127449	B2	B2	B2	B2/3 V n			B3

Table 4.3(1) contd.

HD	β	St	UV	Michigan	Stromlo	Jaschek	HD
135241	B2	B1	B2	B3V			B8
135786	B2	B2	B3	B2/3 IV			B5
147889	B2	B0	B0			B1.5V/B2V	B2.5 V
149065	B2	B1	B1	B2 V			B2 IV
149922	B2	B1	B1	B2 III	B2 IV/V		B5
153084	B2	B1	B3		B1.5 V		B3
156070	B2	B2	B2	B2 II/III			B2 III
163430	B2	B1	B3		B2 IV/V		B5
42204	B3	B3	B5/6				B5
48165	-	B3	B5/6				A0
49188	-	B3	B5/6				B6 IV
60757	B3	B3	B3				A0
64455	B3	B3	B7				B8 III
68030	-	B3	B2				B5
68046	B3	B2	B5/6				B5
71336	-	B3	B5/6	B3 III/IV			B3 V
71945	B3	B5	B5/6				B8
79368	B3	B3	B5/6	B4 V			B9
83866	B3	B3	B7				B8
86385	B3	B5	B5/6	B5 IV			A0
86441	B3	B5	B5/6	B3/4 V			B6 V
87295	B3	B3	B3	B3/4 IV			B3
88556	B3	B5	B3	B5/6 III			B3
89876	B3	B3	B1	B5 IV			A0

Table 4.3(1) contd.

HD	β	St	UV	Michigan	Stromlo	Jaschek	HD
94108	B3	B3	B5/6	B4 V			B8
118553	B3	B3	B3	B3 III			B8
139300	B3	B3	B3	B3 III			B8
146224	B3	B5	B5/6	B3 III	B5 III		B3
149770	B3	B3	B5/6	B5/4 V n			B5
160109	B3	B3	B2		B3 V		B8
161972	B3	B5	B5/6	B3/5III/V			B5
163442	B3	B3	B2				B8
170385	B3	B3	B5/6	B5 III/V			B3 V
172535	B3	B3	B3		B2 V		B8
180124	B3	B3	B2				B8
36629	B5/6	B3	B0			B2 V	B2 V
37526	B5/6	B5	B5/6			B3 V/B5 V	B3.5 V
42551	B5/6	B5	B7				B8
53824	B5/6	B6	B8				B9
63274	-	B5	B5/6				B8
64301	-	B6	B8				B9
69120	-	B6	B5/6				B8
77904	-	B6	B8				B7 V
81769	B5/6	B3	B3	B4 V			B8
82111	B5/6	B5	B5/6	B5 IV/V			B6 V
82811	B5/6	B5	B7	B7 V			B9
83335	B5/6	B5	B5/6	B6 V			B8
91041	B5/6	B6	B3	B8 III			A0

Table 4.3(1) contd.

HD	β	St	UV	Michigan	Stromlo	Jaschek	HD
118256	B5/6	B5	B8	B5 IV			AO
143156	B5/6	B5	B7	B3/5 III			B5
162973	B5/6	B5	B2				B8
163927	B5/6	B5	B7	B5 III			B8
164320	B5/6	B6	B8		B7 III		B8
165477	B5/6	B5	B5/6				AO
66134	-	B7	B8				A
72973	-	B7	B8				AO
155600	B7	B7	B5/6				B8
174395	B7	B7	B5/6				B9
175934	B7	B6	B5/6	B7/8 IV			AO
70550	B8	B9	B8				AO
81694	B8	B8	B1				AO
130903	B8	B9	B5/6	B(2)p			B9
139579	B8	B8	B7	B8 V			B8
172850	B8	B8	B8				B9
81307	B9	B9	B3				AO
81921	B9	B9	B9				B9

TABLE 4.3(2)

STARS WITH CLASSIFICATIONS INCONSISTENT BY TWO OR MORE SUBCLASSES

HD	β	St	UV	Michigan	Stromlo	Jaschek	HD
95275	B0	B0	B3	08/9		09V/B0I	09.5II/III
88844	B0	B1	B5/6	B0.5III	B0.5III		B8
167003	B0	B0	B7		B1 II		B2
72771		B1	B3				B4V
51285	B2	B1	B5/6				B3
52942	B2	B1	B0				B5
68982		B2	B0			B3V	B3V
147889	B2	B0	B0			B1.5V/B2V	B2.5V
153084	B2	B1	B3		B1.5V		B3
163430	B2	B1	B3		B2IV/V		B5
64455	B3	B3	B7				B8III
68046	B3	B2	B5/6				B5
83866	B3	B3	B7				B8
89876	B3	B3	B1	B5IV			A0
36629	B5/6	B3	B0			B2V	B2V
53824	B5/6	B6	B8				B9
64301		B6	B8				B9
77904		B6	B8				B7V
91041	B5/6	B6	B3	B8III			A0
118256	B5/6	B5	B8	B5IV			A0
162973	B5/6	B5	B2				B8
164320	B5/6	B6	B8		B7III		B8
81694	B8	B8	B1				A0
130903	B8	B9	B5/6	B(2)p			B9
81307	B9	B9	B3				A0

5. SPECTRAL ENERGY DISTRIBUTIONS

5.1 Introduction

Monochromatic flux magnitudes of the program stars at 3500 Å, 4100 Å, 4700 Å and 5500 Å were derived from the photometric data. They were combined with the ultraviolet flux magnitudes of Thompson et al (1978) to plot spectral energy distributions, which could be compared with those of model stellar atmospheres.

5.2 Derivation of flux magnitudes from photometric data

5.21 Correction for interstellar reddening

The standard uvby indices for the program stars were unreddened, using -

(a) the reddening ratios of Crawford (1975):

$$(c_1)_o = c_1 - 0.20\ E(b-y)$$
$$(m_1)_o = m_1 + 0.32\ E(b-y)\ .$$

(b) the intrinsic colours $(b-y)_o$ for each MK class by Crawford (1978). The class adopted for each star was obtained from the [u-b] vs β diagram, or the $[m_1]$ vs $[c_1]$ diagram where β had not been observed. The colour excess for each star is

$$E(b-y) = (b-y)_{observed} - (b-y)_o$$

(c) the absorption A_V in magnitudes, given (e.g. Johnson, 1964) as

$$A_V = V_{observed} - V_{o(intrinsic)}$$
$$= 3\ E(B-V)$$

Since $E(b-y) = 0.74\ E(B-V)$ (Crawford 1975),

$$A_y = \frac{3}{0.74}\ E(b-y)$$

whence $y_o = y - 4.05\ E(b-y)$.

5.22 Transformation from standard indices to "absolute indices"

Using the absolute calibration of α Lyr by Hayes and Latham (1975), "absolute indices" were calculated and compared with the standard system indices for α Lyr by Crawford and Barnes (1970).

Table 5.22(a) gives magnitudes $m(1/\lambda)$ interpolated from the tabulation of Hayes and Latham (1975), and the corresponding values of $m(\lambda)$. Magnitudes $m(\lambda)$ were used for consistency with the ultraviolet data, and were obtained in the following way:

Hayes and Latham (1975) define

$$m(1/\lambda) = -2.5\ \log_{10}F(\nu) + k_1 \qquad \ldots(1)$$

where $F(\nu)$ is the flux per unit frequency, and k_1 is a constant.

From Thompson et al (1978) we obtain

$$m(\lambda) = -2.5\ \log_{10}F(\lambda) + k_2 \qquad \ldots(2)$$

where $F(\lambda)$ is the flux per unit wavelength, and k_2 is a constant; also,

$$F(\nu) = F(\lambda) \times \frac{\lambda^2}{c} \qquad \ldots(3)$$

Combining the three equations gives

$$m(\lambda) = m(1/\lambda) + 5\ \log_{10}\lambda + k \qquad \ldots(4)$$

where $k = k_2 - k_1 - 2.5\ \log_{10}c$.

Normalizing both magnitudes to zero at 5556 Å, the wavelength used by Hayes and Latham (1975), gives -

$$m(\lambda) = m(1/\lambda) + 5 \log_{10}\lambda - 18.724 \qquad ...(5)$$

TABLE 5.22(a)

MONOCHROMATIC MAGNITUDES OF αLYR

WAVELENGTH (Å)		$m(1/\lambda)$	$m(\lambda)$
3500	(u)	+1.097	+0.093
4100	(v)	-0.289	-0.949
4700	(b)	-0.171	-0.031
5500	(y)	-0.009	-0.031

Indices (b-y), m_1 and c_1 calculated from the magnitudes $m(\lambda)$ of Table 5.22(a) are shown in Table 5.22(b) together with those of the standard system for αLyr (Crawford and Barnes, 1970). The standard y magnitude is assumed equal to V, given as 0.03 by Wilson (1978).

TABLE 5.22(b)

COMPARISON OF "ABSOLUTE" AND "STANDARD" INDICES FOR αLYR

Index	"Absolute" after Hayes and Latham	"Standard" after Crawford & Barnes
y	-0.031	0.030
b-y	-0.504	0.004
m_1	0.090	0.157
c_1	1.456	1.089

Applying the zero-point corrections implied by Table 5.22(b) and correcting for reddening, the observed photometric indices were converted to "absolute indices" according to the equations:

$$y(abs) = y(obs) - 4.05\ E(b-y) - 0.061$$
$$m_1(abs) = m_1(obs) + 0,32\ E(b-y) - 0.067$$
$$c_1(abs) = c_1(obs) - 0.20\ E(b-y) + 0.367$$
$$(b-y)(abs) = (b-y)_o - 0.508$$

where $(b-y)_o$ is the Crawford (1978) intrinsic colour.

The monochromatic flux magnitudes are obtained from the "absolute" indices using Stromgren's (1966) index definitions:

$$y(abs) = y\ (obs) - 4.05\ E(b-y) - 0.061$$
$$b(abs) = (b-y)(abs) + y(abs)$$
$$v(abs) = m_1(abs) + y(abs) + 2(b-y)(abs)$$
$$u(abs) = c_1(abs) + 2m_1(abs) + y(abs) + 3(b-y)(abs)$$

Table 5.23 lists the ultraviolet (see section 4.21) and visible flux magnitudes $m(\lambda)$.

TABLE 5.23

UNREDDENED MONOCHROMATIC FLUX MAGNITUDES m(λ)

HD	1550	1965	2350	2740	3500	4100	4700	5500 Å
36629	2.87	3.55	4.18	4.91	6.06	5.88	6.34	6.91
37526	5.01	5.44	5.92	6.40	6.64	6.37	6.92	7.49
42204	5.53	6.05	6.51	6.98	7.30	7.17	7.72	8.31
42551	5.32	5.76	6.22	6.63	6.76	6.49	7.01	7.59
48165	4.92	5.37	5.79	6.42	6.90	6.70	7.24	7.83
49188	4.71	5.19	5.66	6.15	6.55	6.36	6.90	7.49
51255	5.05	5.55	6.07	6.57	6.96	6.91	7.47	8.07
51285	4.97	5.54	5.89	6.51	6.87	6.91	7.49	8.10
52942	2.89	3.63	4.01	5.01	5.77	5.86	6.41	7.01
53824	5.77	5.96	6.61	6.98	7.17	6.83	7.83	7.95
54197	3.57	4.25	4.68	5.43	5.95	6.15	6.75	7.37
58441	4.60	5.09	5.49	6.21	6.71	6.66	7.22	7.83
60757	4.84	5.43	5.86	6.38	6.70	6.56	7.11	7.70
61193	3.78	4.55	4.82	5.65	6.20	6.37	6.97	7.59
63274	4.99	5.46	5.86	6.52	6.98	6.73	7.27	7.85
64301	5.81	6.24	6.63	6.90	7.18	6.74	7.23	7.80
64455	5.00	5.49	5.82	6.42	6.63	6.45	7.01	7.60
66134	5.42	5.54	5.93	6.76	7.20	6.71	7.21	7.77
68030	4.45	4.98	5.41	6.19	6.64	6.51	7.04	7.63
68046	5.15	5.64	6.12	6.60	6.95	6.85	7.40	7.99
68982	2.74	3.49	3.98	4.80	5.44	5.41	5.95	6.56
69120	5.63	6.00	6.46	7.16	7.69	7.28	7.81	8.38
70550	6.58	6.93	7.34	7.80	7.87	7.25	7.79	8.34

Table 5.23 contd.

Monochromatic flux magnitudes

HD	1550	1965	2350	2740	3500	4100	4700	5500 Å
71336	4.77	5.20	5.63	6.34	6.77	6.59	7.13	7.72
71945	4.99	5.50	5.84	6.43	6.68	6.50	7.08	7.67
72771	3.84	4.34	4.72	5.47	6.14	6.18	6.76	7.38
72973	5.93	6.52	6.66	7.27	7.57	7.04	7.55	8.11
73215	4.07	4.60	5.05	5.76	6.41	6.53	7.12	7.74
77904	5.44	5.74	5.89	6.82	7.22	6.83	7.35	7.91
79368	5.32	5.74	6.17	6.82	7.15	7.01	7.56	8.15
81307	4.32	4.84	5.25	5.91	6.03	5.31	5.74	6.28
81694	4.42	5.05	5.63	6.16	6.37	5.69	6.15	6.70
81769	4.58	5.06	5.60	6.15	6.54	6.33	6.86	7.44
81921	5.65	5.72	6.08	6.37	6.33	5.48	6.00	6.55
82111	4.85	5.28	5.78	6.23	6.66	6.42	6.98	7.55
82811	5.78	6.10	6.71	7.09	7.36	7.03	7.55	8.12
83335	5.20	5.48	6.07	6.63	6.95	6.65	7.18	7.76
83866	4.65	4.96	5.42	6.03	6.31	6.17	6.75	7.34
84361	3.57	4.17	4.45	5.57	6.02	6.25	6.86	7.48
86385	-	5.31	5.89	5.60	6.78	6.56	7.12	7.69
86441	4.69	5.22	5.67	6.09	6.30	6.13	6.71	7.30
87295	4.30	4.58	5.35	5.82	6.22	6.09	6.66	7.25
88556	4.71	5.09	5.69	6.36	6.59	6.38	6.96	7.55
88844	4.45	4.74	5.15	6.02	6.54	6.84	7.48	8.10
89403	3.96	4.57	4.95	5.60	5.99	5.96	6.56	7.16
89876	4.36	5.08	5.51	6.06	6.35	6.17	6.73	7.32

Table 5.23 contd.

Monochromatic flux magnitudes

HD	1550	1965	2350	2740	3500	4100	4700	5500 Å
90288	4.01	4.50	5.08	5.84	6.33	6.56	7.18	7.80
90786	4.56	5.31	-	6.42	6.95	7.07	7.67	8.28
91041	5.22	5.47	6.16	6.83	7.04	6.70	7.24	7.81
94108	4.95	5.36	5.88	6.30	6.65	6.46	7.02	7.61
95275	3.77	4.20	4.57	5.51	6.14	6.56	7.20	7.83
118256	5.38	5.87	6.08	6.76	6.88	6.60	7.15	7.73
118553	5.11	5.59	6.11	6.75	7.04	6.86	7.40	7.99
118571	3.88	4.87	5.19	5.79	6.35	6.68	7.31	7.94
119926	3.68	4.18	4.64	5.43	5.76	5.70	6.30	6.90
127449	3.89	4.73	4.92	5.55	5.99	5.96	6.52	7.13
130903	5.86	5.98	7.15	7.03	7.34	6.65	7.19	7.74
135241	3.95	4.58	4.92	5.76	6.21	6.32	6.89	7.49
135786	4.44	4.99	5.36	6.06	6.41	6.33	6.90	7.50
139300	4.34	4.90	5.33	5.98	6.19	6.01	6.56	7.15
139579	6.22	6.73	7.26	7.38	7.57	7.00	7.52	8.08
143156	5.47	5.81	6.32	6.80	7.10	6.86	7.40	7.98
146224	4.15	4.65	5.27	5.49	6.03	5.84	6.42	7.01
147889	-0.92	-0.31	0.06	2.66	3.48	3.68	4.20	4.81
149065	4.29	4.58	5.50	6.01	6.49	6.58	7.17	7.77
149770	4.84	5.37	5.73	6.33	6.78	6.66	7.22	7.81
149922	3.90	4.44	5.06	5.69	6.17	6.22	6.79	7.40
153084	4.31	4.81	5.29	5.94	6.47	6.59	7.16	7.76
153140	1.27	2.02	2.18	3.61	4.13	4.39	4.98	5.60

Table 5.23 contd.

Monochromatic Flux Magnitudes

HD	1550	1965	2350	2740	3500	4100	4700	5500 Å
154535	3.14	3.74	4.22	5.14	5.79	6.03	6.66	7.29
155600	4.98	5.25	5.96	6.36	6.49	6.01	6.53	7.10
155754	3.25	3.95	4.40	5.18	5.74	5.96	6.58	7.20
156070	3.73	4.31	4.80	5.35	5.82	5.76	6.33	6.94
160109	3.79	4.44	4.89	5.47	5.88	5.68	6.23	6.82
161972	5.33	5.68	6.26	6.77	7.14	6.94	7.51	8.10
162973	5.39	5.91	6.40	7.02	7.21	6.95	7.48	8.06
163430	4.46	5.10	5.41	6.03	6.51	6.53	7.09	7.69
163442	3.69	4.33	4.83	5.36	5.75	5.63	6.20	6.79
163927	5.56	5.90	6.26	6.97	7.19	6.91	7.47	8.05
164320	4.82	5.16	5.56	6.16	6.33	5.97	6.52	7.09
165132	2.41	3.22	3.77	4.69	5.39	5.76	6.39	7.02
165246	1.86	2.61	3.11	4.08	5.02	5.38	6.00	6.63
165477	5.70	6.18	6.62	7.07	7.32	7.05	7.59	8.17
167003	4.28	4.75	4.90	5.80	6.41	6.74	7.37	7.99
170385	4.86	5.33	5.83	6.35	6.73	6.60	7.16	7.75
172535	4.54	5.05	5.53	6.13	6.49	6.35	6.91	7.50
172850	5.75	6.11	6.43	6.91	7.01	6.41	6.92	7.48
174395	5.38	5.96	6.35	6.80	6.98	6.53	7.07	7.63
175934	5.76	6.05	6.81	7.09	7.33	6.93	7.45	8.01
180124	3.39	4.04	4.50	5.05	5.46	5.32	5.91	6.50

5.3 Uncertainties in Flux Magnitudes

5.31 Possible errors in observed fluxes

Possible errors in the photometric data (indicated by night to night scatter of standards) are of the order of 0.01 magnitudes.

Possible errors between 0.1 and 0.5 magnitudes are given by Thompson et al (1978) for the ultraviolet data for 29 stars; the data for the remaining 61 stars are accurate to better than 0.1 magnitudes.

5.32 Possible errors due to unreddening

From the reddening relationships in sections 4.21 and 5.21, the ratios of the colour excesses may be found and are given in Table 5.3:

TABLE 5.3

RATIOS OF COLOUR EXCESSES

NAME	CENTRAL WAVELENGTH λ (Å)	$\frac{E(\lambda-y)}{E(b-y)}$
y	5460	0.00
b	4680	1.00
v	4110	1.68
u	3490	2.56
A_1	2740	4.19
A_4	2365	7.33
A_3	1965	7.07
A_2	1565	6.87

Most of the program stars have $E(b-y) \leq 0.1$, with an error due mainly to uncertainty in the intrinsic values for (b-y), which Crawford (1978) obtained by averaging over values with a range of ±0.06 magnitudes for classes B0 to B6, and ±0.1 for B7 to B9.

An error in E(b-y) results in a systematically increasing error towards shorter wavelengths. A 0.1 magnitude error in E(b-y) results in a deviation of up to 0.7 magnitudes at the shortest ultraviolet wavelengths observed.

Figures 5.3(1) to 5.3(11) plot the monochromatic magnitudes. The stars in Table 4.3(2) (classifications inconsistent by two or more subclasses) are indicated by asterisks (*) for classes B0, B1, B8 and B9, and are plotted in separate figures for classes B2, B3, and B5/6.

Observational uncertainties in the ultraviolet fluxes (before unreddening) are shown by error bars for individual points when these are significantly larger than the plotted point - i.e., larger than 0.15 magnitudes.

The possible systematic error due to faulty unreddening for the stars in each figure are shown by the error bars at the bottom of each figure.

The stellar model atmosphere fluxes fitted to the plotted points are shown in Figure 5.3(12). The 100K, 75K and 50K models are by Hummer and Mihalas (1970); the 37K and 29K models by Bradley and Morton (1968) and the 10-20K models by Klinglesmith (1971).

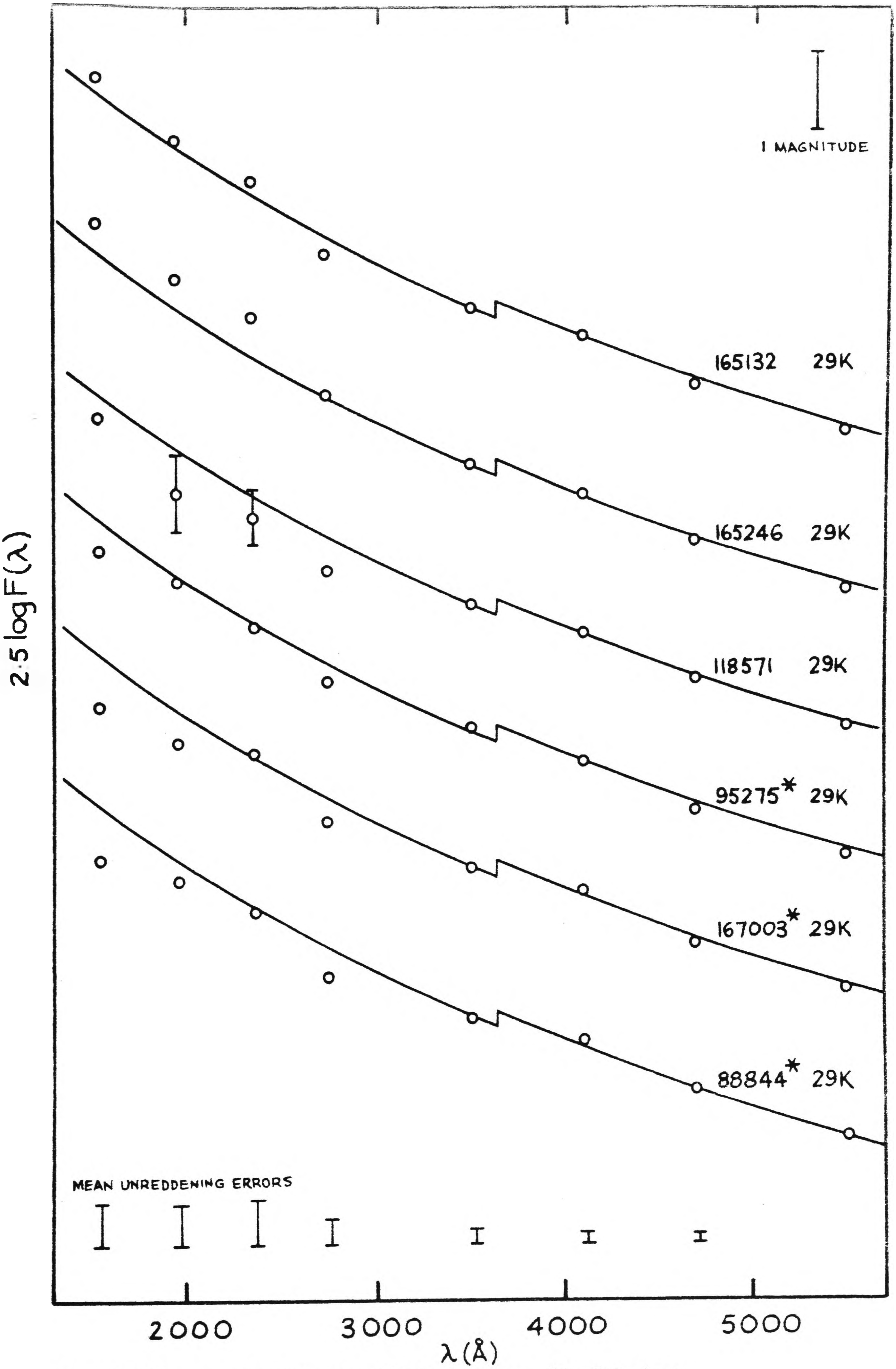

Fig. 5.3(1) Spectral Energy Distribution: All B0 stars.

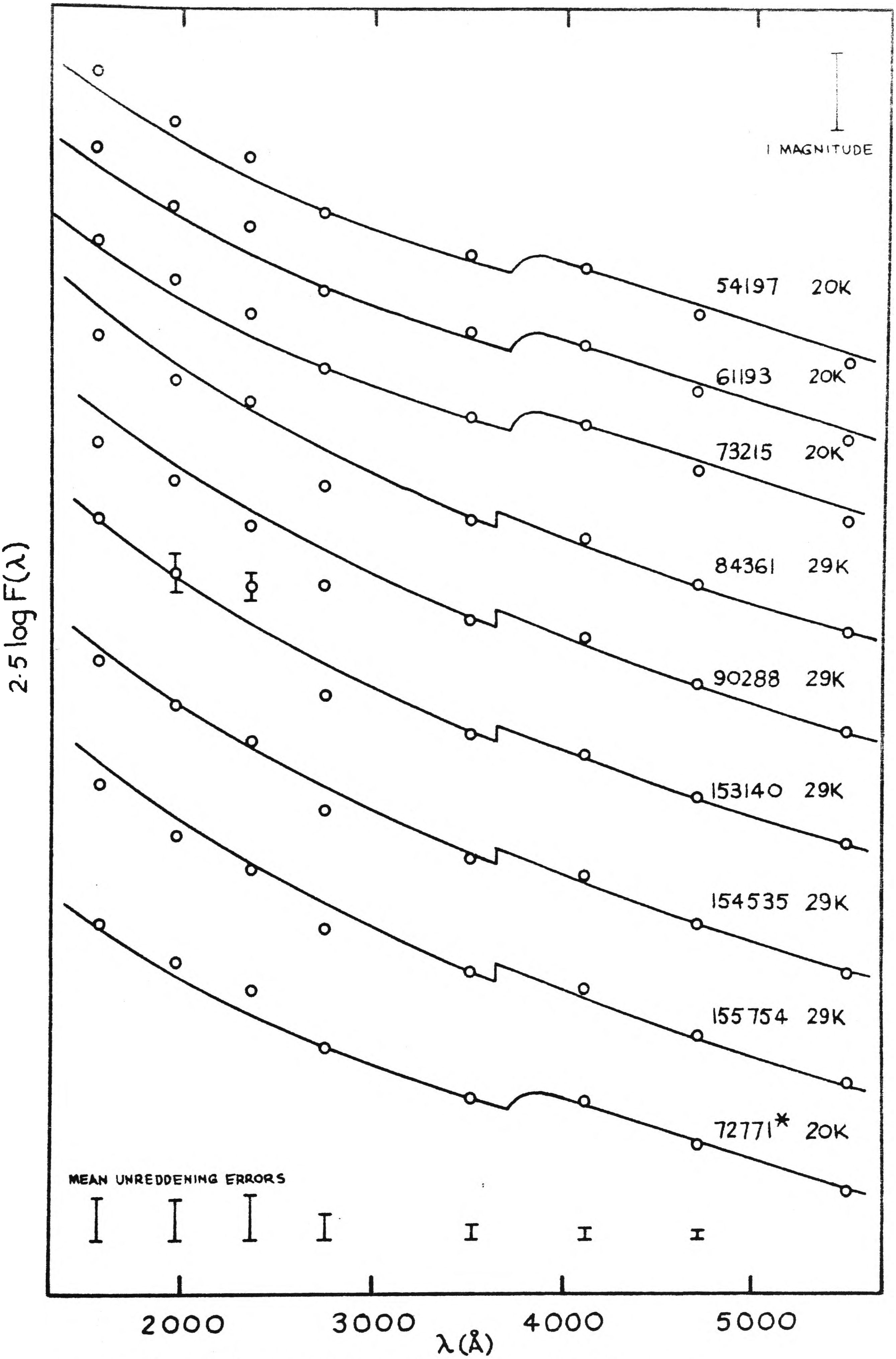

Fig 5.3(2) Spectral Energy Distribution: All B1 stars.

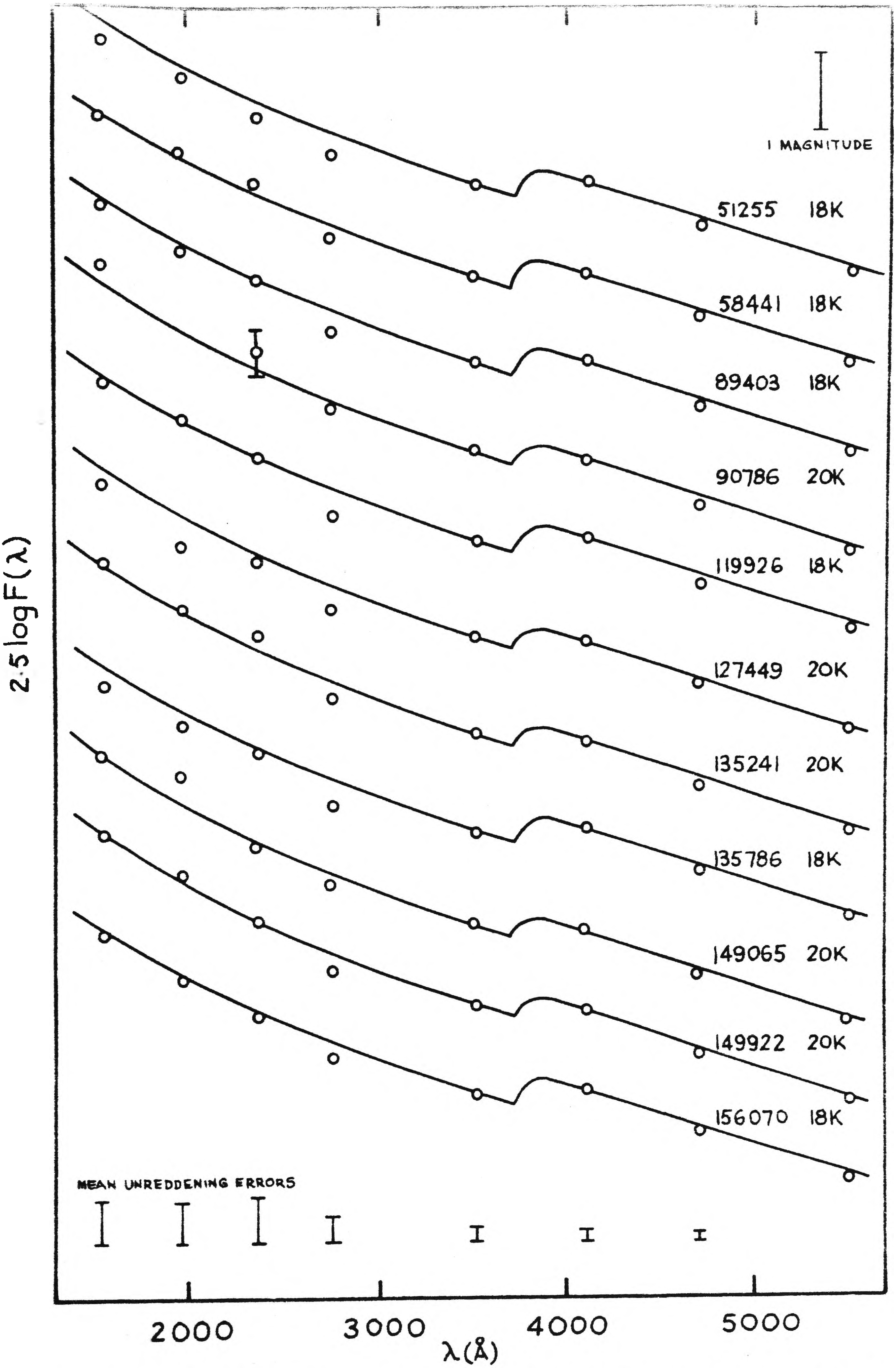

Fig. 5.3(3) Spectral Energy Distribution: B2 - classification consistent.

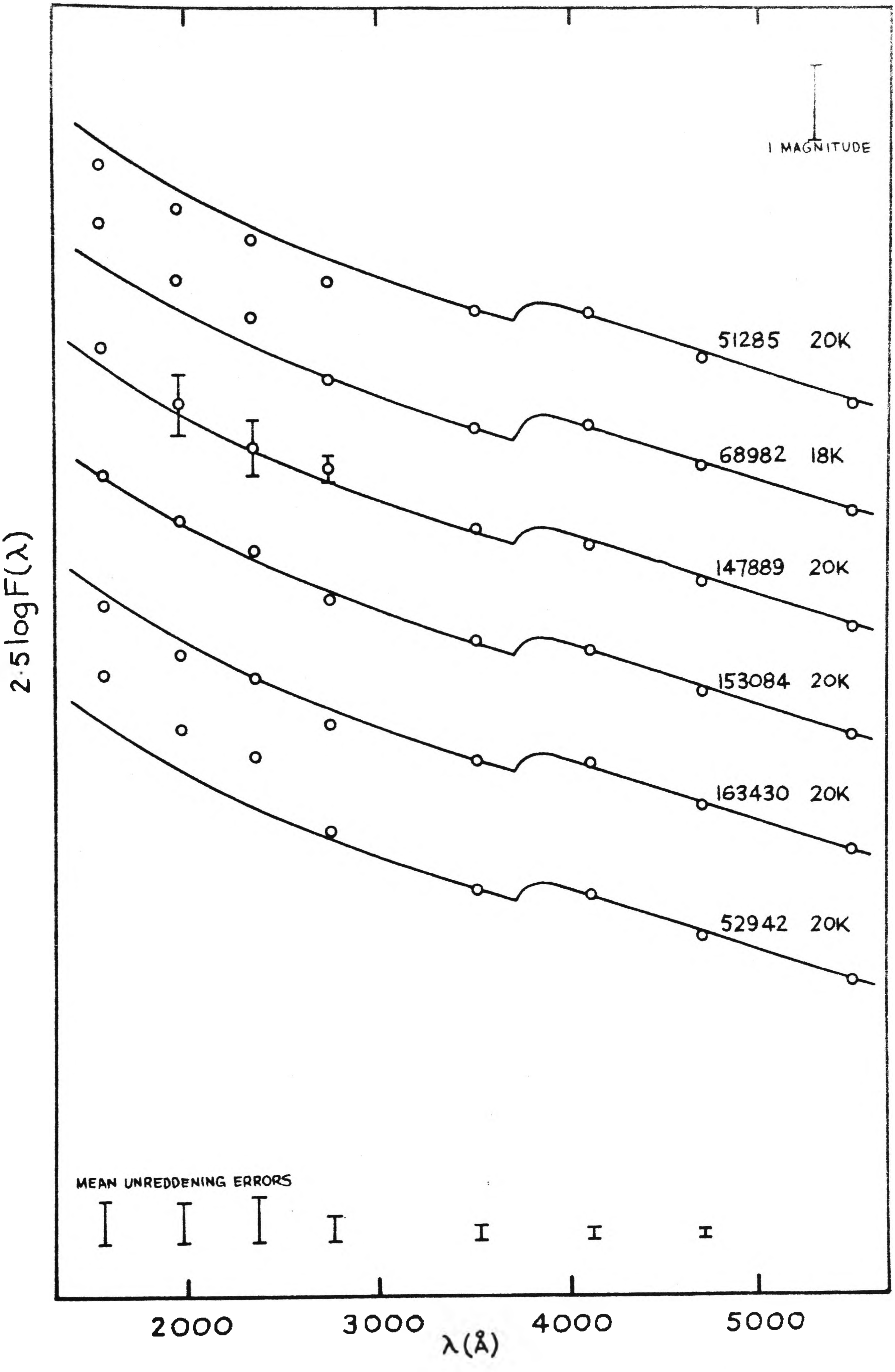

Fig. 5.3(4) Spectral Energy Distribution: B2 - classification not consistent.

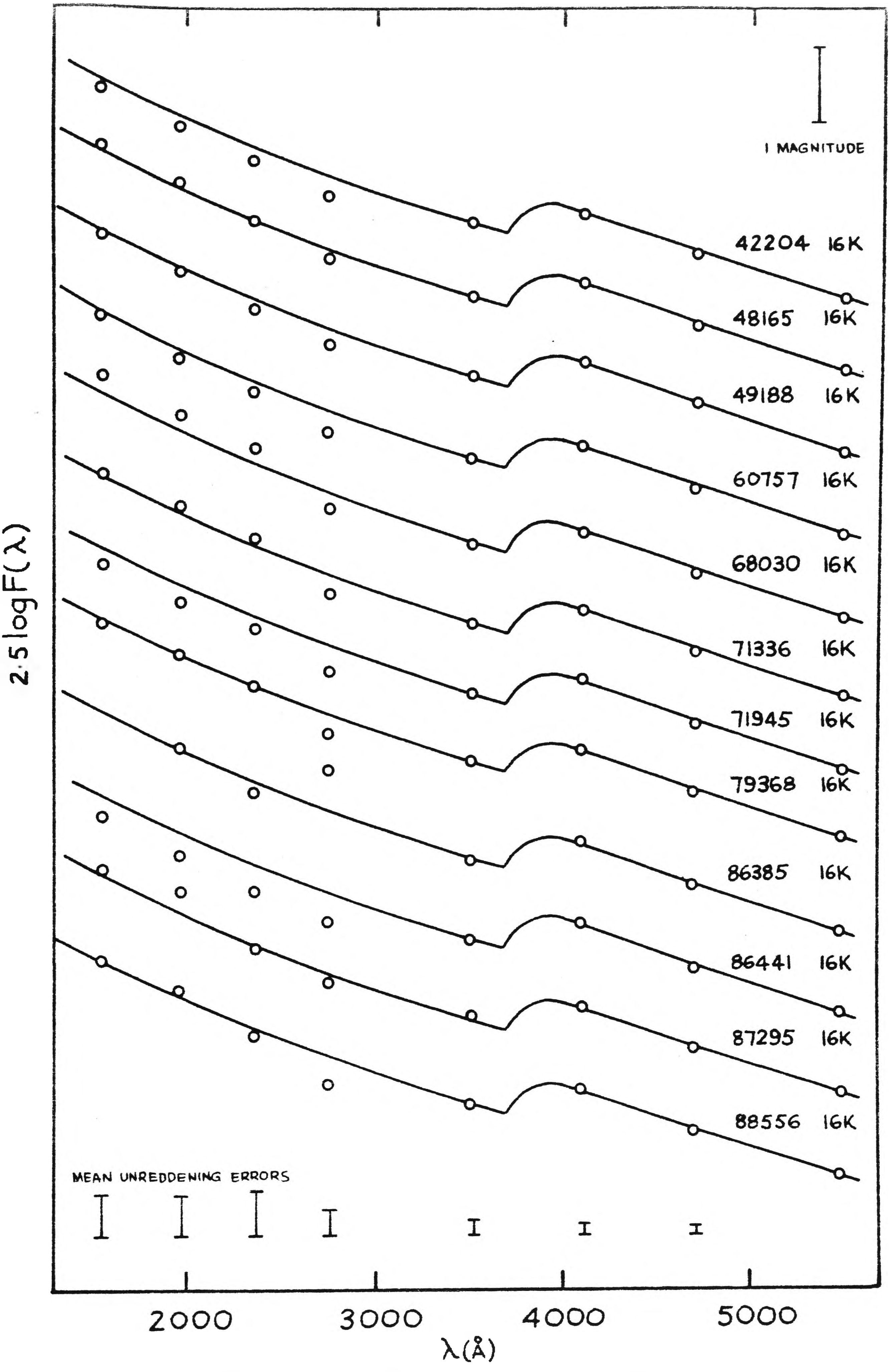

Fig 5.3(5) Spectral Energy Distribution B3 - classification consistent.

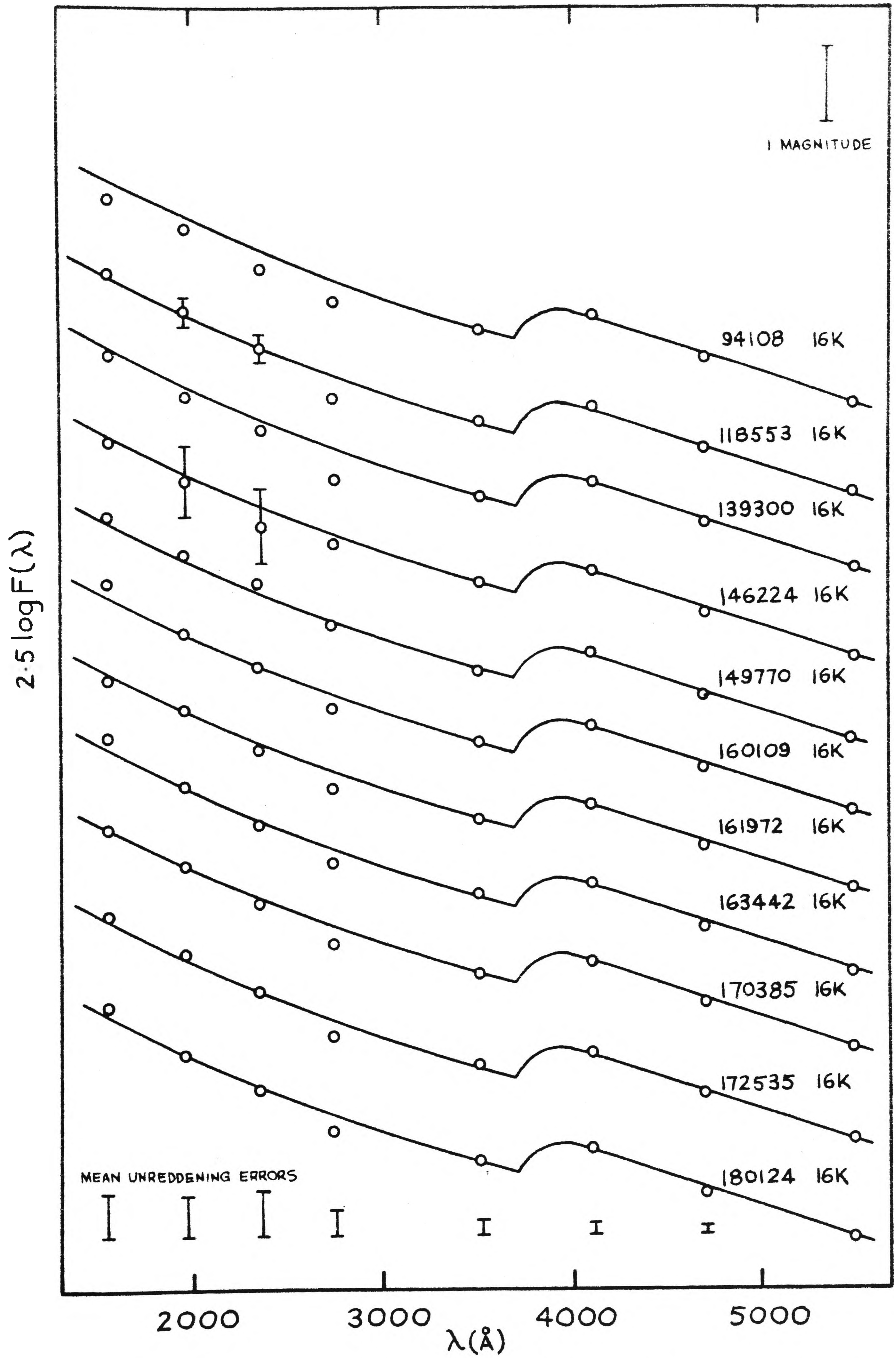

Fig. 5.3(6) Spectral Energy Distribution: B3 - classification consistent.

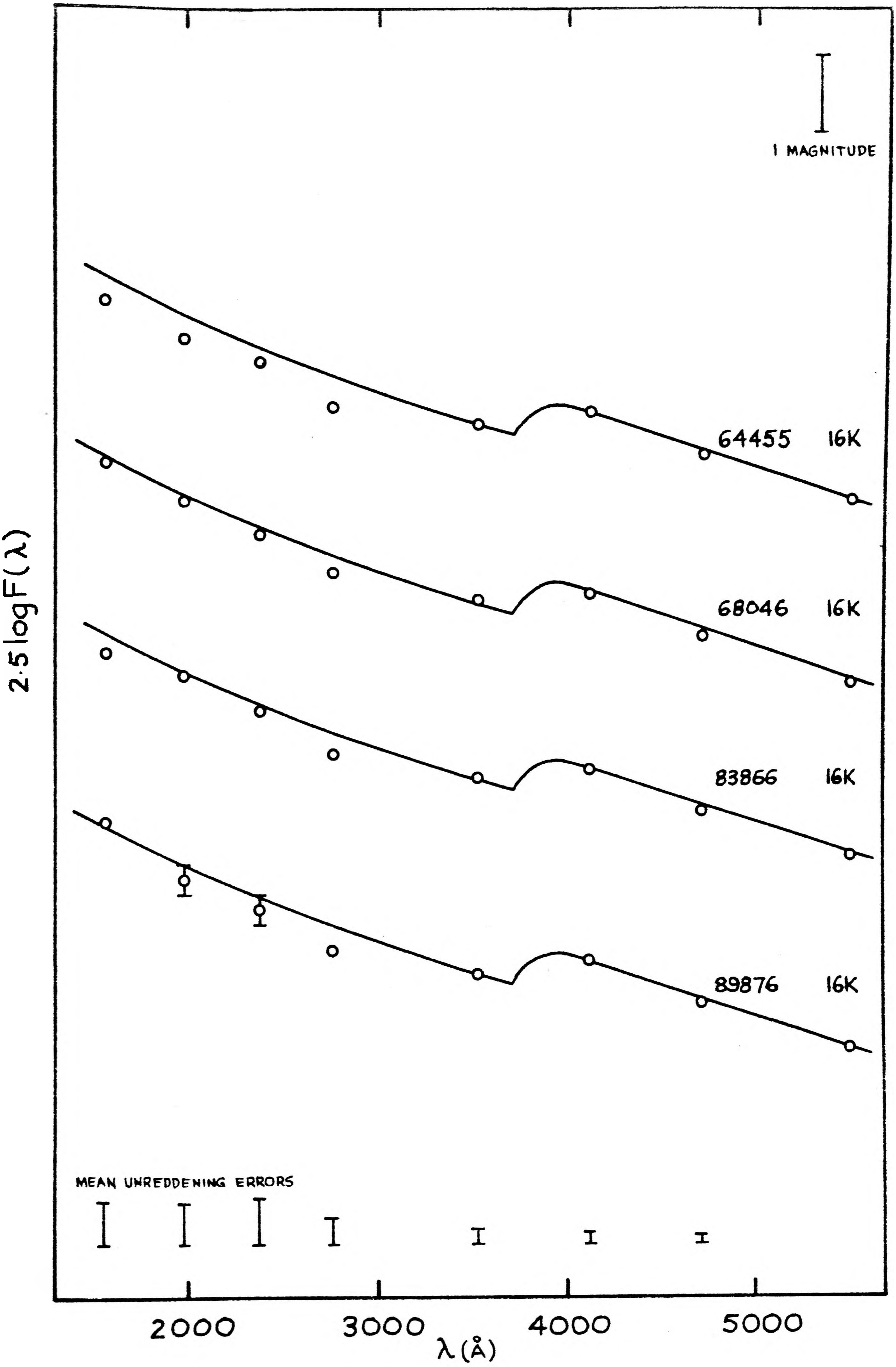

Fig 5.3(7) Spectral Energy Distribution: B3 - classification not consistent.

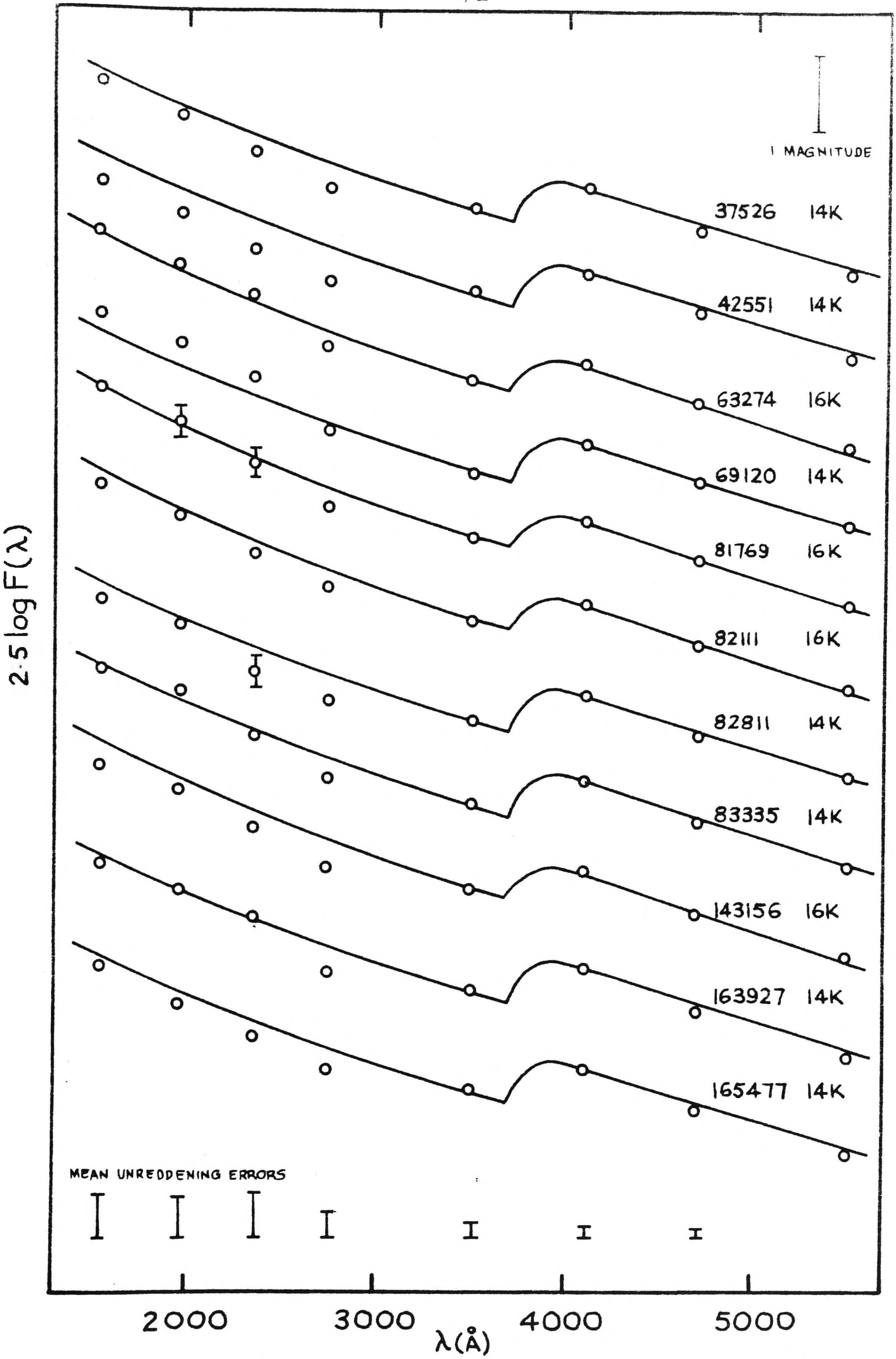

Fig 5.3(8) Spectral Energy Distribution : B5/6 - classification consistent.

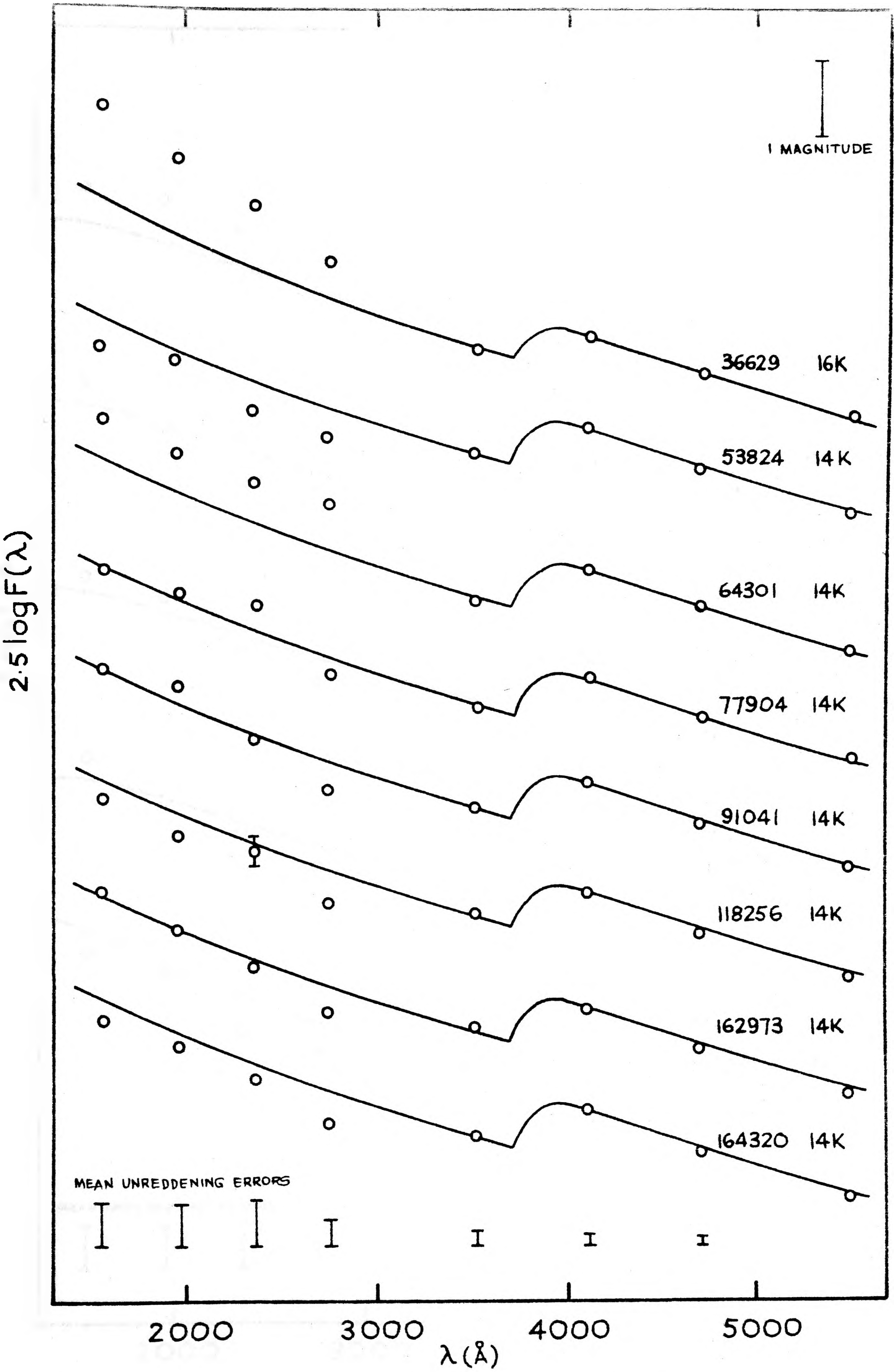

Fig 5.3(9) Spectral Energy Distribution : B5/6 - classification not consistent

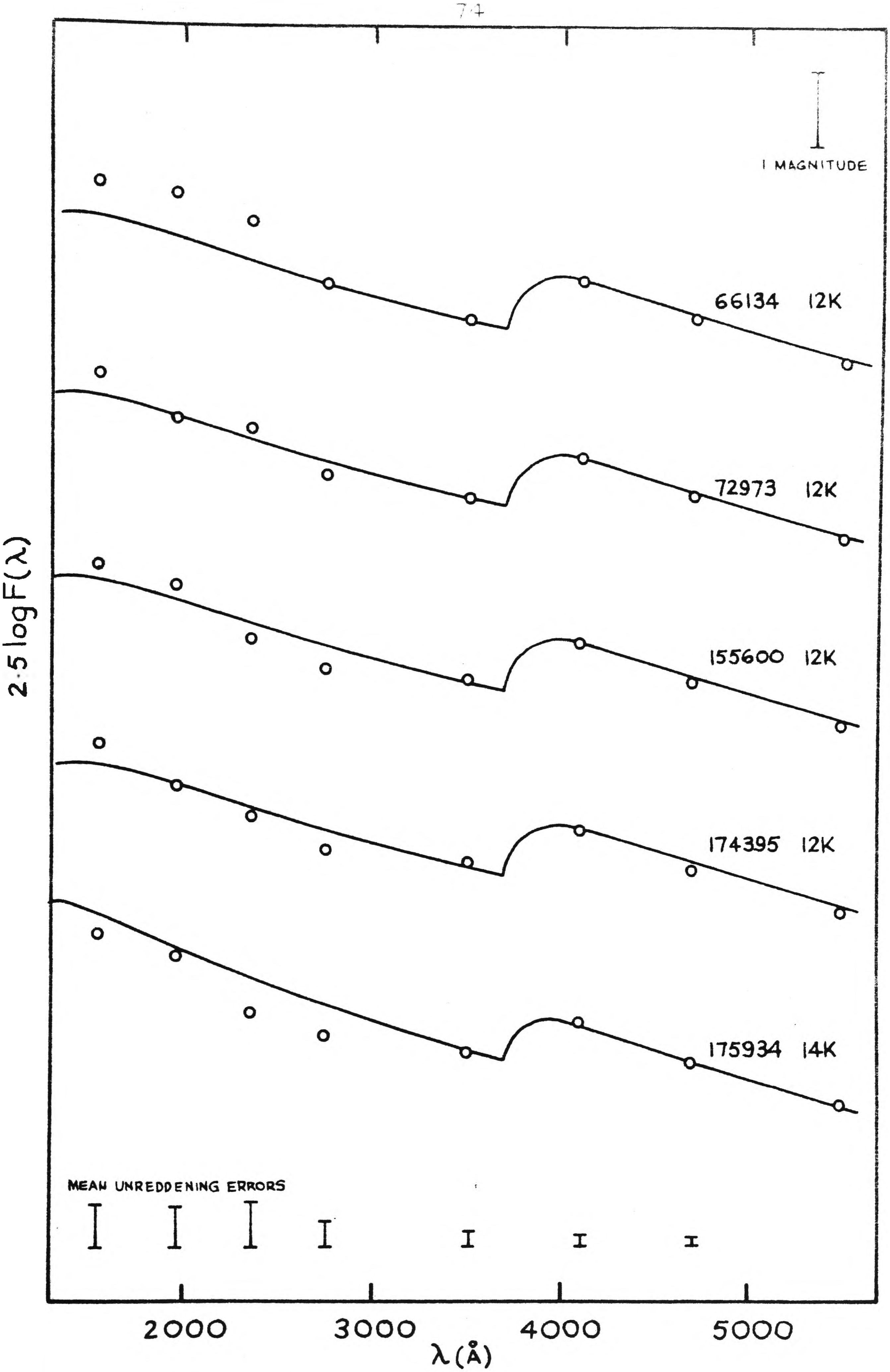

Fig. 5.3(10) Spectral Energy Distribution: B7 - classification consistent.

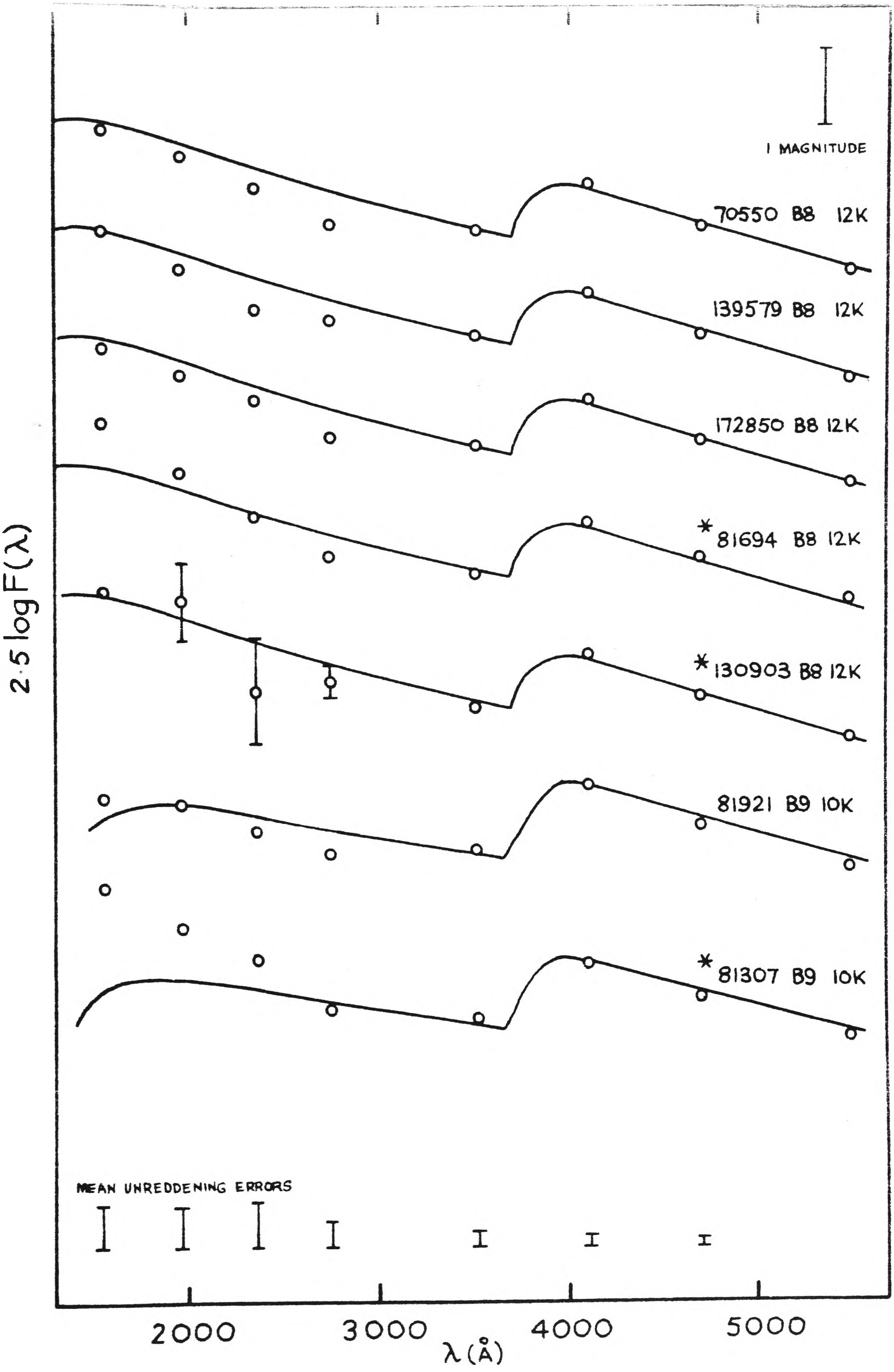

Fig 5.3 (II) Spectral Energy Distribution : All B8 and B9 stars

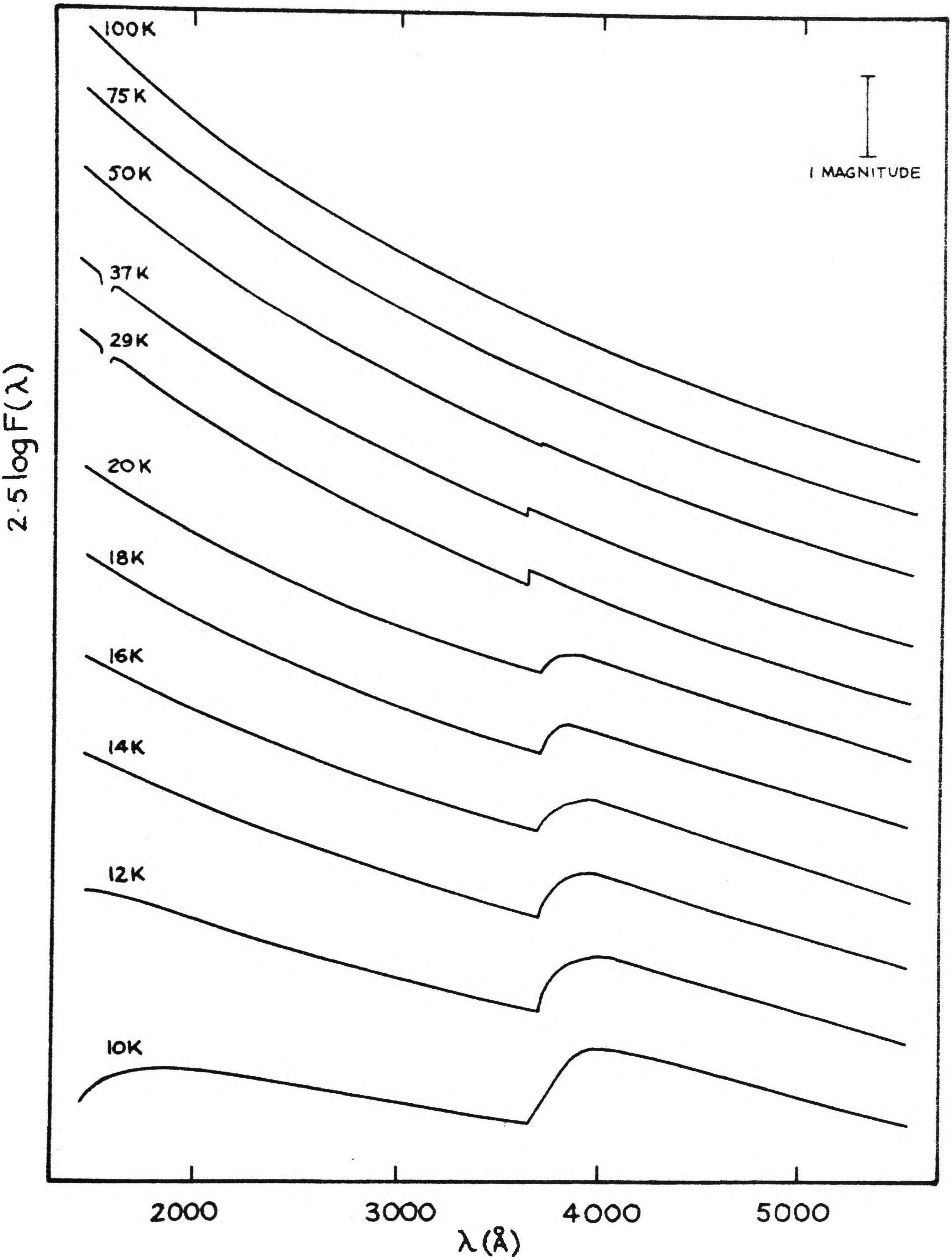

Fig. 5.3 (12) Spectral Energy Distribution - Model Atmospheres.

6. DISCUSSION OF RESULTS

6.1 The Search for Anomalies

Two diagrams have been presented that test the flux distribution of the stars in this program for anomalies. The first (Figure 4.3) compares the classification derived from the visible photometry with that derived from the ultraviolet photometry. The classifications of most stars from the two domains agree or disagree by only one subclass. The number disagreeing by two subclasses does not appear inconsistent with the distribution expected from random errors.

There are six stars that differ substantially. They fall into two distinct groups. HD36629, HD81307 and HD81694 have earlier UV types than visual types and are discussed in section 6.2. HD88844, HD95275 and HD167003 have later UV types than visual types; they are discussed in section 6.3.

Figure 4.22 presents the UV colour-colour diagram from which the UV classifications were made. The stars in this diagram were unreddened according to the colour excess determined from visible photometry. Thus, no assumption was made about the normalcy of UV colours, and any irregularity between the three UV fluxes will affect these colours.

Most of the stars fall around the MS line defined by CW, as expected. However, nine stars fall above and four fall below. Of these, HD90786, HD146224, HD147889 and HD153140 suffer from severe uncertainties in the UV data and are discounted. Four early B stars remain: HD84361, HD88844, HD95275 and HD167003 (the last three are in common with stars singled out by Figure 4.3); they are discussed in section 6.3. One other star is added to the list of peculiar early B stars: HD51285, for reasons explained in that section.

The late B stars HD66134, HD77904, HD130903, HD139579 and HD175934 are discussed in section 6.4 .

The normality of the majority of stars observed casts some doubt on the suggestion by Carnochan and Wilson (1975, 1983) that the catalogue contains a high proportion of stars falling significantly below the main sequence. This is discussed in section 6.5 .

6.2 HD36629, HD81307 and HD81694

These show UV fluxes rising much more steeply than would be expected from the visible spectrum. For HD81694 however these fall above expected values for A_2 and A_3 only.

The discrepancies could be due to binaries comprising a bright main sequence star and a faint hot companion.

Temperatures and relative radii of the possible hot companions can be obtained by the following procedure:

1. The observed spectral energy distribution of each pair of stars is plotted as open circles in Figure 6.21, in the form

$$m(\lambda) = +2.5 \log_{10} F(\lambda) + k \quad (k = \text{constant})$$

2. A model atmosphere flux distribution from Klinglesmith (1971) was chosen to give best agreement to the observed visible flux distribution. The temperature of the visible star was taken to be that of the model. The observed ultraviolet magnitudes were assumed to lie above the model because of a contribution from a hot companion.

3. The ultraviolet magnitudes required of the hot companion were found from the difference between the observed ultraviolet magnitudes and the ultraviolet magnitudes of the visible star predicted by the model atmosphere. If the UV-bright and visible stars have fluxes and magnitudes F_1, F_2 and m_1, m_2 respectively, then:

$$m_1 = 2.5 \log F_1 + k \quad \text{and} \quad m_2 = 2.5 \log F_2 + k \,.$$

Let the observed magnitude of the pair, which combines the fluxes of both stars, be

$$m = 2.5 \log (F_1 + F_2) + k$$

Then the magnitude of the UV-bright star is

$$m_1 = m_2 + 2.5 \log \left[10^{(m-m_2)/2.5} - 1 \right]$$

Figure 6.21 shows m_1 plotted as filled circles.

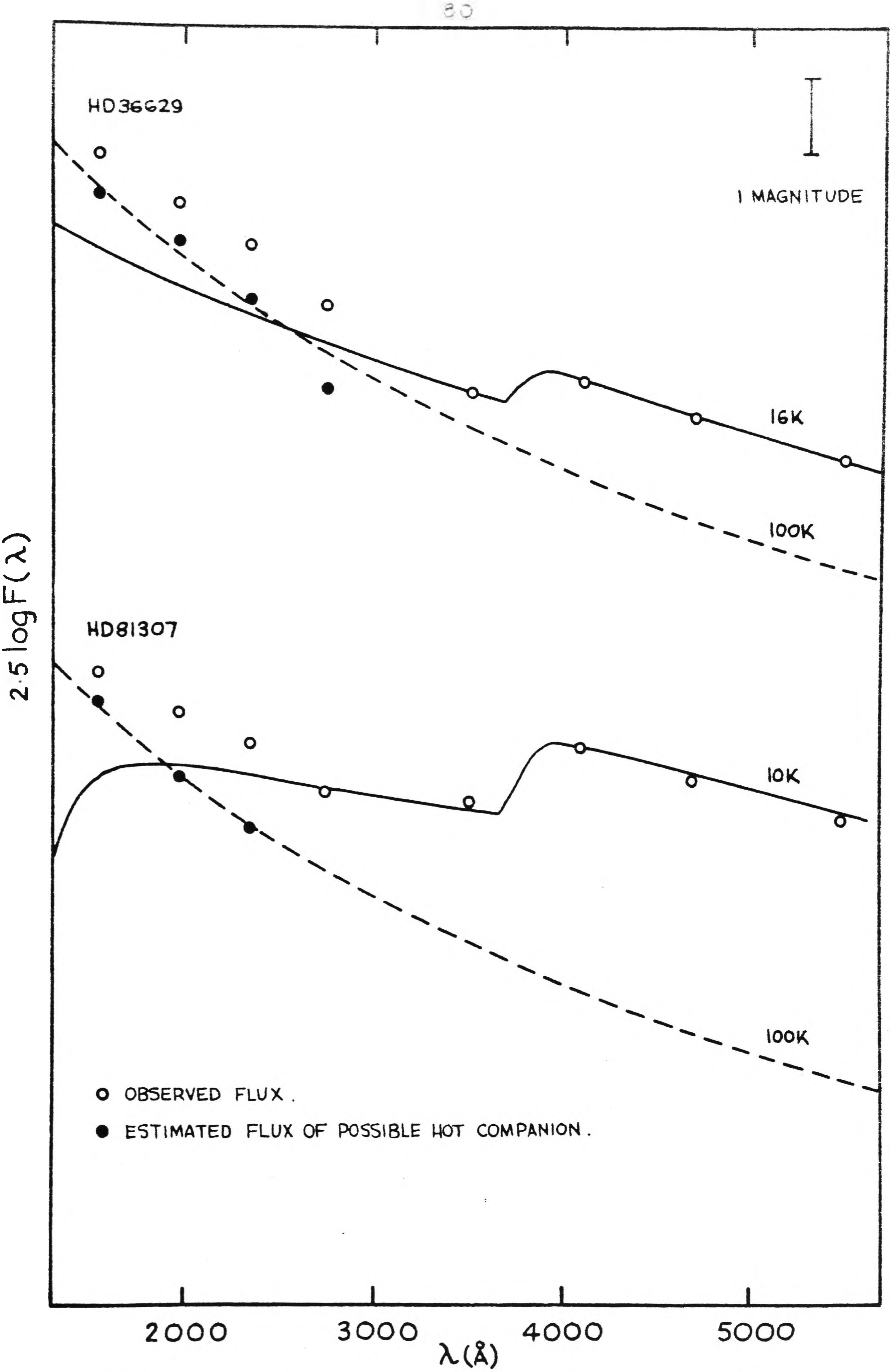

Fig. 6.21 Flux of possible hot companions for HD36629 and HD81307.

4. The black body flux distribution that best fitted the calculated ultraviolet flux distribution is shown, the choice of curve indicating the temperature. (Gebbie and Seaton 1963, and Bohm and Deinzer 1965, suggest that to a reasonable approximation, the central stars of planetary nebulae radiate as black bodies.)

5. The ratio of the radius of the UV-bright star to that of the visible star (R_1/R_2) was calculated using the flux per unit area of each star at a given wavelength (f_1 and f_2) according to the respective models. Since $F_1 \propto f_1 R_1^2$ and $F_2 \propto f_2 R_2^2$, with the same proportionality constant, then

$$m_1 - m_2 = 2.5 \log f_1 R_1^2 - 2.5 \log f_2 R_2^2$$

whence

$$R_1/R_2 = \sqrt{f_2/f_1 \times 10^{(m_1 - m_2)/2.5}}$$

The value of $m_1 - m_2$ is found from Figure 6.21.

6. Luminosities were calculated from the star temperatures and radii using the equations (Allen 1962):

$$m_{bol} = 4.72 - 2.5 \log(\mathcal{L}/\mathcal{L}_\odot)$$

and

$$m_{bol} = 42.35 - 10 \log T_e - 5 \log (R/R_\odot)$$

whence

$$\log (\mathcal{L}/\mathcal{L}_\odot) = 0.4(10\log T_e + 5\log(R/R_\odot) - 37.63)$$

Table 6.2 shows that both HD36629 and HD81307 appear to have companions with T_{eff} of $100,000^{o}$. The estimates of radii of the visible components are based on the measurements by Code et al (1976).

(The same procedure applied to HD81694 yields unreal results due to the A_4 flux being less than the model, and no results are reproduced here.)

Oke and Shipman (1971) give radii of five known white dwarfs ranging from $0.008R_{\odot}$ to $0.015R_{\odot}$. Thus the hot companions in HD36629 and HD81307 appear to be rather larger and more luminous than white dwarfs and are more comparable to luminosities of planetary nuclei.

In Figure 6.22 their position is shown in Webster's (1969) diagram which shows nuclei of planetary nebulae in the Magellanic Clouds together with Seaton's (1966) proposed evolutionary track.

The hot companions fall in the region expected for transition objects from planetary nuclei to white dwarfs.

TABLE 6.2

POSSIBLE HOT COMPANIONS OF HD81307 and HD36629

	HD81307	HD36629
T_{eff} of visible star T_{eff} of hot companion	$10{,}000^{\circ}$ $100{,}000^{\circ}$	$16{,}000^{\circ}$ $100{,}000^{\circ}$
Flux of visible star at 2292 Å in erg $cm^{-2}sec^{-1}Å^{-1}$ (Klinglesmith, 1971)	3.23×10^{7}	2.72×10^{8}
Flux of $100{,}000^{\circ}$ black body at 2292 Å	6.18×10^{10}	6.18×10^{10}
Flux of visible star at 3530 Å (Klinglesmith, 1971)	2.20×10^{7}	1.01×10^{8}
Flux of $100{,}000^{\circ}$ black body at 3530 Å	1.40×10^{10}	1.40×10^{10}
R_1/R_2	0.017	0.066
Estimated radius of visible star (Code et al, 1976)	$1.7R_{\odot}-2.8R_{\odot}$	$1.9R_{\odot}-8.3R_{\odot}$
Estimated radius of hot companion	$0.03\ R_{\odot}$ to $0.07\ R_{\odot}$, or $2.1-4.9\times10^{9}$cm	$0.13\ R_{\odot}$ to $0.55\ R_{\odot}$, or $9.0-38\times10^{9}$cm
$\log \mathcal{L}/\mathcal{L}_{\odot}$	1.9-2.6	3.18-4.4

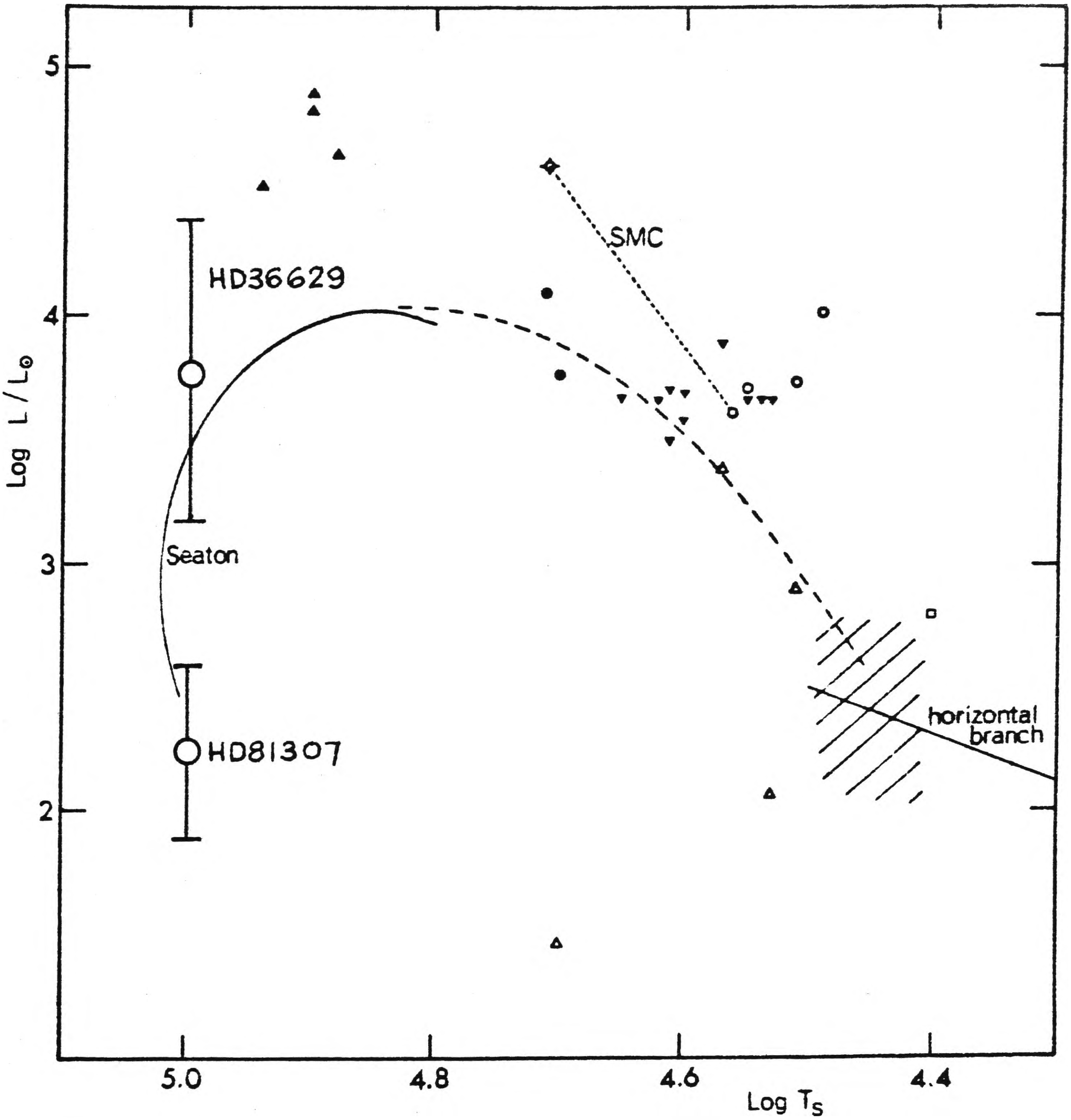

The theoretical H–R diagram of planetary nuclei. The symbols represent the following:

- ● *the spectrum shows measurable He I λ 4471;*
- ○ *low excitation SMC planetaries;*
- -○- *low excitation planetaries with temperatures corrected;*
- ▲ *T_s calculated from He II λ 4686;*
- ▼ *T_s calculated from Hβ and is a lower limit;*
- □ *H 138;*
- △ *taken from Seaton's diagram.*

Ɨ○ Possible hot companions.

FIG. 6.22: Possible hot companions of HD36629 and HD81307 on Webster's (1969) diagram of planetary nuclei.

6.3 Anomalous early B stars: HD51285, HD84361, HD88844, HD95275 and HD167003

Some relevant data on these stars is collected in Table 6.3 .

The last three stars are picked out as anomalous by Figures 4.22 and 4.3; the second is picked out by Figure 4.3 only. HD51285 is added to the list of anomalous early B stars because in Table 6.3(2) it shares with HD84361 and HD167003 the distinction of having a calculated distance larger than 3.5 kpc. Since these three stars have low reddening (0.00, 0.20 and 0.10 respectively) and since the large distances result in large $|z|$ values (650, 439 and 1074 pc respectively), the calculated distances are suspect.

The distances are based on absolute magnitudes assigned from the β calibration of Crawford (1978). It is clear from Figure 4.13 that the three stars have among the lowest β indices measured (hence the highest luminosities) and fall above MS values for early B stars. However, HD84361, with a β index corresponding to luminosity class I has a luminosity class V assigned by Houk et al (1975). If MS luminosities are applied to all three stars, their distances and $|z|$ values are significantly reduced, and only HD167003 remains of any note, with D = 2.34 kpc and $|z|$ = 310 pc, only marginally high for a B0 star. Such a re-assignment of luminosity implies that either the observed β indices are in error or the stars have anomalously weak H lines. Two of the three have spectrographic luminosity classification: HD84361 is class V (Houk et al 1975) and HD167003 is class II (Garrison et al 1977). The matter appears quite inconclusive. Further spectrographic investigation seems warranted.[1]

All stars in Table 6.3 except HD51285 were picked out by their unusual position in the UV colour-colour diagram high and to the right, indicating an anomaly in the UV distribution. Figures 5.3(1), 5.3(2) and 5.3(4) indicate that the anomaly shared by the four stars is a lower than expected flux in A2, A3 and A1. A4 is on or near the expected flux of the model atmosphere (assigned mainly on the strength of the Balmer discontinuity). In three of the four cases this UV distribution results in a UV classification that is significantly later than the visible classification. For HD51285, the uniformly lower than expected flux might be due to error in unreddening; there is no obvious explanation for the deviations in the other three stars.

---

[1] To add to the confusion, Dworetski et al (1982) in a paper published after this manuscript was completed, classify HD51285 as B2Vnn indicating very broad H lines.

HD	Sp(β)	l	b	β	M_V	D(kpc)	z pc	y	E_{b-y}	Sp
51285	B2	235.59	-10.10	2.585	-4.65	3.65	650	8.16	0.00	
84361	B1	280.07	-3.87	2.507	-6.51	6.49	439	8.35	0.20	B2/3V
167003	B0	359.41	-7.49	2.555	-6.51	8.17	1074	8.45	0.10	B1II
88844	B0	284.99	-3.95	2.623	-3.17	1.85	128	8.52	0.09	B0.5III
95275	B0	287.17	+4.51	2.596	-4.12	2.52	199	8.55	0.16	O9V/B0I

TABLE 6.3: ANOMALOUS EARLY B STARS

6.4 Anomalous Late B Stars: HD66134, HD77904, HD130903, HD139579 and HD175934

HD66134 and HD77904 fall far to the right in the UV colour-colour diagram. The others fall low in the same diagram. They appear to be a mixed group.

The position of HD77904 results from a higher than expected A4 flux coupled with a lower than expected A1 flux; A2 and A3 fluxes agree with the model. Errors seem to be the most likely cause.

The position of HD66134 results from high fluxes in the three shortest wavelengths A2, A3 and A4, but normal A1 (resulting in a very negative A2-A1). This excess in the far UV looks convincing, but has no obvious explanation. A similar flux distribution is displayed by HD165246 (B0), HD52942 (B2) and HD68982 (B2).

HD175934 and HD139579 have lower than expected UV fluxes, especially in A4, giving a more negative A2-A4. It is not evident from the flux distributions shown in Figures 5.3(9) and 5.3(10) that the deviations are really significant.

The position of HD130903 could be due to large uncertainties in the UV data; however, it is a peculiar object for another reason. Its classifications in this thesis are B8 from the [u-b] vs β diagram, B9 from the

$[m_1]$ vs $[c_1]$ diagram, and B5/6 from the UV diagram. However, the spectrographic classification is B(2)p (Houk et al, 1975). One other star in Table 4.3(2) has a noteworthy disagreement between photometric and spectrographic classifications. HD91041 has photometric classifications B5/6, B6, B3 and spectrographic classification B8 (Houk et al, 1975).

There is one further type of anomaly in the flux distributions that does not show up in Figures 4.22 and 4.3 or in Table 4.3(2). Some stars in Figures 5.3 (1) to (11) have all UV fluxes falling higher (HD64301) or lower (HD64455 (B3), HD86441 (B3), HD42551 (B5/6), HD118256 (B5/6) and HD64301 (B6)) than expected. This looks like a zero point error. No obvious source of such an error presents itself.

The later stars generally show poorer agreement between observed UV fluxes and the models, which may be in part because for later stars, the effects of line absorption in the UV become stronger (Nandy and Schmidt, 1975) and the models (Klinglesmith 1971) are unblanketed except for hydrogen.

The A1 flux fall consistently below the models through most of the stars, which suggests a systematic error in A1.

6.5 Subdwarfs

Carnochan and Wilson (1983), henceforth referred to as CW, suggest that a large number of the objects with very ultraviolet colours are subdwarfs, with luminosities two magnitudes below the main sequence. This is of great interest because such stars would be candidates for the intermediate stage between red giants and white dwarfs.

According to Weidemann (1967) the local space density of white dwarfs is $10^{-2}pc^{-3}$, requiring a birthrate of $2 \times 10^{-12}pc^{-3}yr^{-1}$.

Comparison with birth rates of planetary nebulae which are $1 \times 10^{-13}pc^{-3}yr^{-1}$ for Seaton's (1966) distance scale and $11 \times 10^{-13}pc^{-3}yr^{-1}$ for Abell's (1966) distance scale, indicates (Weidemann, 1967) that planetary nebulae can provide 5-50% of the white dwarfs observed. It follows that non-planetary nebula precursors to white dwarfs might have a birth rate of $1.9 \times 10^{-12}pc^{-3}yr^{-1}$ for Seaton's distance scale and $0.9 \times 10^{-12}pc^{-3}yr^{-1}$ for Abell's distance scale.

Adopting lifetimes of the same order as for planetary mebulae, about 35,000 years (O'Dell, 1967), leads to space densities of $7 \times 10^{-8}pc^{-3}$ and $3 \times 10^{-8}pc^{-3}$ for the two distance scales. These compare well with the sum of values $1.3 \times 10^{-8}pc^{-3}$ and $4.2 \times 10^{-8}pc^{-3}$ given by CW for stars with $A_2-A_1 < -1.8$, many of which have already been identified as subdwarfs.

However, CW proposed a space density of $2.5 \times 10^{-7} pc^{-3}$ for subdwarfs in the colour range A_2-A_1 = -1.6 to -1.8 magnitudes. This is greatly in excess of the numbers required to provide the observed white dwarfs. It appears that CW have seriously overestimated, as suggested below; or the lifetime of these subdwarfs is much less than that of planetary nebulae; or these stars are not progenitors of white dwarfs.

CW derive luminosities for stars with no spectroscopically determined luminosity classification as follows:

1. The position of the unreddened colour-colour line in the plot of (A_2-A_1) versus (A_2-A_4) is determined from the observed colours of stars at high galactic latitude, assuming average extinction.

2. The relationship between colour excess and distance (for intervals of galactic longitude of 30°) is determined from stars known to be main sequence stars.

3. The (A_2-A_1) versus (A_2-A_4) diagram is broken into bands bounded by lines with the slope of the reddening line.

4. The <u>average</u> colour excess E of luminosity-unclassified stars in each band is determined.

5. The average distance D of these stars is determined on the assumption that the relationship between colour excess and distance is the same as for the known MS stars.

6. Individual absolute magnitudes for the stars are derived from the values of E and D.

Table 6.5(1) summarises CW's longitude groups, their mean ratio E_{B-V}/D for each group, the corresponding ratios E_{b-y}/D, and the HD numbers of stars observed in this program corresponding to each group.

TABLE 6.5(1)

LONGITUDE GROUPS AND REDDENING

GROUP	GALACTIC LONGITUDE (°)	$\frac{E_{B-V}}{D}$	$\frac{E_{b-y}}{D}$	HD
1	90-180 300-60	0.29	0.22	118256-180124
2	60-90 180-240 270-300	0.15	0.11	36629-54197, 60757,79368, 81769, 82111-95275
3	240-270	0.10	0.07	58441, 61193-77904, 81307,81694

CW found that there were many stars which fell two or more magnitudes below the expected luminosity for MS stars of that colour, and concluded that the stars were subdwarfs. The resulting space densities are very high.

The essence of CW's argument is that there are more faint objects with very negative ultraviolet colours than would be expected, considering that faint objects are usually distant and should therefore suffer from interstellar reddening. Figure 6.5 shows the distribution of stars in the CW catalogue over colour (A_2-A_1) in progressive intervals of m_v. (Wolf-Rayet stars are excluded.) The shaded regions indicate stars which are known to be subdwarfs from Giddings (1980) catalogue and other references cited by CW. Subdwarfs with no m_v listed in the catalogue are assumed to be fainter than 10.

Nearly all the stars with A_2-A_1 < -1.8 and $m_v > 9$ are known to be subdwarfs. Excluding all known subdwarfs, the distribution in UV colour appears to be independent of m_v. In fact there are as many stars with A_2-A_1 between -1.6 and -1.8 in the magnitude interval 9 to 10 as in any other magnitude interval except the very brightest ($m_v < 4$). This is indeed surprising and CW's interpretation would appear to be justified. We examine it further, however, on the basis of results of the present study.

There is little doubt that a high proportion of the stars with A_2-A_1 < -1.8 are subdwarfs. The interesting question is what proportion of the stars with A_2-A_1 between -1.6 and -1.8 are subdwarfs. Only one star in

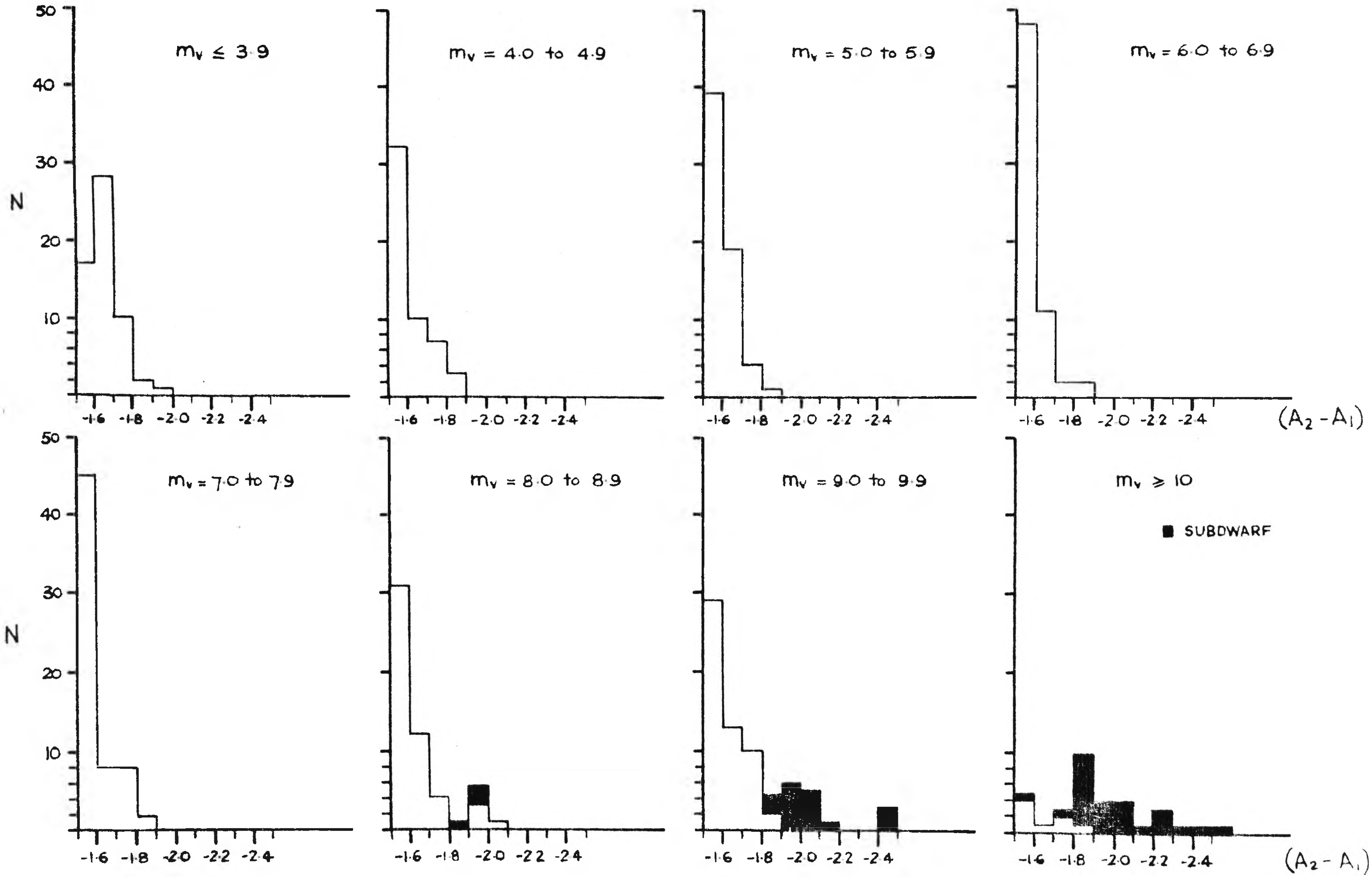

Fig 6.5 Distribution of Carnochan and Wilson (1983) stars over colour $(A_2 - A_1)$.

the catalogue is known to fall in this category: DM-31°4800 has (A_2-A_1) = -1.79 and so qualifies (just). There is also, however, HD200516 with (A_2-A_1) = -1.54. It is possible that the less UV objects have not yet been as intensively studied, and subdwarfs have avoided detection.

CW find that of the 268 objects with unreddened colours between -1.6 and -1.8 (B2 and B3 stars), about 58 (or 22%) are subdwarfs.

The present sample of 90 stars is essentially limited to stars brighter than 8.5 magnitudes, but is otherwise random. There appear to be two objects which have excessive UV flux for their spectral types and appear to have subdwarf companions. None of the other stars appear to be subdwarfs.

This strongly implies that, of the 298 stars in the CW catalogue brighter than m_v = 8, none are subdwarfs. This is not a great surprise; subdwarfs are intrinsically faint and their observed numbers are expected to increase with apparent magnitude. However, since the stars brighter than 8th magnitude comprise about 65% of the stars in the catalogue, in all colour ranges, an overall proportion of 22% subdwarfs requires that about 63% of stars fainter than m_v = 8 are of this type. This does not seem likely.

Another explanation for CW's results is suggested by the present data and is outlined below.

The interstellar extinction is very irregular. Stars with greater than average distance, but less than average extinction will have average colour and will be included in the catalogue. To assess the importance of this effect, Table 6.5(2) contains calculated distances for the stars observed in this program, together with the resulting ratio of E_{b-y}/D. The range of the latter is very large, especially for CW's longitude group 1 ($\ell^{II} = 300^{o}$ to 60^{o}) where the average extinction is the highest, being 0.01 to 0.55 compared with CW's mean of 0.22.

By the procedure adopted by CW, a star which is faint because it is distant, but happens to have lower than average reddening, will be assigned a luminosity according to the average reddening and distance of stars in the same band of the (A_2-A_1) vs (A_2-A_4) diagram. Table 6.5(3) shows the determination of M_V by a method comparable to CW for B2 and B3 stars (intrinsic (A_2-A_1) = -1.6 to -1.8) in longitude group 1 ($\ell^{II} = 300^{o}$ to 60^{o}). The method differs from CW only in that it uses E_{b-y} determined from the present photometry and assumes normal intrinsic colours; CW use colour excesses derived from the (A_2-A_1) vs (A_2-A_4) diagram and a special intrinsic colour line which, for these classes, lies lower (more negative) than the line for MS stars. The effect of this difference is that colour excesses derived here will be slightly greater and absolute magnitudes brighter than would be derived by CW; consequently this method is <u>less</u> likely to assign a star a low luminosity.

The average E_{b-y} for the B2 program stars in Table 6.5(3) is 0.130 magnitudes and for the B3 stars is 0.095 magnitudes, corresponding to E_{B-V} of 0.175 and 0.128 respectively. The resulting distances, using CW's E_{B-V} versus D line, are 0.59 kpc and 0.43 kpc respectively. The individual values of m_{2740} are in column 4 and are to be compared with CW's values for these spectral classes of -4.40 for B2 and -3.68 for B3. With a dividing line between ordinary stars and subdwarfs that is 2 magnitudes below the main sequence, CW would have assigned four of the fourteen stars (29%) to the subdwarfs. The four stars are HD162973, HD118553, HD163430 and HD153084. The spectra (Table 4.3(1)) and the flux distributions (Figs 5.3(1)-(11)) indicate firmly that none of the stars are subdwarfs, all being normal MS or giant stars. For reasons given above, CW's errors in luminosity assignment would have been even greater.

CW, for the same boundaries of colour and longitude, find that 36 out of 128 stars (28%) fall more than two magnitudes below the main sequence, and conclude that the stars are subdwarfs. The above calculation shows that a large proportion and perhaps all of the low-luminosity stars in CW's diagram result from the statistical treatment applied to the data.

On this interpretation, the unexpectedly large numbers of faint objects in the range $(A_2-A_1) = -1.6$ to -1.8 result from the very strong selection effect in favour of objects with unusually low interstellar extinction. A 9th magnitude B2 star with no interstellar extinction is located at a distance of about 2 kpc. Holes in the local dust distribution to this distance do not seem unlikely.

There are 27 objects in the CW catalogue with (A_2-A_1) between -1.6 and -1.8 and $m_v > 9$. One of these is a known subdwarf. Whether the rest owe their colour to low interstellar extinction or to also being subdwarfs, they deserve further investigation.

TABLE 6.5 (2)

ABSOLUTE MAGNITUDES AND DISTANCES

HD	Sp [1]	$(b-y)_o$ [2]	E_{b-y} [3]	V_o [4]	M_V [5]	V_o-M_V	D (kpc) [6]	$\frac{E_{b-y}}{D}$
36629	B5/6	-0.069	0.193	6.98	-0.87	7.85	0.37	0.52
37526	B5/6	-0.069	0.007	7.55	-0.27	7.82	0.37	0.02
42204	B3	-0.082	0.022	8.37	-1.12	9.49	0.79	0.03
42551	B5/6	-0.069	-0.018	7.65	-1.69	9.34	0.74	0.02
48165	B3	-0.082	0.051	7.89	-1.70	9.59	0.83	0.06
49188	B3	-0.082	0.022	7.55	-1.70	9.25	0.71	0.03
51255	B2	-0.095	0.017	8.13	-1.69	9.82	0.92	0.02
51285	B2	-0.095	0.001	8.16	-4.65	12.81	3.65	0.00
52942	B2	-0.095	0.264	7.07	-2.01	9.08	0.65	0.41
53824	B5/6	-0.069	0.023	8.01	-0.65	8.66	0.54	0.04
54197	B1	-0.114	0.132	7.43	-3.17	10.60	1.32	0.10
58441	B2	-0.095	0.043	7.89	-2.50	10.39	1.20	0.04
60757	B3	-0.082	0.022	7.77	-3.62	4.15	0.07	0.33
61193	B1	-0.114	0.133	7.66	-2.01	9.67	0.86	0.15
63274	B5	-0.069	0.034	7.91	-1.00	8.91	0.61	0.06
64301	B6	-0.060	-0.008	7.86	-0.70	8.56	0.52	-0.02
64455	B3	-0.082	0.017	7.66	-1.12	8.78	0.57	0.03
66134	B7	-0.054	0.048	7.83	-0.40	8.23	0.44	0.11
68030	B3	-0.082	0.136	7.69	-2.50	10.19	1.09	0.12
68046	B3	-0.082	0.014	8.05	-0.65	8.70	0.55	0.03
68982	B2	-0.095	0.234	6.62	-2.50	9.12	0.67	0.35
69120	B6	-0.060	0.045	8.44	-0.70	9.14	0.67	0.07
70550	B8	-0.045	0.027	8.40	0.18	8.22	0.44	0.06

Table 6.5(2) contd.

HD	Sp	$(b-y)_o$	E_{b-y}	V_o	M_V	V_o-M_V	D (kpc)	$\frac{E_{b-y}}{D}$
71336	B3	-0.082	0.054	7.78	-1.30	9.08	0.65	0.08
71945	B3	-0.082	0.020	7.73	-1.39	9.12	0.67	0.03
72771	B1	-0.114	0.109	7.44	-3.60	11.04	1.61	0.07
72973	B7	-0.054	0.025	8.17	-0.60	8.77	0.57	0.04
73215	B1	-0.114	0.080	7.80	-3.60	8.16	0.43	0.19
77904	B6	-0.060	0.045	7.98	-0.70	8.68	0.54	0.08
79368	B3	-0.082	0.044	8.21	-0.65	8.86	0.59	0.07
81307	B9	-0.037	0.049	6.35	1.31	5.04	0.10	0.48
81694	B8	-0.045	0.030	6.77	1.03	5.74	0.14	0.21
81769	B5/6	-0.069	0.135	7.50	-0.65	8.15	0.43	0.32
81921	B9	-0.037	0.044	6.61	-0.27	6.88	0.24	0.19
82111	B5/6	-0.069	0.039	7.61	-1.39	9.00	0.63	0.06
82811	B5/6	-0.069	0.032	8.19	0.04	8.15	0.43	0.08
83335	B5/6	-0.069	0.034	7.82	-0.45	8.27	0.45	0.08
83866	B3	-0.082	0.059	7.40	-0.87	8.27	0.45	0.13
84361	B1	-0.114	0.199	7.55	-6.51	14.06	6.49	0.03
86385	B3	-0.069	0.035	7.76	-0.87	8.63	0.53	0.07
86441	B3	-0.082	0.035	5.97	-2.75	8.72	0.55	0.06
87295	B3	-0.082	0.088	7.31	-1.69	9.00	0.63	0.14
88556	B3	-0.082	0.057	7.61	-0.87	8.48	0.50	0.11
88844	B0	-0.114	0.089	8.16	-3.17	11.33	1.85	0.05
89403	B2	-0.095	0.111	7.22	-2.01	9.23	0.70	0.16
89876	B3	-0.082	0.134	7.38	0.04	7.34	0.29	0.46

Table 6.5(2) contd.

HD	Sp	$(b-y)_o$	E_{b-y}	V_o	M_V	V_o-M_V	D (kpc)	$\frac{E_{b-y}}{D}$
90288	B1	-0.114	0.064	7.86	-4.12	11.98	2.49	0.03
90786	B2	-0.095	0.113	8.34	-2.01	10.35	1.17	0.10
91041	B5/6	-0.069	0.054	7.87	-0.45	8.32	0.46	0.12
94108	B3	-0.082	0.023	7.67	-0.65	8.32	0.46	0.05
95275	B0	-0.120	0.164	7.89	-4.12	12.01	2.52	0.06
118256	B5/6	-0.069	0.056	7.79	-1.12	8.91	0.61	0.09
118553	B3	-0.082	0.119	8.05	-0.87	8.92	0.61	0.20
118571	B0	-0.114	0.189	8.00	-3.62	11.62	2.11	0.09
119926	B2	-0.095	0.156	6.97	-2.36	9.33	0.73	0.21
127449	B2	-0.095	0.133	7.19	-1.69	8.88	0.60	0.22
130903	B8	-0.045	0.037	7.81	-2.36	10.17	1.08	0.03
135241	B2	-0.095	0.119	7.55	-1.69	9.24	0.70	0.17
135786	B2	-0.095	0.094	7.57	-1.39	8.96	0.62	0.15
139300	B3	-0.082	0.071	7.21	-1.12	8.33	0.46	0.15
139579	B8	-0.045	0.055	8.14	0.18	7.96	0.39	0.14
143156	B5/6	-0.069	0.027	8.04	-0.87	8.91	0.61	0.04
146224	B3	-0.082	0.114	7.07	-0.87	7.94	0.39	0.29
147889	B2	-0.095	0.750	4.87	-4.12	8.99	0.63	1.19
149065	B2	-0.095	0.150	7.83	-1.39	9.22	0.70	0.21
149770	B3	-0.082	0.043	7.87	-2.75	10.62	1.33	0.03
149922	B2	-0.095	0.117	7.46	-4.12	11.58	2.07	0.06
153084	B2	-0.095	0.126	7.82	-1.69	9.51	0.80	0.16
153140	B1	-0.114	0.453	5.66	-5.84	11.50	2.00	0.23

Table 6.5(2) contd.

HD	Sp	$(b-y)_o$	E_{b-y}	V_o	M_V	V_o-M_V	D (kpc)	$\frac{E_{b-y}}{D}$
154535	B1	-0.114	0.241	7.35	-3.62	10.97	1.56	0.15
155600	B7	-0.054	0.197	7.16	-0.65	7.81	0.36	0.54
155754	B1	-0.114	0.171	7.26	-2.36	9.62	0.84	0.20
156070	B2	-0.095	0.134	7.00	-3.17	10.17	1.08	0.12
160109	B3	-0.082	0.149	6.88	-0.65	7.53	0.32	0.46
161972	B3	-0.082	0.048	8.16	-1.69	9.85	0.93	0.05
162973	B5/6	-0.069	0.069	8.12	-1.12	9.24	0.70	0.10
163430	B2	-0.095	0.104	7.75	-3.17	10.92	1.53	0.07
163442	B3	-0.082	0.128	6.85	-1.39	8.24	0.44	0.29
163927	B5/6	-0.069	0.060	8.11	0.30	7.81	0.36	0.16
164320	B5/6	-0.069	0.101	7.16	-1.12	8.28	0.45	0.22
165132	B0	-0.120	0.253	7.08	-5.22	12.30	2.88	0.09
165246	B0	-0.120	0.254	6.69	-4.65	11.34	1.85	0.14
165477	B5/6	-0.069	0.080	8.23	-0.10	8.33	0.46	0.17
167003	B0	-0.114	0.099	8.05	-6.51	14.56	8.17	0.01
170385	B3	-0.082	0.020	7.82	-1.39	9.21	0.70	0.03
172535	B3	-0.082	0.058	7.56	-0.65	8.21	0.44	0.13
172850	B8	-0.045	0.061	7.54	0.30	7.24	0.28	0.22
174395	B7	-0.054	0.117	7.69	-0.10	7.79	0.36	0.32
175934	B7	-0.054	0.030	8.07	-0.27	8.34	0.47	0.06
180124	B3	-0.082	0.153	6.56	-0.65	7.21	0.28	0.55

Table 6.5(2): Footnote.

[1] Spectral type is from the [u-b] vs β classification, or from the $[m_1]$ vs $[c_1]$ classification where the former was not available.

[2] Intrinsic colour given by Crawford (1978).

[3] $E_{b-y} = (b-y)_{observed} - (b-y)_o$

[4] V_o is assumed equal to y_o, where $y_o = y - 4.05E_{b-y}$.

[5] Absolute magnitude M_V is as given by Crawford (1978) in his $M_V(\beta)$ calibration; where β is not known, the Schmidt-Kaler (1965) value of M_V for each MK class as listed by Crawford (1978) is given.

[6] D is calculated from $M_V = V_o + 5 - 5\log D$ where D is measured in parsecs.

TABLE 6.5(3)

DETERMINATION OF M_{2740} FOR B2 AND B3 STARS

HD	Sp[1]	A_2-A_1	A_2-A_4	E_{b-y}[2]	m_{2740} unred.	M_{2740}	E_{B-V}[3]	E_{B-V}[4]
119926	B2	-1.33	-1.03	0.156	6.71	-2.67	0.15	0.21
127449	B2	-1.31	-1.09	0.133	6.65	-2.73	0.19	0.18
135241	B2	-1.50	-1.03	0.119	6.74	-2.64	0.08	0.16
156070	B2	-1.25	-1.13	0.134	6.45	-2.93	0.23	0.18
160109	B2	-1.28	-1.16	0.149	6.70	-2.86	0.24	0.20
162973*	B2	-1.45	-1.04	0.069	7.59	-1.79	0.10	0.09
163442	B2	-1.32	-1.20	0.128	6.41	-2.97	0.25	0.17
180124	B2	-1.25	-1.18	0.153	6.32	-3.06	0.26	0.21
118553*	B3	-1.32	-1.05	0.119	7.73	-0.83	0.16	0.16
135786	B3	-1.37	-0.97	0.094	6.84	-1.72	0.09	0.13
139300	B3	-1.45	-1.03	0.071	6.56	-2.00	0.10	0.10
153084*	B3	-1.29	-1.03	0.126	6.98	-1.58	0.16	0.17
163430*	B3	-1.29	-1.01	0.104	6.88	-1.68	0.15	0.14
172535	B3	-1.43	-1.02	0.058	6.61	-1.95	0.10	0.08

* indicates stars which by CW's criteria are subdwarfs.

[1] spectral type from UV photometry.

[2] excess from uvby photometry.

[3] $E_{B-V} = 0.40(A_2-A_1) - 0.57(A_2-A_4) + 0.09$ (CW, 1983).

[4] $E_{B-V} = 1.35E_{b-y}$ (Crawford 1975).

Footnote:

Since completion of this manuscript, Dworetsky et al (1982) have published spectral classifications for 103 stars in CW's 1981 list. Six stars are in common with this work and spectral classes agree satisfactorily.

Of the stars observed fainter than this survey, i.e., $m_v > 8$, four have $(A_2-A_1) < -1.8$. Of these, one is a subdwarf and one is suspect because of high galactic latitude. Six stars have (A_2-A_1) in the range -1.6 to -1.8. None of these shows any peculiarity. The results of Dworetsky et al (1982) support our conclusion that few if any of the stars with $(A_2-A_1) > -1.8$ are subdwarfs.

7. AN ENCODING SYSTEM FOR THE 18-INCH TELESCOPE

7.1 INTRODUCTION

The University of Wollongong operates an 18-inch telescope located on the escarpment behind Wollongong. The greatest contribution from a telescope of this size is gained by photoelectric observations such as those reported in chapters 1-6 of this thesis. It was originally intended that the program be conducted with that telescope, however time factors dictated use of MSSSO telescopes instead.

Photometric observations require photometric weather, i.e., constant atmospheric transmission. The sky in Wollongong is photometric often enough to support a viable program. However, it is vital that the telescope (and its instruments) works quickly and efficiently to utilise the fine periods. To that end the digital encoder system described below was designed and installed.

As originally constructed, the position of the telescope was determined only from setting circles, which are neither fast nor convenient. It was therefore decided to develop a position encoding system, using optical shaft encoders which would give the best possible angular resolution consistent with the limited budget and of the order of 0.1 minutes of arc. The encoders would operate a low-cost digital display using components which were readily available from local suppliers.

A block diagram of the electronic system is shown in Figure 7.1.

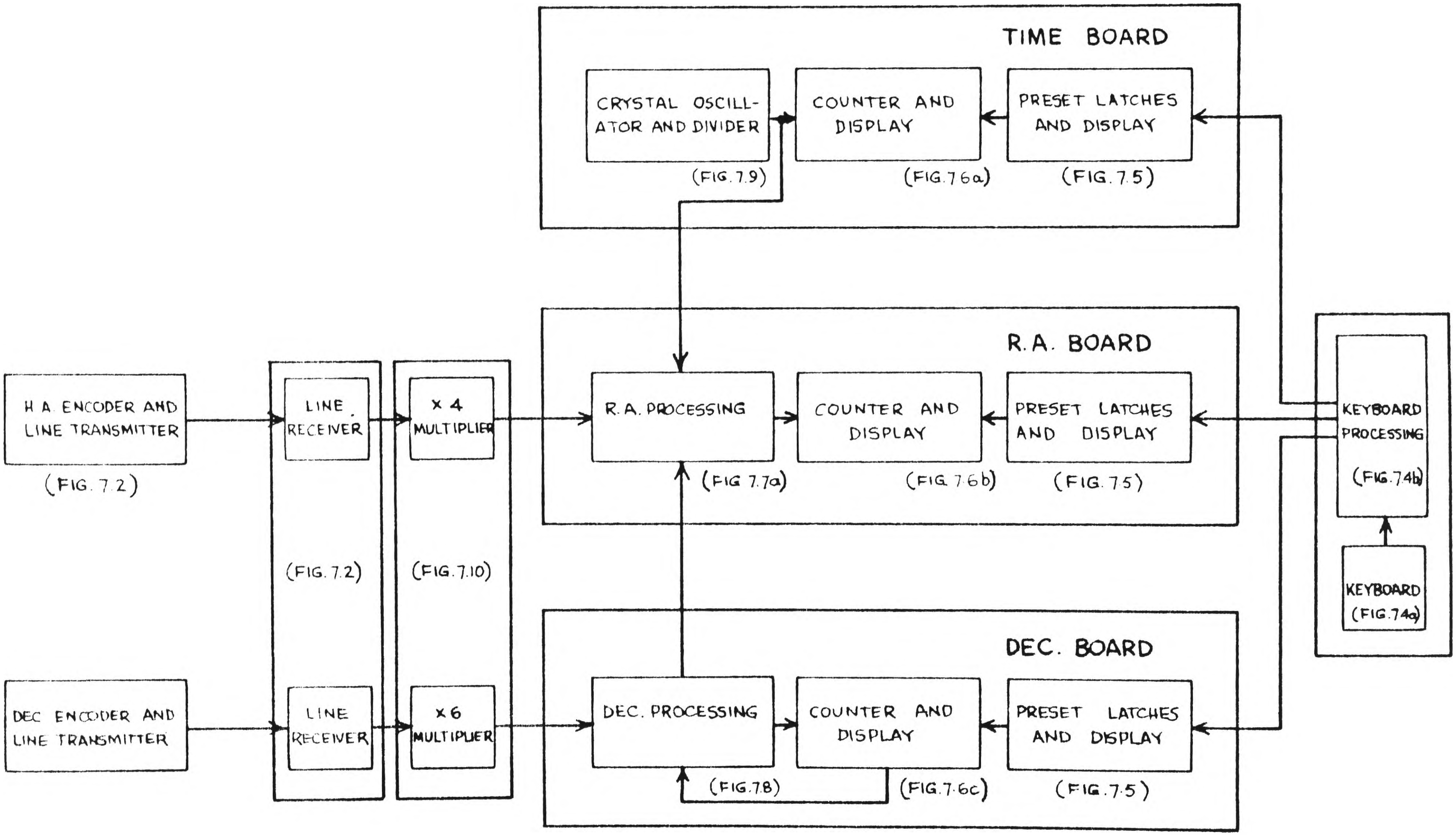

FIG. 7.1 ENCODING SYSTEM BLOCK DIAGRAM

7.2. THE OPTICAL SHAFT ENCODERS

The telescope drive system uses separate fast and slow motors on both axes, with separate clutches to impart motion to the telescope. The shaft encoders must therefore be driven from the axes of the telescope itself, which immediately presents the difficulty of obtaining sufficiently high angular resolution. The approach adopted was -

(1) to use incremental encoders rather than absolute position encoders, since the former provided substantially better angular resolution for a given cost;

(2) to drive each encoder via a step-up gearbox.

The incremental shaft encoders chosen were Baldwin 5V676 encoders, which produce one output pulse for 36 arc-seconds of shaft rotation, and they are driven by 6:1 step-up gearboxes, to produce one output pulse per 6 arc-seconds rotation of the telescope. The gearboxes use "PIC" brand anti-backlash stainless steel spur gears.

Each encoder requires about 50 milliamps at 5.0 volts for its internal TTL circuitry, and about 300 milliamps at 5 volts for the exciter lamp. An unregulated supply of 12 volts DC is fed to a 5-volt integrated circuit regulator mounted in each encoder case, together with associated filter capacitors. Placing the regulator and filter capacitors at the encoders avoids the problem of voltage drop in the supply lines and suppresses the introduction

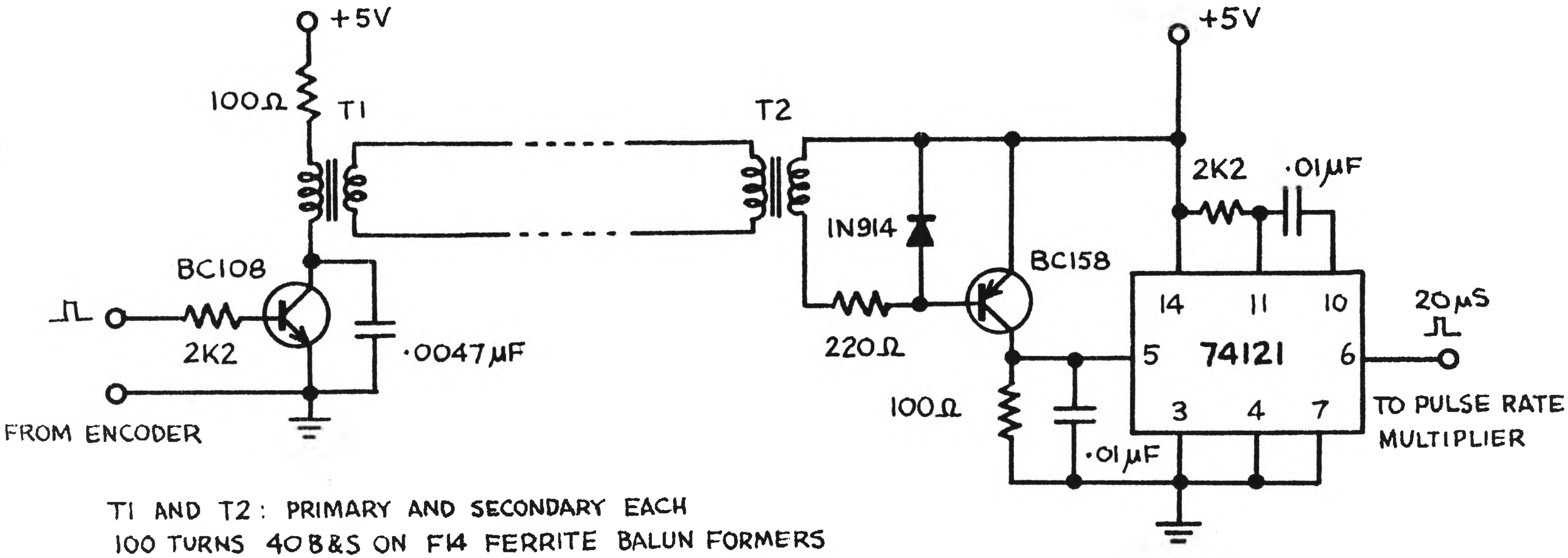

T1 AND T2: PRIMARY AND SECONDARY EACH
100 TURNS 40 B&S ON F14 FERRITE BALUN FORMERS

FIG. 7.2 LINE TRANSMITTER AND RECEIVER

of electrical noise into the encoder via the supply lines.

The pulses from each encoder appear at TTL level on one of two output terminals depending on the direction of rotation, and are transformer-coupled to balanced transmission lines, as shown in Figure 7.2. The DC isolation and balanced output provided by the transformers was needed to prevent spurious signals from the telescope drive motors appearing in the system.

Four-conductor shielded cable provides two pairs of balanced lines to carry pulses from each encoder to the desk console.

7.3. THE DESK CONSOLE

At the desk console, pulses from the transmission lines are received, converted to TTL level, and the pulse rate multiplied by four (for R.A.) or by six (for DEC). The R.A. counting circuitry thus receives pulses at the rate of one per tenth of a second of R.A. and the DEC counters receive one pulse per second of arc.

The sidereal clock is based on a crystal oscillator with frequency 4.011 MHz, which is divided down to produce pulses at intervals of one-tenth of a sidereal second. The pulses increment a ripple counter made of presettable 74192 up-down counters, and the time is displayed by seven-segment LED readouts. Multiplexing was not used with any of the displays, in order to avoid high-frequency interference to adjacent equipment which might have been caused by rapid switching of the displays.

A modified hexadecimal keyboard is used to set the time, R.A. and DEC displays. The required setting is read into latches on each board, which drive seven-segment LED readouts (to display the setting to the operator) and which can have their contents loaded into the main counters by the operator pressing the "load" button at the telescope.

R.A. is obtained by incrementing the counter from the clock, decrementing it by encoder pulses as hour angle increases, and incrementing it by encoder pulses as the hour angle decreases, in accordance with the relationship:

(Right Ascension) = (Local Sidereal Time) - (Hour Angle).

When DEC passes through -90°, as read by the DEC counter, the R.A. counter is incremented by 12 hours.

Declination is obtained by counting pulses from the declination shaft encoder and by detecting, from the counter, when -90° and 0° are reached, at which points the counting direction is reversed. When DEC passes through 0°, the sign (+/-) is also changed.

7.4. KEYBOARD PROCESSING

The keyboard comprises 15 SPST pushbuttons. The ten numerical keys operate a 74C922 key encoder (see Figures 7.4a and 7.4b) which produces a debounced binary output and a "data available" pulse. A 4049 buffer interfaces the CMOS encoder to the following TTL circuitry.

The pushbuttons for R.A., DEC, TIME, +/- and QUAD SET are debounced by IC10, a 7414 Schmitt trigger, and the RC input circuits shown.

Consider the sequence of operation if a time is to be entered into "time" preset latches and display.

The TIME button is pushed, which sets the time board enable line high, and the other board enables low.

IC04 (a 74121 monostable) delivers a "set" pulse to six of the D-flipflops in IC's 06, 07, 08 and 09, which sets all the digit enable lines high. Since the data outputs A, B, C and D are all low (the keyboard encoder has a tri-state output which is pulled low by the 47K resistors) zeros are entered into all the preset latches and the preset display shows all zeros.

The rising edge of the "set" pulse triggers a second monostable, IC05, which delivers a "clear" pulse to all except for the first flipflop in the shift register, thus leaving only the first digit enabled.

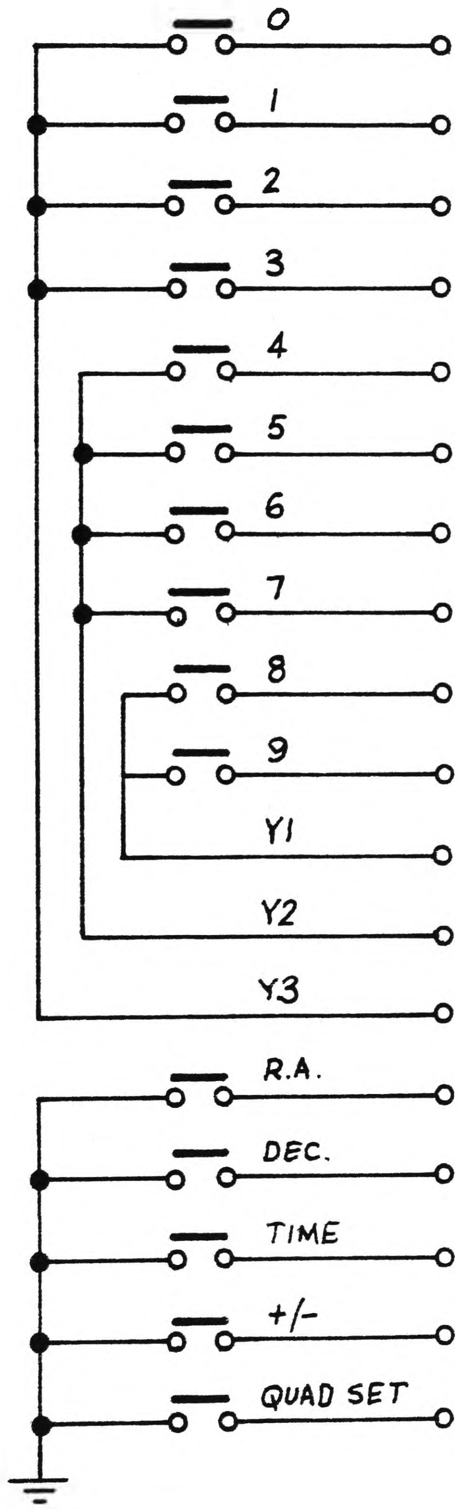

FIG 7.4a KEYBOARD CONNECTIONS

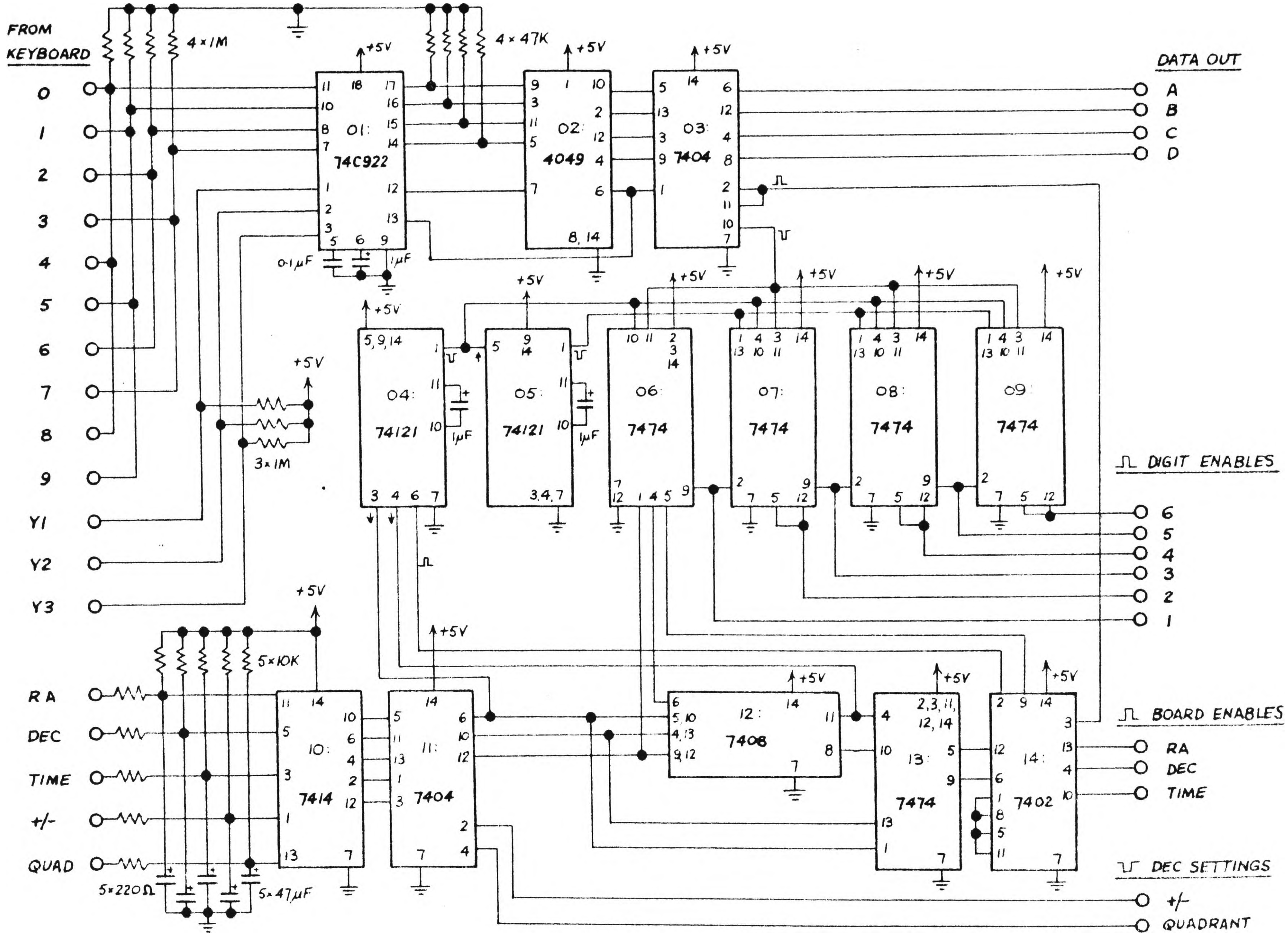

FIG. 7.4b KEYBOARD PROCESSING

When a number key is pressed, the corresponding data appearing on lines A, B, C and D is entered into the preset latch and readout for the first digit.

The rising edge of the "data available" pulse from pin 10 of IC03 clocks the shift register, enabling the second digit latch on the preset board.

When six digits have been entered (hours, minutes and seconds) all the digit enable lines are low and no further entry can be made until the "TIME" button is pressed again.

R.A. and DEC are entered in the same way, except that for DEC a "QUADRANT SET" entry is made if the telescope is "below" the pole, and the "+/-" button sets the appropriate sign.

7.5. PRESETTING THE MAIN COUNTERS AND DISPLAYS

Time, R.A. and DEC are entered into the preset latches and displays from the keyboard. "Load Enable" buttons (which operate 7472 flipflops on each board) are pressed for each quantity to be entered into the main readouts. The "Load" button at the telescope completes the entry and immediately becomes inactive, to prevent subsequent accidental operation.

LED indicators on the desk console show which quantities will be entered when the load button is pushed. Pressing a "Load Enable" button a second time will disable the load function.

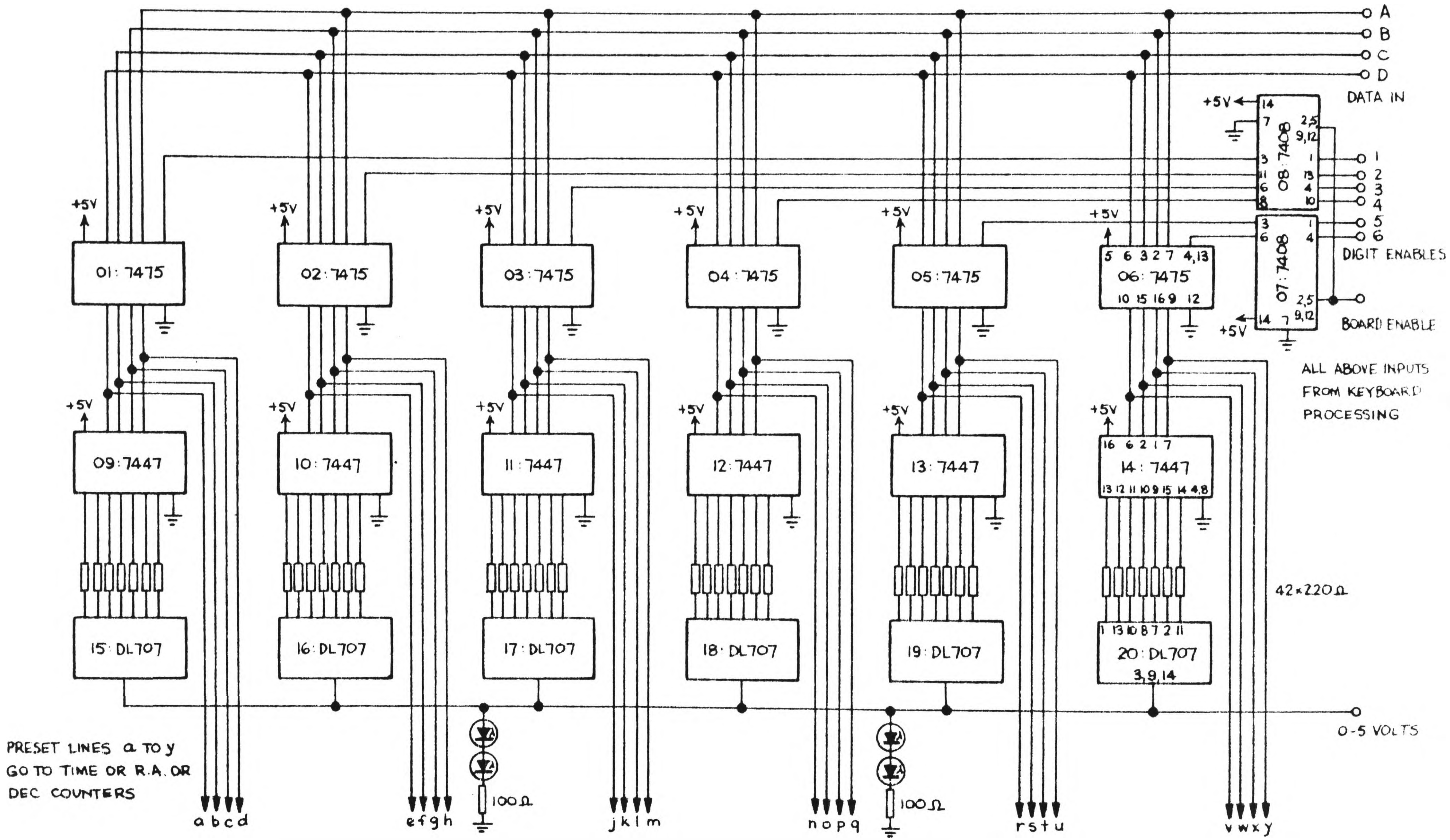

FIG. 7.5 PRESET LATCHES AND DISPLAYS ON TIME, R.A. AND DEC BOARDS.

7.6. THE TIME, RA, AND DEC COUNTERS AND DISPLAYS

The main counting is performed by 74192 up-down presettable counters. (See Figures7.6a, 7.6b and 7.6c.)

The counter outputs are passed to 7475 latches which, although not used at present, were included in case latching was needed at a later time to avoid invalid outputs while the counters were changing states. The binary outputs from the latches have been connected to rear sockets (see the contacts shown in Figures 7.6a, 7.6b and 7.6c) to be readily available if needed.

Type 7447 decoder-drivers operate the DL747 LED readouts, whose supply voltage can be varied from 0 to 5 volts for dimming.

When counting up, second-to-minutes conversion is performed by detecting 6 tens of seconds, using it to increment the minutes counter and reset the tens of seconds counter to zero.

When counting down, 9 tens of seconds is detected, which then decrements the minutes counter and loads a 5 into the tens of seconds counter via the presetting inputs.

The minutes-to-hours transition is dealt with in the same way.

Time and RA hours are reset to zero when, counting up, they reach 24. When the RA tens of minutes, counting down, goes from zero to 9, and the hours go from zero to 99, the tens of minutes counter is immediately loaded with a 5 and the hours counter loaded with a 23.

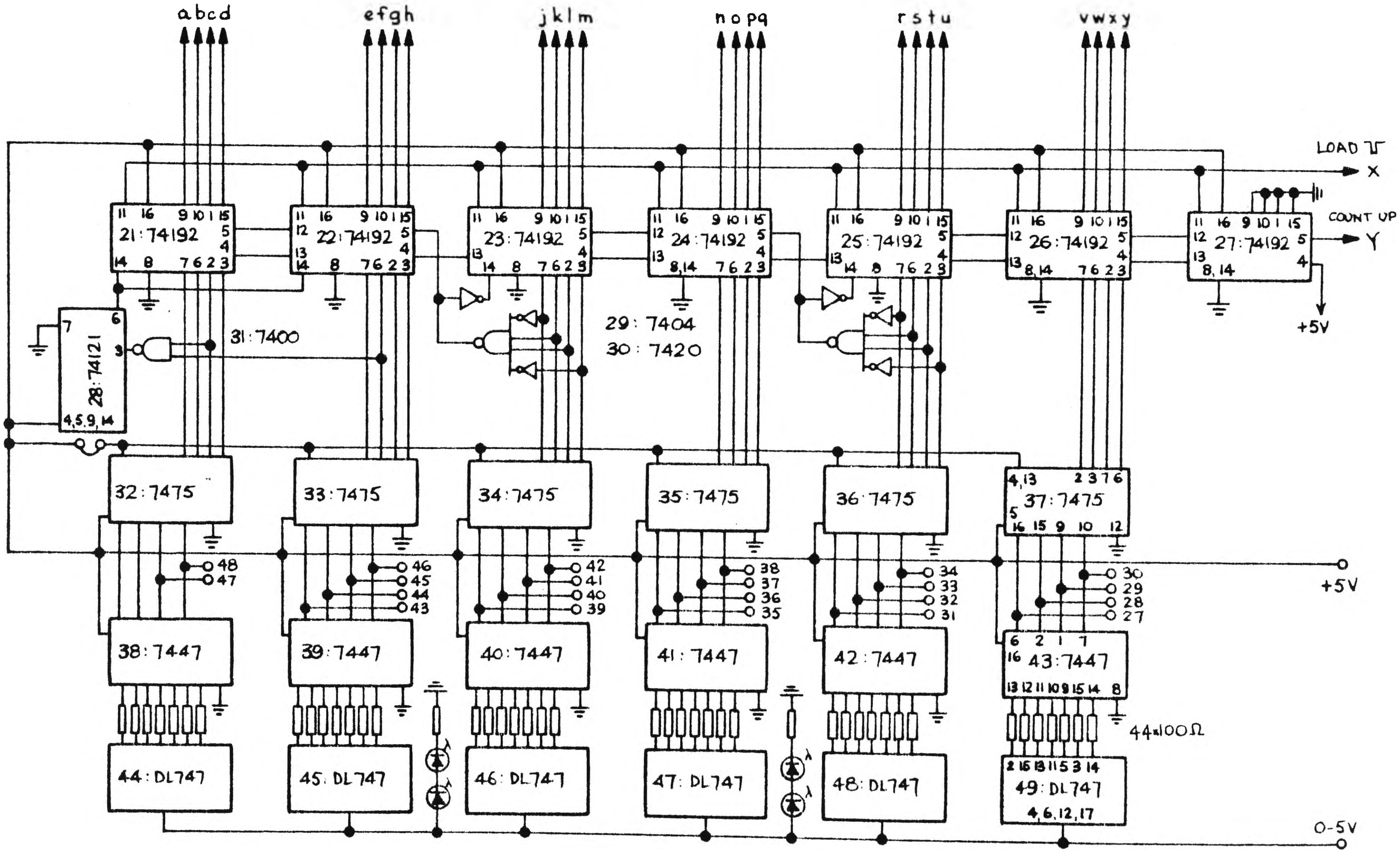

FIG. 76a TIME COUNTER AND DISPLAY

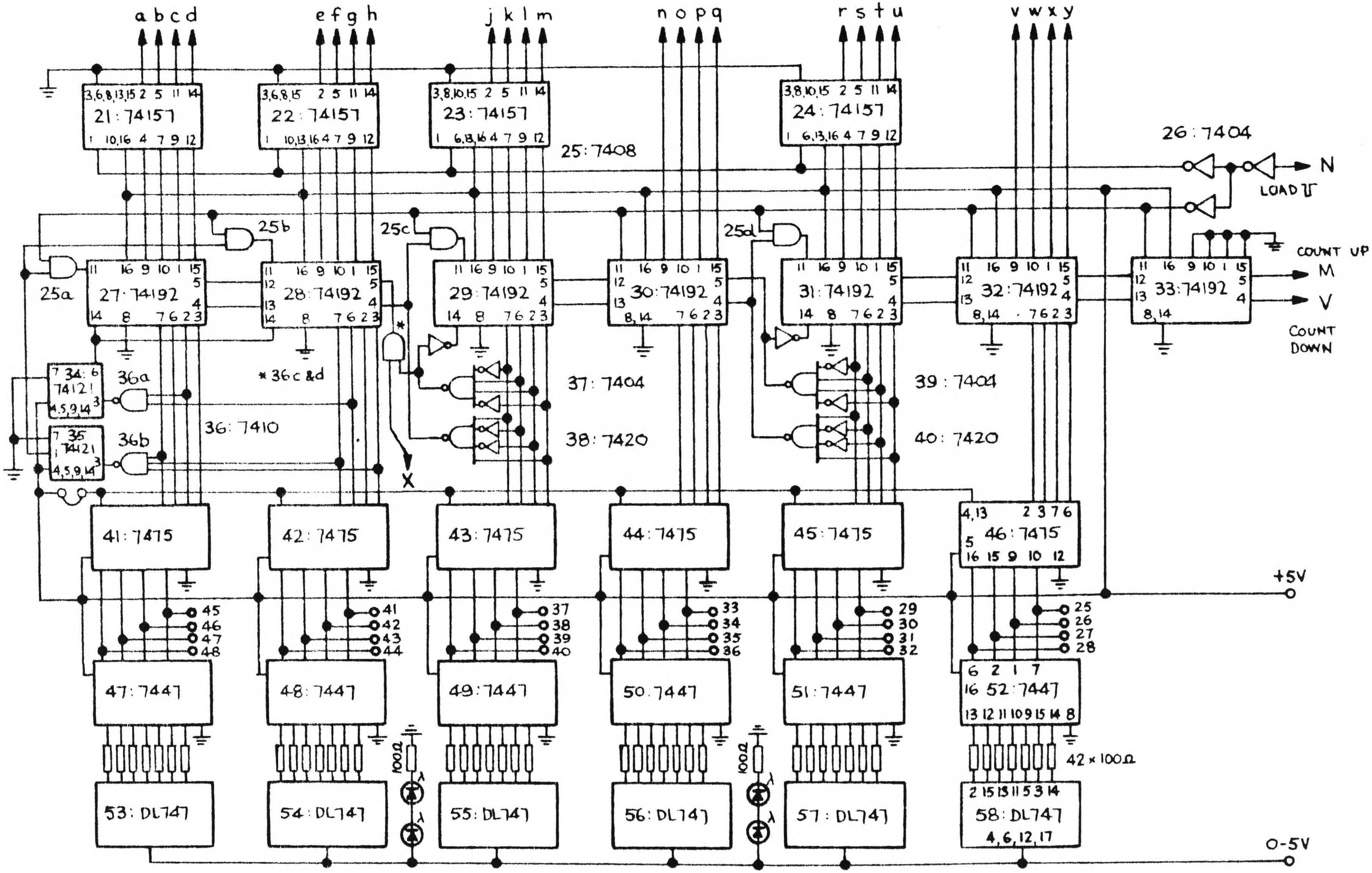

FIG 7.6b R.A. COUNTER AND DISPLAY.

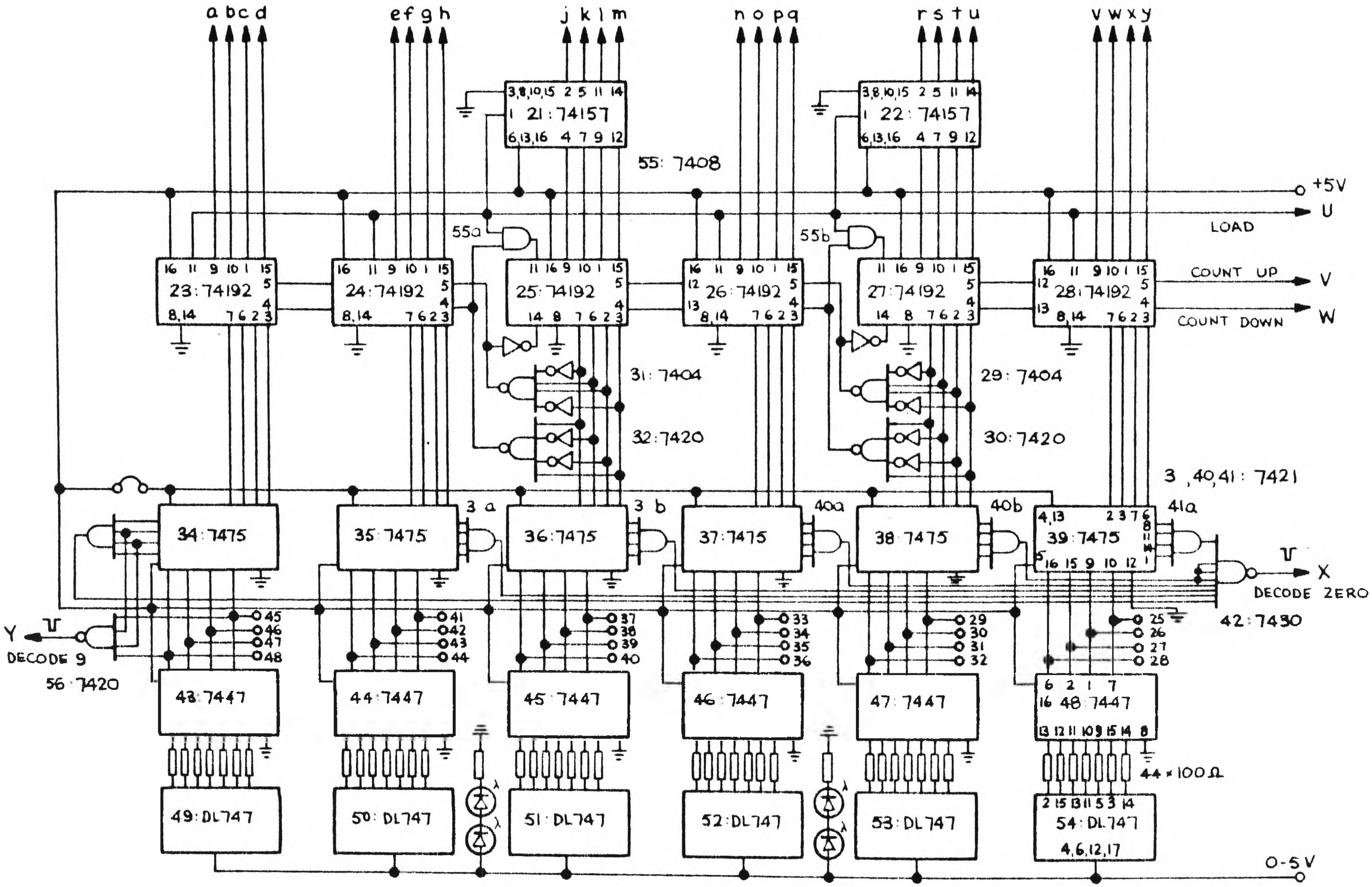

FIG. 7.6c DEC COUNTER AND DISPLAY.

Type 74157 data selectors direct either the preset 5, 2 or 3 or the keyboard data to the affected counters.

The DEC counter has counts of 0^{o} and 90^{0} decoded to produce pulses which reverse the direction of counting and in the case of 0^{o} change the sign as well.

7.7. R.A. PROCESSING

The RA counter must accept pulses from the HA encoder, the clock, and a set of 12 "hour" pulses whenever DEC passes -90^{o}. (See Figure 7.7a.)

The incoming pulses are each latched by a D flipflop and read into the counter in sequence by a pulse distributer.

The pulse distributer (see Figure 7.7a) comprises a 10 MHz oscillator, driving a 74161 synchronous counter and a 74154 data distributor. Alternate outputs of the data distributer are inverted, since each latch is scanned by two successive pulses: the first a positive-going pulse, and the second a negative-going pulse.

For the operation of each memory latch, refer to Figure 7.7b .

A random pulse arriving at Clock input 1 will set Q_1 high on its trailing (rising) edge.

A pulse (1) from the pulse distributor then sets Q_2 high on its leading (rising) edge.

The NAND gate will output a negative-going pulse which goes to the RA counter, and which also resets Q_1 low.

A clearing pulse from the pulse distributor then

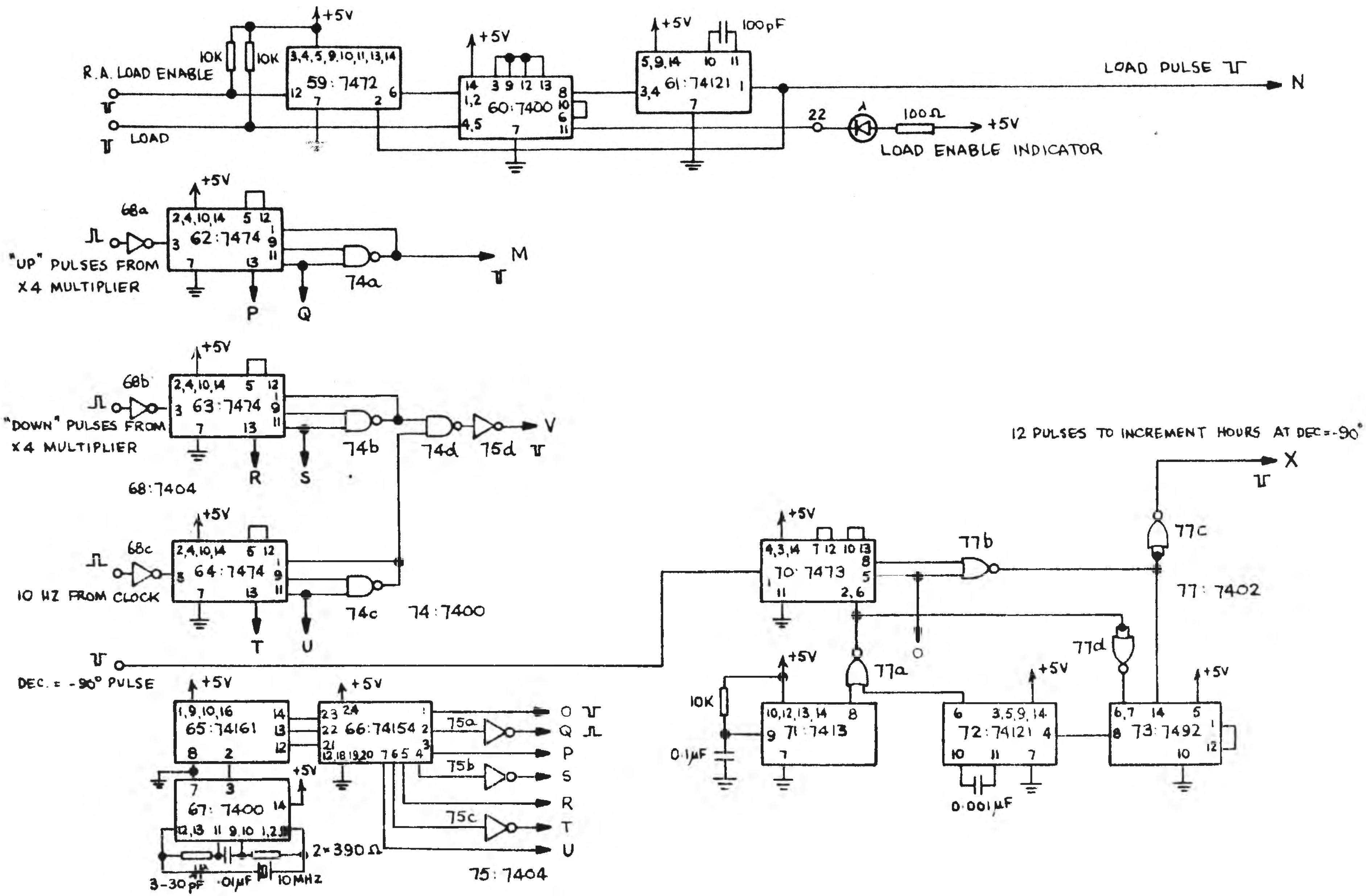

FIG 7.7a R.A. PROCESSING

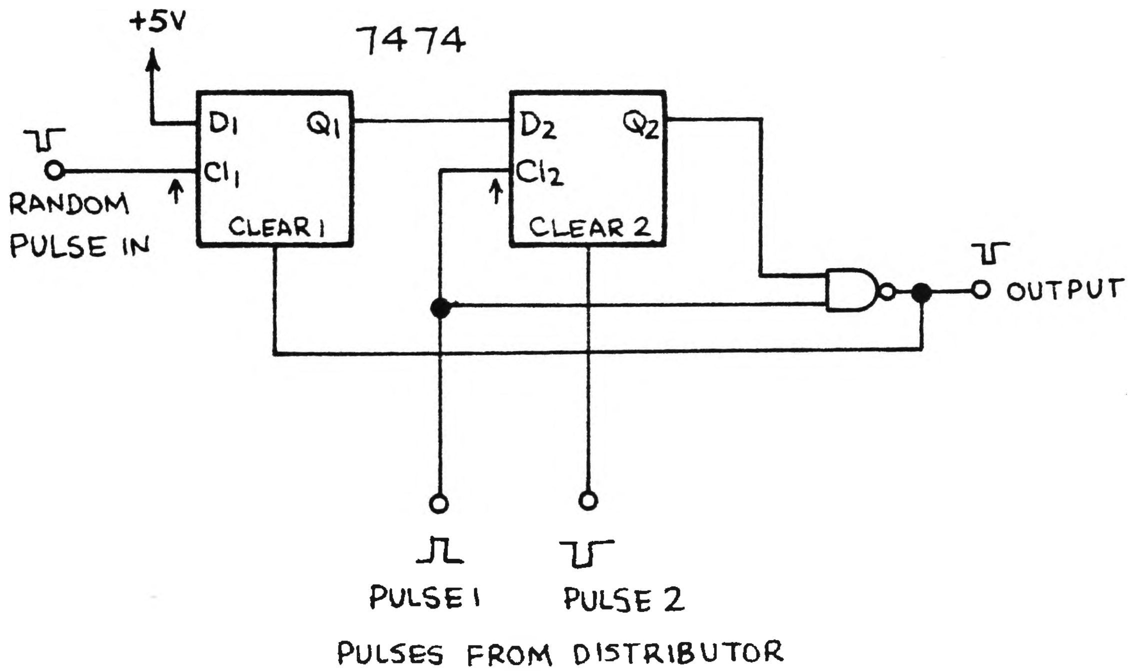

FIGURE 7.7b Memory latches on RA board.

sets Q_2 low.

The above sequence occurs in about 0.2 microseconds, and is repeated 0.8 microseconds later, while the incoming random pulses will be separated by at least 2 microseconds. Therefore the scanning rate is quite adequate.

If Q_1 should go high just after pulse (1) rises, Q_2 remains low and a pulse is not clocked out until the next pulse (1).

Memory latches for HA up, HA down, and the clock are scanned in sequence.

When a DEC = -90^{o} pulse arrives, the output of IC70 (a 7473 flipflop) at pin 8 goes low. Pulses from the "0" output of the distributor are passed by the NOR gate 77b to increment the RA hours counter. At the end of the 12th pulse, IC73 (a 7492 divider) triggers IC72 (a 74121 monostable) which clears IC70, causing pin 8 to go low, preventing the passage of further pulses through NOR gate 77b. IC71 (a 7413 Schmitt trigger) provides a clearing pulse for IC70 and IC73 when power is switched on, to ensure that exactly twelve pulses will be delivered when needed.

7.8. DEC PROCESSING

The main function of the DEC processing circuit is to change the counting direction when DEC passes through -90^{o} and 0^{o}, a function performed by the gates in IC 60 and IC 61 (see Figure 7.8).

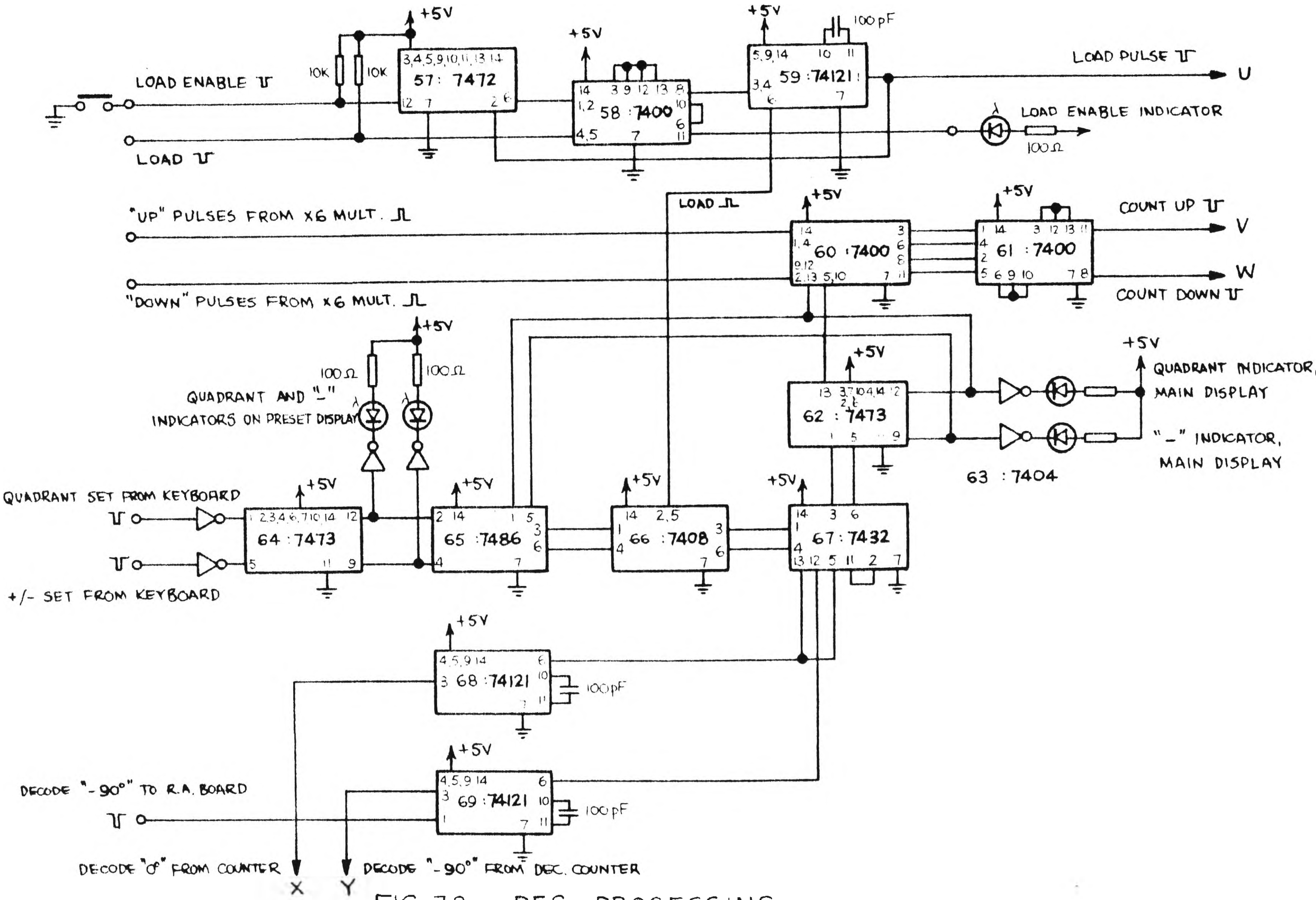

FIG. 7.8 DEC. PROCESSING

The gates are controlled by flipflops (IC 62 and IC64) which are set by the detected -90° or 0° from the DEC counter, or by command from the keyboard (the "QUAD SET" and "+/-" keys).

LEDs on the preset and main displays indicate the status of the QUAD SET and +/- setting.

7.9. THE CLOCK OSCILLATOR AND DIVIDER

The oscillator uses a 4.011 MHz crystal and two NAND gates, with the output buffered by a third NAND gate. (See Figure 7.9.) A 5-60 pF trimmer capacitor enables fine adjustment of the frequency to be made.

The oscillator is followed by a divide by four stage (IC 54), and then five 7490 decade dividers to produce an output signal with a period of 0.1 sidereal seconds.

7.10. PULSE-RATE MULTIPLIERS

The counter designs initially envisaged that the shaft encoders would be driven by gear boxes with high step-up ratios (1:36 for DEC, and 1:24 for RA). However, financial and mechanical restraints dictated ratios of 1:6 for both DEC and RA encoders. A pulse-rate multiplier was made up which delivers four pulses for every RA pulse received, and six pulses for every DEC pulse.

The sequence of operation is as follows (see Figure 7.10) :

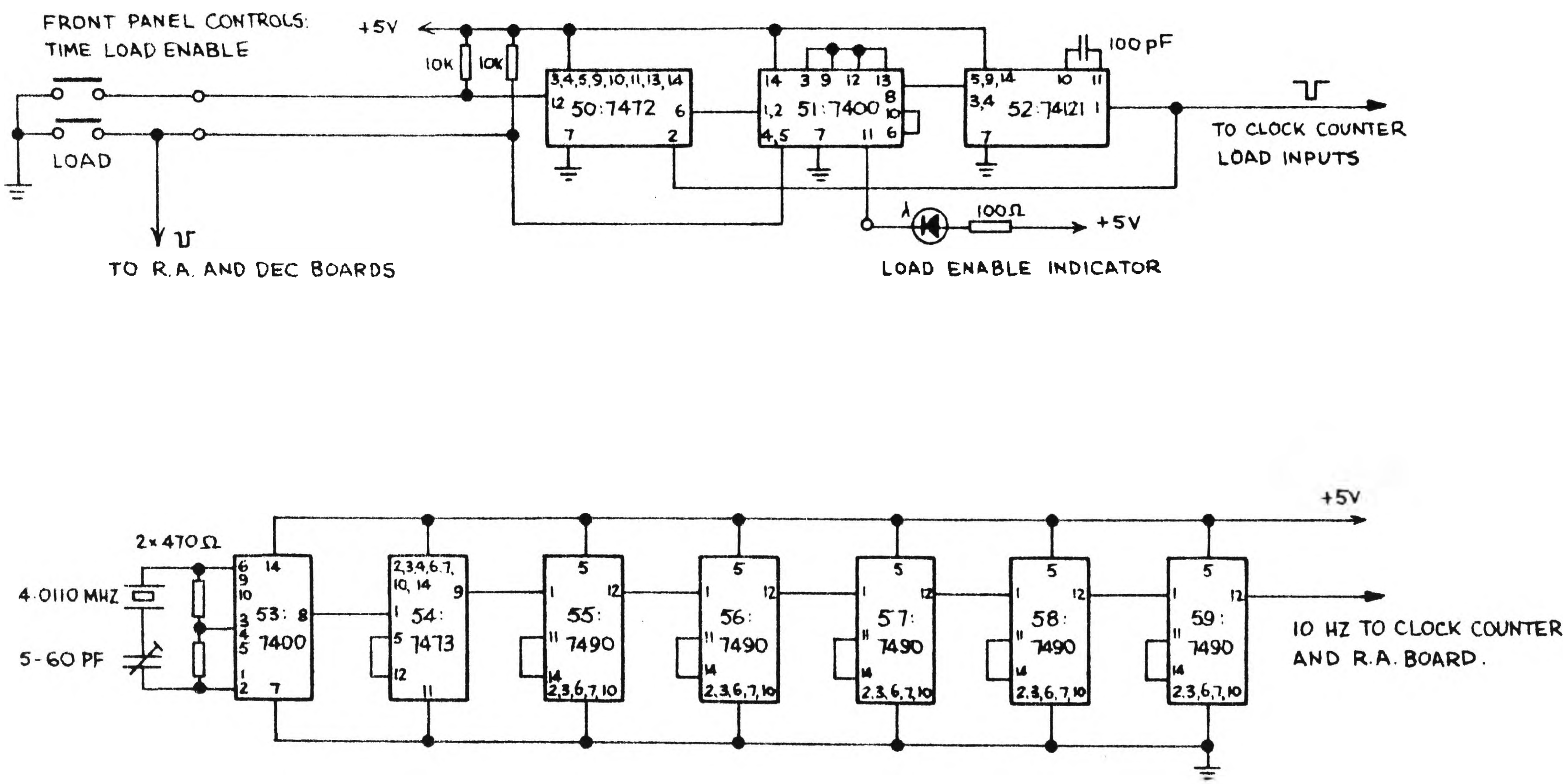

FIG 7.9 CRYSTAL OSCILLATOR, DIVIDER, AND TIME LOAD.

A positive-going pulse arriving on either DEC input line triggers the 74121 monostable (IC1) on the rising edge. The 74121 puts out a 0.1 microsecond pulse (negative-going) to the "set" pin of IC2, a 7474 flipflop, so the Q output (pin 5) goes high. (A short pulse is needed at the set pin, since "set" and "reset" must not be taken low at the same time).

The high output from pin 5 is applied to the D input of the second half of the 7474 flipflop. The first rising edge of the clock pulse train (at pin 11) transfers the high level at the D input to the Q output (pin 9).

The high level from the flipflop is applied to AND gates (IC3) together with the still high level on the DEC input line and the clock pulses. The clock pulses pass to IC5, a 7492 connected as a divide by six stage. After 6 input pulses at pin 1, pin 8 goes low, which triggers IC4, a 74121 monostable, which resets both halves of IC2, which prevents further pulses from appearing at the output.

The clock pulses have a nominal frequency of 500 KHz, or a period of 2 microseconds, which enables 6 pulses to fit easily into pulses arriving from the line receivers with periods of 20 microseconds.

The 500 KHz clock is based on half of IC9, a 7413 Schmitt trigger. Timing is determined by the 4K7 resistor and the 220 pF capacitor, and output is buffered by IC7b.

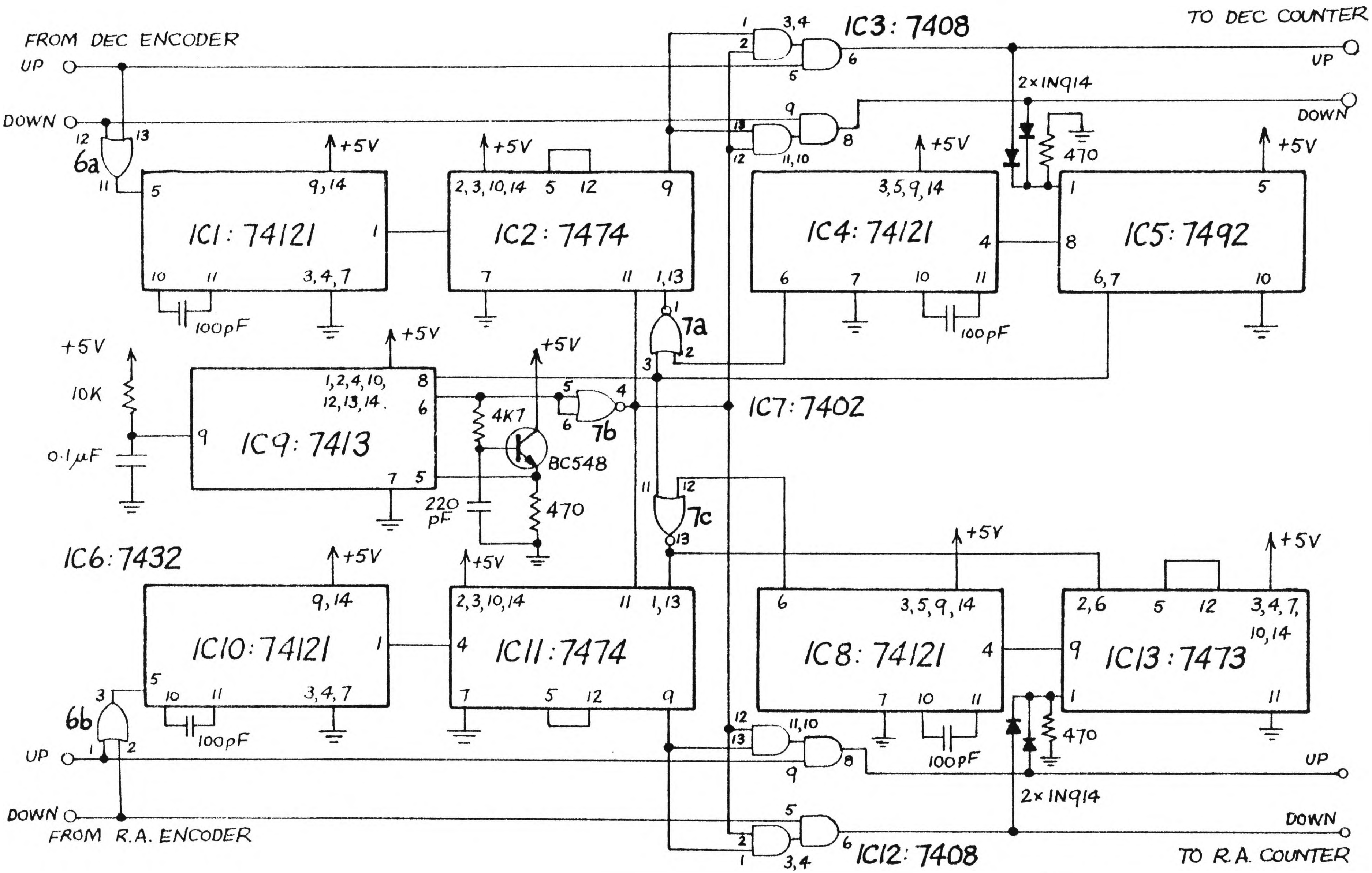

FIG. 7.10 PULSE RATE MULTIPLIER

The other half of IC9 produces one pulse at switch-on, to provide power-on resetting of IC2, IC11, IC5, and IC13.

Multiplication of RA pulses is performed in the same way as for DEC pulses using the same clock, except that IC13 is connected as a divide-by-four counter so that four pulses are delivered for every pulse received.

7.11 POWER SUPPLY

The mains voltage at the telescope site suffers from significant variation and occasional spikes (the line exists to serve coal mining machinery). In addition, the telescope drive motors and particularly the dome drive motor produce substantial mains-borne noise.

In order to isolate the encoding system from mains supply problems, operation is based on a 12 volt lead-acid battery which can be recharged during the day and isolated from the mains when used at night.

The battery powers a 5 volt 10 amp regulator based on a design by Simpson (1977); the 5 volts is used for all of the system except for the encoders and their line transmitters, which have their own 5 volt regulators.

BIBLIOGRAPHY

Abell, G. O. (1966). Astrophys. J. 144, 259.

Allen, C. W. (1964). Astrophysical Quantities (Athlone Press, London).

Berger, J., and Fringant, A.-M. (1980). Astron. Astrophys. 85, 367.

Bohm, K. H., and Deinzer, W. (1965). Z. Astrophys. 63, 177.

Boksenberg, A., Evans, R. G., Fowler, R. G., Gardner, I. S. K., Houziaux, L., Humphries, C. M., Jamar, C., Macau, D., Macau, J. P., Malaise, D., Monfils, A., Nandy, K., Thompson, G. I., Wilson, R., and Wroe, H. (1973). Monthly Notices Roy. Astron. Soc. 163, 291.

Bradley, P. T., and Morton, D. C. (1969). Astrophys. J. 156, 687.

Carnochan, D. J., Dworetsky, M. M., Todd, J. J., Willis, A. J., and Wilson, R. (1975). Phil. Trans. Roy. Soc. London, A279, 479.

Carnochan, D. J., and Wilson, R. (1976). A Catalogue of Ultraviolet Objects. (Private communication.)

Carnochan, D. J., and Wilson, R. (1983). Monthly Notices Roy. Astron. Soc. 202, 317.

Code, A. D., Davis, J., Bless, R. C., and Hanbury Brown, R. (1976). Astrophys. J. 203, 417.

Crawford, D. L. (1975). Publ. Astron. Soc. Pacific <u>87</u>, 481.

Crawford, D. L. (1978). Astron. J. <u>83</u>, 48.

Crawford, D. L., and Barnes, J. V. (1970). Astron. J. <u>75</u>, 978.

Crawford, D. L., and Mander, J. (1966). Astron. J. <u>71</u>, 114.

Dworetsky, M. M., Lanning, H. H., Etzel, D. B., and Patenaude, D. J. (1977). Monthly Notices Roy. Astron. Soc. <u>181</u>, 13P.

Dworetsky, M. M., Whitelock, P. A., and Carnochan, D. J. (1982). Monthly Notices Roy. Astron. Soc. <u>200</u>, 445.

Garrison, R. F., Hiltner, W. A., and Schild, R. E. (1977). Astrophys. J. Suppl. <u>35</u>, 111.

Gebbie, K. B., and Seaton, M. J. (1963). Nature, <u>199</u>, 580.

Giddings, J. R. (1980). PhD. Thesis, University of London.

Giddings J. R., and Dworetsky, M. M. (1978). Monthly Notices Roy. Astron. Soc. <u>183</u>, 265.

Hardie, R. H. (1962). In <u>Stars and Stellar Systems</u>, Vol. II (Astronomical Techniques), edited by W. A. Hiltner (Univ. of Chicago Press, Chicago), p. 180.

Hayes, D. S., and Latham, D. W. (1975). Astrophys. J. <u>197</u>, 593.

Houk, N., and Cowley, A. P. (1975). University of Michigan Cat. of Two-Dimensional Spectral Types for the HD Stars, Vols. I and II (Univ. of Michigan, Ann Arbor, Mich).

Hummer, D. G., and Mihalas, D. (1970). JILA report No. 101, Univ. of Colorado, Boulder, Colorado.

Humphries, C. M., Nandy, K., and Thompson, G. I. (1973). Monthly Notices Roy. Astron. Soc. 163, 1.

Jamar, C., Macau-Hercot,D., Monfils,A., Thompson,G. I., Houziaux,L., Wilson, R. (1976). Ultraviolet Bright Star Spectrophotometric Catalogue. ESA Special Report No. 27.

Jaschek, C., Conde, H., and deSierra, A. C. (1964). Catalogue of Stellar Spectra Classified in the MK System. Astronomical Observatory La Plata, Serie Astronomica XXVIII(2).

Johnson, H. L. (1965). Astrophys. J. 141, 923.

Klinglesmith, D. A. (1971). Hydrogen Line Blanketed Model Stellar Atmospheres. Scientific and Technical Information Office, N.A.S.A., Washington D.C.

Nandy, K., and Schmidt, E. G. (1975). Astrophys. J. 198, 119.

Oblak, S., Considere, S., and Chareton, M. (1976). Astron. Astrophys. Suppl. 24, 69.

O'Dell, C. R. (1967). IAU Symp. No. 34, 371.

Oke, J. B., and Shipman, H. L. (1971). IAU Symp. No. 42, ed. W. J. Luyten (Reidel, Dordrecht) p 67.

Schmidt-Kaler, Th. (1965). Landolt-Bornstein, ed. K. H. Hellwege (Springer-Verlag, Berlin), New Ser., Group 6, Vol.P.,284.

Seaton, M. J. (1966). Monthly Notices Roy. Astron. Soc. 132, 347.

Simpson, L. (1977). Electronics Australia, November.

Stromgren, B. (1966). Ann. Rev. Astron. and Astrophys. 4, 433.

Thompson, G. I., Nandy, K., Jamar, C., Monfils, A., Houziaux, L., Carnochan, D. J., and Wilson, R. (1978). Catalogue of Stellar Ultraviolet Fluxes, The Science Research Council.

Webster, B. L. (1969). Monthly Notices Roy. Astron. Soc. 143, 113.

Weidemann, V. (1967). IAU Symp. No. 34, ed. D. E. Osterbrock and C. R. O'Dell (Reidel, Dordrecht) p 423.

Wilson, R. (1978). University College London Ultraviolet Star Catalogue, U.C.L. Microfiche.